FUNCTIONAL AND MECHANISTIC CHARACTERIZATION OF TWO TRNA MODIFYING ENZYMES

LAURA CAROLE KEFFER-WILKES
Master of Science, University of Lethbridge, 2012

A Thesis
Submitted to the School of Graduate Studies
Of the University of Lethbridge
In Partial Fulfillment of the
Requirements for the Degree

DOCTOR OF PHILOSOPHY

Department of Chemistry and Biochemistry
University of Lethbridge
LETHBRIDGE, ALBERTA, CANADA

FUNCTIONAL AND MECHANISTIC CHARACTERIZATION OF TWO TRNA MODIFYING ENZYMES

LAURA CAROLE KEFFER-WILKES

Date of Defence: June 28, 2016

Dr. Ute Wieden-Kothe Supervisor	Associate Professor	Ph.D.
Dr. Tony Russell Thesis Examination Committee Member	Assistant Professor	Ph.D.
Dr. Stacey Wetmore Thesis Examination Committee Member	Professor	Ph.D.
Dr. Hans-Joachim Wieden Thesis Examination Committee Member	Professor	Ph.D.
Dr. Eugene Mueller External Examiner University of Louisville Louisville, Kentucky	Professor	Ph.D.
Dr. Elizabeth Schultz Internal External Examiner University of Lethbridge	Associate Professor	Ph.D.
Dr. Michael Gerken Chair, Thesis Examination Committee	Professor	Ph.D.

Abstract

The formation of pseudouridine (Ψ) and 5-methyluridine (m^5U) in the T-arm of transfer RNAs (tRNAs) is near-universally conserved. These two modifications are formed in *Escherichia coli* by the pseudouridine synthase TruB and the *S*-adenosylmethionine-dependent methyltransferase TrmA, respectively. In this thesis, I investigate the function and mechanisms of these two tRNA modifying enzymes. First, *in vitro* and *in vivo* analysis of TruB reveals that this enzyme is acting as a tRNA chaperone which proves a long outstanding hypothesis. Secondly, characterization of ligand binding by TrmA shows that binding is cooperative and disruption of tRNA elbow region tertiary interactions by TrmA is essential for efficient tRNA binding and catalysis, leading to future analysis. In conclusion, my studies further our understanding of the mechanism and function of tRNA modifications and modifying enzymes, as well as shed light on why all cells invest substantial resources into fine-tuning the chemical composition of tRNAs.

Acknowledgements

First, I would like to thank my wonderful supervisor, Dr. Ute Wieden-Kothe. She has taught me so much over the years, not only about science, but how to be a better person and grow from your hardships. Being a part of the Kothe lab has been an amazing, rewarding experience and I will be forever grateful for the opportunities you gave me.

Thank you to my committee members, Drs. Tony Russell, Stacey Wetmore, and HJ Wieden. Thank you for sitting through many committee meetings and all the helpful advice and support over the many years.

To the Kothe and Wieden lab members, thank you for providing such a friendly and open work environment, as well as the many, many laughs.

Lastly, thank you to my friends and family. The many times I wanted to talk science and you actually let me and even listened. Love you and thank you.

Table of Contents

List of Tables

List of Figures

Abbreviations

2AP	Deoxyribo-2-aminopurine
Abs	Absorbance
ASL	Anticodon stem loop of tRNA
ATP	Adenosine-5´-triphosphate
Cbf5	Centromere binding factor 5
CD	Circular dichroism
CIP	Calf intestinal alkaline phosphatase
CMCT	*N*-cyclohexyl-*N´*-β-(4-methylmorpholinium)ethylcarbodiimide *p*-tosylate
CTP	Cytidine-5´-triphosphate
D	Dihydrouridine
DEAE	Diethylaminoethyl
DNA	Deoxyribonucleic acid
DPM	Decays per minute
DTT	Dithiothreitol
EDTA	Ethylenediaminetetraacetic acid
EF-Tu	Elongation factor – thermal unstable
FL	Fluorescein-5-thiosemicarbazide
f^5U	5-fluorouridine
Gar1	Glycine and arginine rich protein 1
Gm18	2´-*O*-methylguanosine
GTP	Guanosine-5´-triphosphate
His-tag	Histidine-tag
HEPES	*N*-2-Hydroxyethylpiperazine-*N´*-2-ethanesulfonic acid
iPPase	Inorganic pyrophosphatase
IPTG	β-D-1-thiogalactopyranoside
LB	Lysogeny broth
KAN	Kanamycin
m^5U	5-methyluridine
mRNA	Messenger RNA
MW	Molecular weight
MWCO	Molecular weight cut-off
MWM	Molecular weight marker
NAD(P)	Nicotinamide adenine dinucleotide (phosphate)
Nop10	Nucleolar protein 10
NMR	Nuclear magnetic resonance
NTP	Nucleotide-5´-triphosphate
OD_{600}	Optical density at 600 nm
ORF	Open reading frame
PAGE	Polyacrylamide gel electrophoresis
PDB	Protein data bank
PCR	Polymerase chain reaction
PMSF	Phenylmethanesulfonylfluoride
Ψ	Pseudouridine
PTC	Peptidyl transferase centre

PUA	Pseudouridine synthase and archaeosine transglycosylase
Pus1-10	Pseudouridine synthases 1 – 10
RluA - F	Ribosomal large subunit pseudouridine synthase A – F
RNA	Ribonucleic acid
RNase	Ribonuclease
rRNA	Ribosomal ribonucleic acid
RsuA	Ribosomal small subunit pseudouridine synthase A
rT	Ribothymine
SAH	*S*-adenosylhomocysteine
SAM	*S*-adenosylmethionine
SDS	Sodium dodecyl sulfate
sRNA	Small ribonucleic acid
sRNP	Small ribonucleoprotein
snRNA	Small nuclear ribonucleic acid
snRNP	Small nuclear ribonucleoprotein
snoRNA	Small nucleolar ribonucleic acid
tRNA	Transfer nucleic acid
TCA	Trichloroacetic acid
T_M	Melting temperature
Tris	Tris(hydroxymethyl)aminomethane
TSL	T-arm stem loop of tRNA
TruA - D	tRNA pseudouridine synthase A – D
THUMP	Thiouridine synthases, methylases, and pseudouridine synthases
U1 – U6	Uridyl-rich sn(o)RNAs
UTP	uridine-5´-triphosphate
UV	Ultraviolet
WT	wild type

Chapter 1 - Introduction: tRNA, Modifications and Modifying Enzymes

1.1 Transfer Ribonucleic Acid

Transfer RNA (tRNA) is an essential adaptor molecule that transports amino acids to the ribosome in order to facilitate the synthesis of a polypeptide. The lifecycle of a tRNA is complex and involves transcription, processing, folding, modification, aminoacylation and degradation. tRNA must interact with numerous protein factors during its lifetime such as a variety of modification enzymes, aminoacyl synthetases, and EF-Tu. Finally, tRNAs must be properly accommodated into the A and P sites of the ribosome and decode the mRNA message. This thesis highlights the importance of tRNA modification and modification enzymes for cellular fitness.

1.2 Biogenesis of tRNA in *E. coli*

Transfer RNA is often transcribed as a polycistronic precursor RNA by RNA polymerase (RNA polymerase III in eukaryotes) (Willis 1993; Ishihama 2000). In *Escherichia coli*, there are 86 tRNA genes corresponding to 45 tRNA species (Withers *et al*. 2006). Frequently used tRNAs (i.e. tRNAs used to decode codons that appear often in open reading frames (ORFs) of highly expressed genes) always have at least four copies, whereas less used tRNAs have two or three copies. Genes for rare tRNAs have only a single copy. However, it is not only gene copy number that contributes to tRNA abundance, but also promoter activity. There are ten *E. coli* tRNA genes that are present in the spacer regions of rRNA operons, and six tRNA operons that contain protein genes, such as EF-Tu. Since both EF-Tu and rRNA are highly expressed in cells, these operons are under the control of strong promoters, and as a result, these tRNA genes are abundantly transcribed (Komine *et al*. 1990; Blattner *et al*. 1997).

Once the precursor tRNA is synthesized, it undergoes multiple processing steps to yield the final RNA products (Figure 1.1). RNase E is essential for cell viability and is responsible for generating pre-tRNAs from a polycistronic precursor (Ow and Kushner 2002). The 5´ leader sequence of the tRNA transcript is removed by the endoribonuclease RNase P to produce mature 5´ ends (Altman *et al*. 1995). The maturation of the 3´ end is more complicated as many exoribonucleases are involved with some redundancies, including RNase D, RNase BN, RNase T, RNase PH, RNase II, and polynucleotide phosphorylase (PNP) (Li and Deutscher 1996). In eukaryotes, RNase Z catalyzes the cleavage directly following the discriminator N_{73} nucleotide prior to the addition of the essential 3´CCA sequence (Schiffer *et al*. 2002). Alternatively, genes coding for tRNA in *E. coli* already contain the CCA sequence, but cells still have a CCA-adding enzyme present to assist in tRNA repair (Zhu and Deutscher 1987). Although not all *E. coli* tRNA transcripts contain introns, those that do undergo intron removal via a group 1 self-splicing mechanism (Kuhsel *et al*. 1990; Reinhold-Hurek and Shub 1992).

As precursor tRNA is transcribed in bacteria, it can fold rapidly into the characteristic cloverleaf secondary and L-shaped tertiary conformations. The formation of the canonical cloverleaf structure of sequential polycistronic tRNAs can bring the 5´ RNase P sites together for processing (Seidman and McClain 1975). The formation of the native tertiary structure is dependent on temperature and ion strength, most notably magnesium (Cole and Crothers 1972; Cole *et al*. 1972; Yang and Crothers 1972; Sampson and Uhlenbeck 1988; Serebrov *et al*. 1998). Folding is independent of tRNA modifications, but the level of modification decreases if mutations in the tRNA prevent correct folding (McClain and Seidman 1975; Hall *et al*. 1989). Although most modifications are not

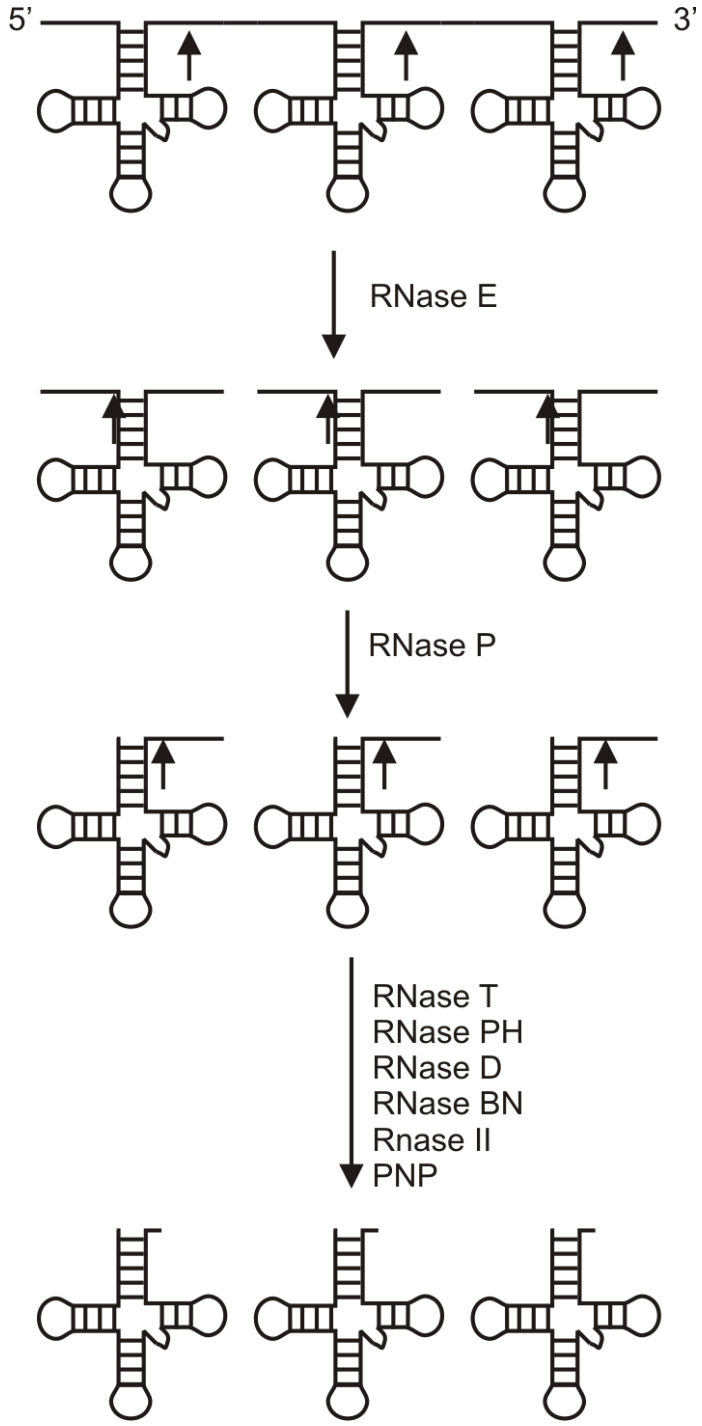

Figure 1.1. Transfer RNA processing in bacteria. Polycistronic precursor tRNA is cleaved by RNase E downstream of the encoded 3´ CCA determinant. Mature 5´ termini are generated by RNase P cleavage. Subsequent trimming of the 3´ terminus proceeds through a number of exonucleolytic cleavage steps producing mature tRNA transcripts. Modification of tRNA nucleosides can possibly occur during any of these maturation steps.

essential for tRNA folding, several studies suggest that they modulate the stability of tRNA tertiary structure, level of aminoacylation, and translational efficiency (Hagervall *et al*. 1990; Urbonavičius *et al*. 2002; Agris *et al*. 2007; Ranjan and Rodnina 2016).

tRNAs are composed of 76 - 90 nucleotides that fold into a cloverleaf secondary structure typically resulting in four stems with a small variable loop region (Class I) or a larger variable region that can form an additional hairpin (Class II) (Figure 1.2) (Sprinzl *et al*. 1998; Giegé *et al*. 2012). The acceptor stem forms by base pairing between the 5´ and 3´ termini, and the conserved CCA 3´ overhang is the site of aminoacylation. Nucleotides 10 to 25 fold into the D-arm, named as such for the common dihydrouridine modifications found in the loop. The anticodon stem loop consists of nucleotides 27 – 43 and contains the anticodon triplet (nucleotides 34 to 36) that is used to decode mRNA codons in the ribosome. Some tRNAs may contain a variable loop, which can range in size and occurs between positions 45 and 46. The last stem loop contains the near-universally conserved modifications of ribothymine (5-methyluridine, m^5U, T) at position 54 and pseudouridine at position 55 (Ψ), as well as the invariant C56 and is thus called the TΨC-arm (Holley *et al*. 1965). The first three-dimensional structure of tRNA was described in 1973 and revealed that the cloverleaf secondary structure folds into an L-shaped conformation (Kim *et al*. 1973). Two helices of the tRNA cloverleaf always stack onto each other coaxially forming two main arms connected through the elbow region. The acceptor arm consists of the T-arm stem loop and the acceptor stem, with the anticodon arm, forming from the D-arm and anticodon stem loops (Figure 1.2).

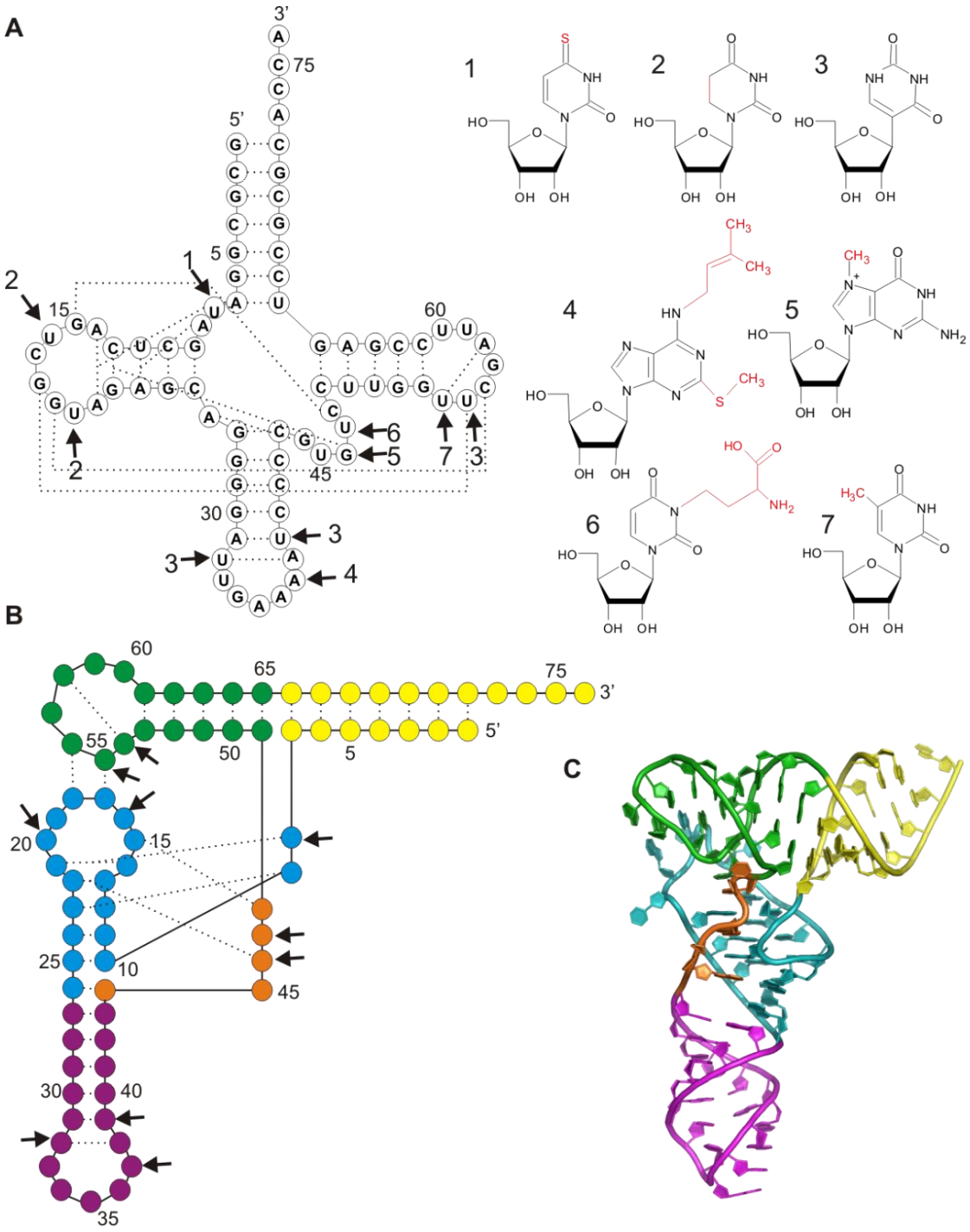

Figure 1.2. Secondary and tertiary structures of *E. coli* tRNA^{Phe} highlighting base pairing and long-range interactions between stem loops as well as modification sites. A) Classical cloverleaf representation of tRNA secondary structure. The nucleotide chain is represented by circles connected by solid lines. Base-pairing and tertiary interactions are shown as dotted lines. Arrows indicate nucleoside modification with corresponding

modifications shown at right: 1. 4-thiouridine, 2. Dihydrouridine, 3. Pseudouridine, 4. 2-methylthio-N^6-isopentenyladenosine, 5. 7-methylguanosine, 6. 3-(3-amino-3-carboxypropyl)uridine 7. 5-methyluridine B) Two-dimensional representation of the tertiary structure of tRNA emphasizing the contacts made between the D-arm (blue) and T-arm (green). Acceptor stem is in yellow, anticodon stem loop in purple, and the variable loop is orange. Arrows indicate modification sites as described in (A) C) Crystal structure of unmodified *E. coli* $tRNA^{Phe}$ (3L0U) with arms coloured as in (B) (Byrne *et al*. 2010).

1.3 Modifications in tRNA

Transfer RNAs in *E. coli* range in length from 74 to 89 nucleotides and can have up to 10% of their sequence modified (Machnicka *et al*. 2012). Most modifications are located in the anticodon stem loop and the elbow region of tRNA. Modifications of the position 34, the wobble position of the anticodon, can be very complex and act to promote, expand, restrict and/or alter codon-anticodon interactions during translation (Hagervall *et al*. 1990; Agris 2004; Agris *et al*. 2007). Additionally, position 37, 3´ to the anticodon, is always conserved as a purine and is often modified to prevent frameshifting errors, and mischarging of certain tRNAs (Miller *et al*. 1976; Putz *et al*. 1994; Lamichhane *et al*. 2013). This position can also be hypermodified to help stabilize codon/anticodon interactions or reinforce stacking to maintain the correct U loop structure. Specifically, the unmodified anticodon loop of *E. coli* $tRNA^{Phe}$ adopts a small three nucleotide loop not observed in the mature tRNA. NMR analysis revealed that with the addition of nucleoside modifications the loop adopts a more native-like conformation (Sundaram *et al*. 2000; Cabello-Villegas and Nikonowicz 2005). While the anticodon loop can contain a variety of unique and complex modifications, the elbow region modifications are far more conserved across species and tRNA subtypes. In fact, these modifications are so common that tRNA secondary structure is named after them. The D-arm, comprised of

nucleotides 11 to 25, is designated as such due to the highly conserved presence of dihydrouridine (D) modifications at positions 16, 17, 20, 20a, or 21 of the stem loop (Figure 1.2). Only 5 tRNAs in *E. coli* lack all D modifications, with the remaining having at least one (Machnicka *et al*. 2012). The 2´-*O*-methylation of G18 in the D-arm stem loop is also common and found in more than 30% of the tRNA species of *E. coli*. In the single glutamate tRNA isoacceptor of *E. coli*, a pseudouridine modification is located at position 13. While the D-arm can have some variability in the number and positioning of the modifications, the T-arm of tRNA has an almost universally conserved modification pattern of 5-methyluridine (m^5U/T) and pseudouridine (Ψ). With few exceptions, nucleotides 53-56 are conserved as GUUC, which is then modified to GTΨC and thus denotes the name of the stem loop (Machnicka *et al*. 2012). The focus of this thesis will be on the TΨC-arm modifications in bacterial tRNAs.

1.4 Pseudouridine in RNA

Pseudouridine is the most common modification found in RNA and is often referred to as the "fifth nucleotide" (Davis and Allen 1957). Discovered more than 50 years ago, pseudouridine can be found in many different functional RNAs, but was recently confirmed to also be present in mRNA (Carlile *et al*. 2014; Li *et al*. 2015). Pseudouridine is the 5-ribosyluridine isomer of canonical 1-ribosyluridine and thereby has a unique C_1´-C_5 bond between the ribose sugar and the uracil base, but retains uracil's ability to base pair with adenine (Figure 1.2). The enhanced rotational freedom of the carbon-carbon bond over the nitrogen-carbon bond allows for greater conformational flexibility of the nucleoside (Figure 1.2; Davis, 1998). However, the additional N_1 imino group, which now has the ability to hydrogen bond as well, has been shown to be involved in

coordinating a water molecule between the base and the preceding backbone phosphodiester bond, resulting in an overall more rigid local RNA structure (Arnez and Steitz 1994; Davis 1995; Davis 1998; Davis *et al*. 1998). Free pseudouridine in solution has a slight preference for the *syn* glycosyl conformation, in contrast to uridine and the other canonical nucleosides (Davis 1998). However, when pseudouridine is part of a polynucleotide chain, only the *anti* conformation has been observed (Yarian *et al*. 1999). Several spectroscopic studies have revealed that pseudouridine, as a part of an oligoribonucleotide sequence, forms A-form helices with increased base stacking compared to the unmodified RNA which is proposed to be the primary effect on RNA structure stabilization (Davis 1995).

Pseudouridine is often found in functionally important regions of non-coding RNA. In some eukaryotes, pseudouridines are integral to the spliceosomal machinery. Many pre-mRNA transcripts contain introns that need to be removed before being used in protein translation. The spliceosome, a large dynamic molecular machine, consists of both proteins and RNA and catalyzes the splicing reaction within pre-mRNA. The RNA components known as “uridyl-rich” small nuclear RNAs (snRNAs), U1, U2, U4, U5, and U6, are extensively post-transcriptionally modified with pseudouridine, among other less common modifications (Reddy and Busch 1988). The pseudouridines in spliceosomal snRNAs are highly conserved across species and are clustered in functionally important regions of the RNA (Massenet *et al*. 1998). In U2 snRNA, pseudouridine modifications are found frequently in the branch site recognition region, which recognizes the branch site of pre-mRNA during splicing. Specifically, in *Saccharomyces cerevisiae*, it was shown that the presence of pseudouridine at position 35 in U2 not only stabilizes the

branch-site interactions, but also changes the orientation of the bulged adenosine relative to the U2 snRNA-intron duplex. These findings suggest that pseudouridine better positions the branch-site adenosine for recognition and subsequent activity during splicing (Newby and Greenbaum 2001; Wu *et al*. 2016).

The ribosome, another large dynamic ribonucleoprotein complex, also contains multiple pseudouridine modifications. While *E. coli* contains only one pseudouridine in the small ribosomal subunit, *S. cerevisiae* 18S ribosomal RNA (rRNA) can have up to 14. The number of pseudouridine modifications increases in the large subunit with 10 in *E. coli*, 30 in *S. cerevisiae*, and 55 in humans (Ofengand 2002). The most highly conserved pseudouridines across all species are found in the loop of helix 69. In *E. coli*, these residues, pseudouridine 1911, 1915, and 1917, help form an important bridge between the small and large ribosomal subunits, as well as interact with translation factors and tRNA during protein synthesis (O'Connor and Gregory 2011). Pseudouridines are also clustered around the peptidyl transferase centre. In *E. coli*, five pseudouridine residues are present in 23S rRNA that are within close proximity to nucleotides that are directly involved in peptide bond formation (Bakin and Ofengand 1993). Pseudouridines may also play a role in antibiotic resistance, as *E. coli* strains lacking pseudouridines at positions 955, 2504, and 2580 showed an increase in their susceptibility towards antibiotics targeting the peptidyl transferase centre of the ribosome (Toh and Mankin 2008). While many of these pseudouridine modifications are conserved in all domains of life, the loss of individual pseudouridine residues does not significantly impact cell survival. King and coworkers (2003) showed that in yeast, the deletion of individual pseudouridines from rRNA does not significantly affect the growth of the cells. However, when multiple pseudouridines

were removed, synergistic effects were observed, resulting in impaired translation (King *et al*. 2003).

As mentioned above, pseudouridine is present at position 55 of almost all tRNAs in all domains of life. In *E. coli*, pseudouridine can also be found at positions 13, 32, 38, 39, 40, and 65 in various tRNA isoacceptors. Lack of individual pseudouridine modifications in tRNA does not result in significant changes in cell viability, but can impair cell survival in co-culture competition (Li *et al*. 1997; Raychaudhuri *et al*. 1999; Gutgsell *et al*. 2000; Kaya and Ofengand 2003). Pseudouridines have also been proposed to aid in extreme temperature resistance in both *E. coli* and the thermophile *Thermus thermophilus* (Kinghorn *et al*. 2002; Ishida *et al*. 2011). Notably, Ishida and coworkers (2011) observed an increase in Gm18, m^5s^2U54, and m^1A58 levels when pseudouridine 55 was absent, signifying that pseudouridine 55 may play an important regulatory role in other tRNA modifications.

1.4.1 Pseudouridine synthases: Stand-alone vs. H/ACA s(no)RNP

Pseudouridine modifications are introduced in RNA by pseudouridine synthases which belong to six different families: the TruA, TruB, TruD, RluA, RsuA, and Pus10 family. Each family is named after the *E. coli* representative enzyme, except for Pus10 which is not found in bacteria, and thus the family is named after the human protein. Crystal structures have been determined for members of each family and reveal a common fold for the catalytic domain (Foster *et al*. 2000; Hoang and Ferré-D'Amaré 2001; Sivaraman *et al*. 2002; Hoang and Ferré-D'Amaré 2004; Hoang *et al*. 2006; McCleverty *et al*. 2007). Outside of the catalytic core, a variety of additional domains can be found. Members of

the RluA and RsuA families can have an N-terminal extension resembling ribosomal protein S4 (Sivaraman *et al*. 2002; Mizutani *et al*. 2004). Enzymes belonging to the TruB family have a C-terminal *p*seudo*u*ridine synthase and *a*rchaeosine transglycosylase (PUA) domain (Figure 1.3) (Hoang and Ferré-D'Amaré 2001; Li and Ye 2006; Sabina and Söll 2006). Within the catalytic core, pseudouridine synthases have five loosely conserved sequence motifs: I, II, IIa, III, and IIIa (McCleverty *et al*. 2007). Motif I plays a structural role, where its function is to reinforce the active site loop in motif II (Spedaliere *et al*. 2000; Hamma *et al*. 2005; Hoang *et al*. 2005). The only consistently conserved residue, a catalytic aspartate, is found within motif II in the active site cleft (Foster *et al*. 2000; Hoang and Ferré-D'Amaré 2001; Sivaraman *et al*. 2002; Hoang and Ferré-D'Amaré 2004; Hoang *et al*. 2006; McCleverty *et al*. 2007). Motif II also contains a histidine (in TruB family members) or an arginine (in RluA, RsuA, and TruA enzymes) that inserts itself between the RNA bases and ensures that the target uridine flips into the active site (Hoang and Ferré-D'Amaré, 2001; Hoang *et al*., 2006). A tyrosine (or phenylalanine in TruD family) as part of the conserved K/RxY in motif IIa helps to maintain the structural integrity of the active site through hydrophobic interactions (Phannachet *et al*. 2005). The basic residue (K/R) within this conserved sequence interacts with the phosphate of the target nucleotide through a salt bridge (Hoang and Ferré-D'Amaré 2001; Pan *et al*. 2003; Phannachet and Huang 2004; Phannachet *et al*. 2005). In motif III, a conserved lysine or arginine residue interacts with the catalytic aspartate through a salt bridge (Hoang *et al*., 2006). Although TruB lacks motif III, it too has an arginine (R181) that forms a salt bridge with the catalytic residue and helps to activate the aspartate for catalysis (Hoang and Ferré-D'Amaré 2001; Friedt *et al*. 2014).

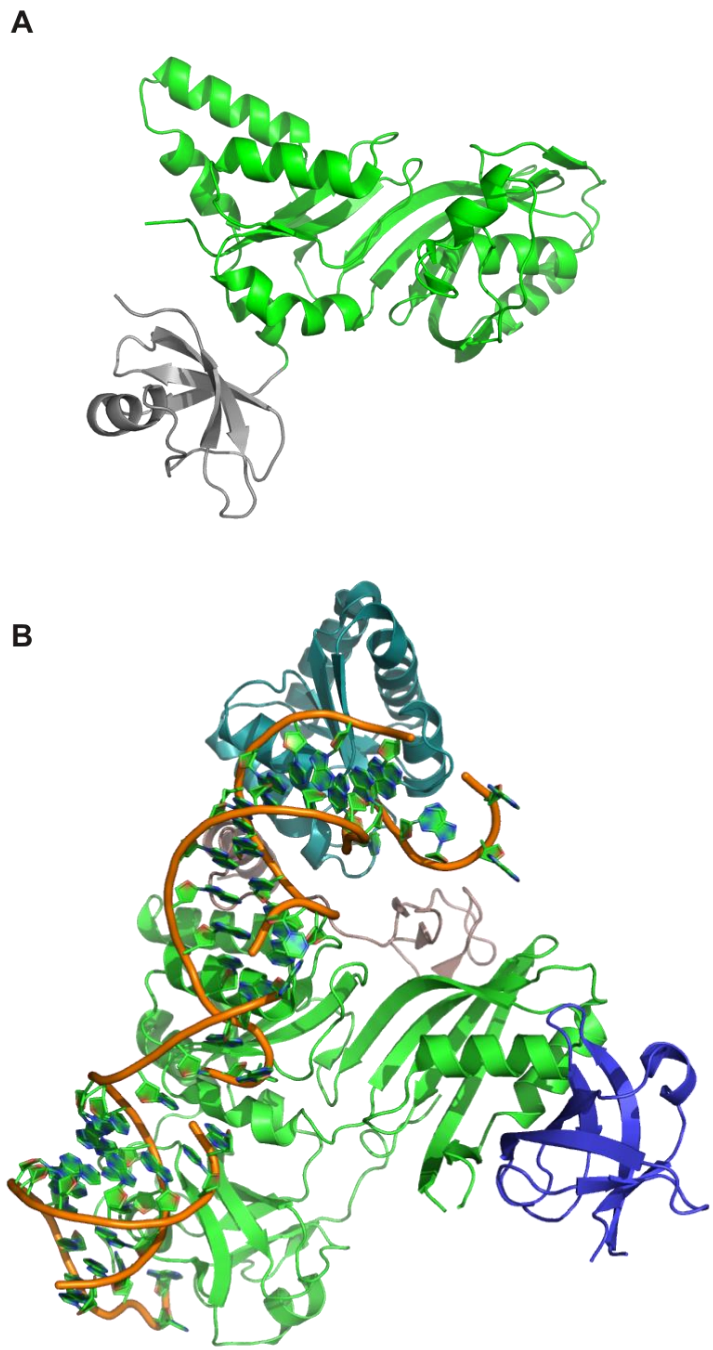

Figure 1.3. Stand-alone and H/ACA sRNP pseudouridine synthases share common core architecture. A) *E. coli* pseudouridine synthase TruB crystal structure (1K8W) with characteristic catalytic domain (green) and C-terminal PUA extension (grey) (Hoang and Ferré-D'Amaré 2001). B) Archaeal H/ACA sRNP (2HVY) composed of the catalytic pseudouridine synthase subunit Cbf5 (green), Gar1 (blue), Nop10 (light grey), L7ae (cyan), and guide H/ACA RNA (orange backbone) (Li and Ye 2006).

In yeast and other eukaryotes, the stand-alone Pus enzymes are responsible for many pseudouridine modifications. Pus1 from *S. cerevisiae* is a multisite, multisubstrate targeting enzyme that forms pseudouridines in the anticodon stem loop of some tRNAs, as well as U2 snRNA (Motorin *et al*. 1998; Massenet *et al*. 1999). While Pus1 acts on cytoplasmic tRNAs, Pus2p is imported into the mitochondria and modifies positions 27 and 28 of mitochondrial tRNAs in yeast (Behm-Ansmant *et al*. 2007). Both Pus1 and Pus2 belong to the TruA family of pseudouridine synthases, along with another yeast enzyme, Pus3, which targets positions 38 and 39 in the anticodon loop of cytoplasmic tRNAs (Lecointe *et al*. 1998). Pus4 is the eukaryotic homolog of TruB, accordingly shares remarkable sequence similarity with *E. coli* TruB and catalyzes the same formation of pseudouridine 55 in both mitochondrial and cytoplasmic tRNAs (Becker *et al*. 1997a). Like Pus2, Pus5 is mitochondrial specific, targeting U2819 in mitochondrial 21S rRNA (Ansmant *et al*. 2000). Another anticodon stem targeting enzyme, Pus6 modifies position 31 in both cytoplasmic and mitochondrial tRNAs (Ansmant *et al*. 2001). Similarly to Pus1, Pus7 targets multiple sites in cytoplasmic tRNAs as well as position 35 in U2 snRNA and is a member of the TruD family (Behm-Ansmant *et al*. 2003; Urban *et al*. 2009). Pseudouridylation at position 32 of tRNAs in yeast, which is accomplished by RluA in *E. coli*, requires two enzymes, Pus8 and Pus9, where Pus8 targets cytoplasmic tRNAs and Pus9 modifies mitochondrial tRNAs (Behm-Ansmant *et al*. 2004). The most recently identified family of pseudouridine synthases, Pus10, has been identified in some archaea and eukaryotes, but is for example not present in *S. cerevisiae*. This enzyme is responsible for the formation of pseudouridine 55 in tRNA, as well as pseudouridine 54 in certain archaeal species (Gurha and Gupta 2008). Members

of this family have a large N-terminal THUMP domain, which contributes to substrate binding, whereas the catalytic domain shares features similar to other pseudouridine synthase enzymes (McCleverty *et al*. 2007; Kamalampeta *et al*. 2013).

Although all organisms have stand-alone pseudouridine synthases, in archaea and eukaryotes, most pseudouridines are introduced by H/ACA small (nucleolar) ribonucleoproteins (H/ACA s(no)RNPs) comprised of four different proteins and a guide RNA (Kiss *et al*. 2010). The complex is comprised of proteins Nop10, Gar1, Nhp2 (L7Ae in archaea), and the only essential pseudouridine synthase, the catalytic subunit Cbf5 (Dyskerin in humans). Archaeal H/ACA sRNAs are typically composed of 60 – 75 nucleotides that fold into a long hairpin (Dennis and Omer 2005). In most eukaryotes such as yeast and humans, the H/ACA snoRNA forms two hairpins each containing a single-stranded pseudouridylation pocket. The stem loops are connected by the characteristic single-stranded ANANNA Hinge region, and the 3´ end of H/ACA snoRNA harbors a conserved 3´ACA box motif (Balakin *et al*. 1996). The H/ACA s(no)RNA is bound to the active site of the pseudouridine synthase subunit and base pairs with the target RNA to position the uridine for modification. Nhp2 or L7Ae can directly and independently bind to the H/ACA s(no)RNA stem loop (Baker *et al*. 2005; Charpentier *et al*. 2005; Li and Ye 2006). Nop10 and Gar1 interact with Cbf5, but do not associate with the sRNA nor do they require the s(no)RNA presence to form a stable ternary protein subcomplex (Rashid *et al*. 2006).

1.4.2 Conserved Catalytic Mechanism for Pseudouridine Formation?

Since all pseudouridine synthases share a common catalytic core and all require an aspartate residue, it is hypothesized that they all share the same catalytic mechanism (Mueller 2002). The first step of pseudouridine synthesis is the breakage of the N_1-C_1' glycosidic bond between the uracil base and ribose sugar. The base can then be rotated or flipped within the catalytic pocket and then reattached to the ribose through C_5. Three possible pathways have been proposed (Figure 1.4). The first mechanism proposed that the catalytic aspartate attacks the C_6 position of the target uracil forming a stable Michael adduct. The final product is then released by hydrolysis of the ester linkage between the aspartate and the pyrimidine ring. This mechanism is supported by experiments with RNA containing 5-fluorouridine (f^5U). Santi and coworkers showed that TruA formed a complex with f^5U-tRNA that could survive denaturing gel conditions but could be disrupted upon heating. HPLC analysis revealed the RNA was hydrated, unrearranged f^5U with the intact N-glycosidic bond, resulting from ester hydrolysis (Huang *et al*. 1998; Gu *et al*. 1999). The second proposed mechanism proceeds through an acylal intermediate, where the catalytic aspartate attacks the C_1' of the ribose ring. This method was proposed based on experiments with TruB and f^5U-tRNA. The crystal structure of TruB was completed in the presence of f^5U substituted RNA with the aim of observing the Michael adduct. Instead, the f^5U was converted to 5-fluoro-6-hydroxypseudouridine. However, labeling studies with ^{18}O showed that hydrolysis of an ester adduct with the catalytic aspartate would not give rise to this product which speaks against the Michael addition mechanism (Huang *et al*. 1998; Hoang and Ferré-D'Amaré 2001; Hoang *et al*. 2006). In 2011, a third mechanism was proposed suggesting the

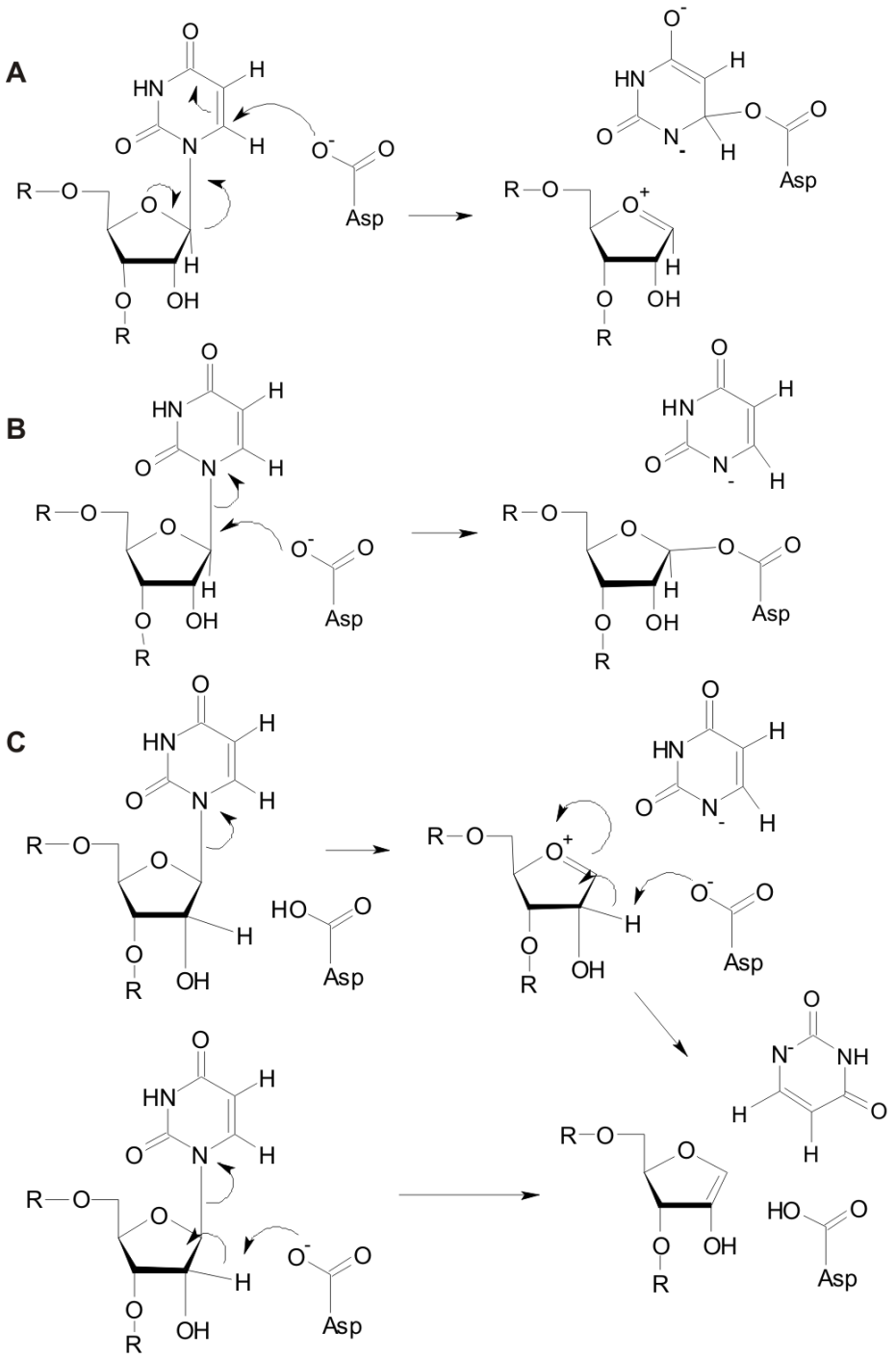

Figure 1.4. Proposed catalytic strategies for pseudouridine formation. A) During the Michael Addition mechanism, the catalytic aspartate attacks the C_6 position of the uracil base. B) As part of the acylal intermediate mechanism, the catalytic aspartate instead attacks the C_1' position of the ribose sugar. C) Miracco and Mueller (2011) proposed the glycal intermediate mechanism for pseudouridine formation, where uracil extraction can be stepwise (top) or concerted (bottom).

reaction progresses through a glycal intermediate (Miracco and Mueller 2011). They found that f^5U products could differ in their stereochemistry at C2´, which would require epimerization through the formation of a glycal intermediate. New evidence points to the glycal mechanism as being most likely the common mode of action for all pseudouridine synthases (Veerareddygari 2014).

1.4.3 A Model Enzyme: TruB

In *E. coli,* the stand-alone pseudouridine synthase responsible for Ψ55 formation in all tRNAs is TruB (Figure 1.3A). The N-terminal catalytic domain folds into a curved β-sheet of 11 antiparallel strands, in addition to 11 α-helices, two short strands and multiple loops forming the active site cleft. TruB also has a C-terminal PUA domain that consists of a four-stranded β-sheet and one α-helix (Hoang and Ferré-D'Amaré 2001; Pan *et al*. 2003). The TruB homolog Cbf5 also has a C-terminal PUA domain which is used to bind the ACA trinucleotide motif of guide RNA. TruB's PUA domain most likely interacts with tRNAs acceptor stem 3´CCA sequence in a similar manner (this work; (Pan *et al*. 2003)). Within the active site, TruB's thumb loop, composed of residues from strands β8, β9 and helix α4, pinches the major groove of the T-arm stem loop. TruB differs from Cbf5 in the active site by the addition of Insertions 1 and 2 that form the tRNA binding cleft. Upon binding tRNA, TruB undergoes only a slight movement of Insertion 1, whereas Insertion 2 moves almost 26 Å in order to interact with the tRNA. In the *apo* structure, Insertions 1 and 2 interact through nonspecific Van der Waals contacts as well as specific interactions, including hydrogen bonds (between D87 and Y126) and hydrophobic stacking (between V96 and Y126) (Phannachet and Huang 2004). In order for RNA to bind, these interactions must be broken and in doing so new contacts are

made with the substrate. Residue D90 of Insertion 1 interacts with N_4 of T-arm nucleotide C56 via a hydrogen bond, but also interacts with the catalytic residue D48 prior to RNA binding (Phannachet and Huang 2004; Friedt *et al*. 2014). The number of contacts increase between substrate RNA and Insertion 2 residues upon binding, specifically the phosphate ester backbone of T-arm nucleotides G52, G53, and U54 which interact with G124, K121, and K120, respectively. Additionally, the main chain amide group of A119 hydrogen bonds with the phosphate group of the invariant C56 nucleotide, whereas the 2´-oxygen of C56 interacts via a hydrogen bond with R132. Finally, Y128 stacks on G57 in its flipped out conformation (Hoang and Ferré-D'Amaré 2001; Phannachet and Huang 2004). TruB modifies U55 in all tRNAs in *E. coli*, as such TruB has 40 different substrates with various nucleotide sequences. It has been described previously that the only RNA sequence requirements for TruB are nucleotides U54, U55, C56, and A58 within the T-arm stem loop. Furthermore, TruB can modify stem loop substrates consisting of only 11 nucleotides, but does require a folded stem structure of at least four base pairs (Becker *et al*. 1997b; Gu *et al*. 1998). Pseudouridine 55 has also been found in precursor tRNAs suggesting that TruB and its homologs don't require a fully processed or possibly even fully transcribed tRNA in order to modify its target nucleotide (Schaefer *et al*. 1973; Nishikura and De Robertis 1981). In order to gain access to its target nucleotide, TruB binds the T-arm in the active site cleft between Insertions 1 and 2. Residue H43, located in a loop region between strands β2 and β3, is forced into the RNA stem loop by the closing of the thumb loop into the major groove. This results in U55 vacating the stem loop in order to avoid steric clashes with residues C-terminal to H43. Nucleotides C56 and G57 are also flipped out of the stem loop into

the active site, whereas the reverse Hoogsteen base pair of U54:A58 stacks on top of H43 (Hoang and Ferré-D'Amaré 2001). The invariant C56 is coordinated by interactions with Y126 and D90 within the active site. The nonconserved nucleotide at position 57 makes hydrogen bonds to both R141 and Y137. The target nucleotide is coordinated by Y76 which is conserved in pseudouridine synthases from the TruB, TruA, RluA, and RusA families (Phannachet *et al*. 2005). Another aromatic residue Y179 stacks against the ribose of U55, whereas D48, the catalytic aspartate residue, makes hydrogen bonds to the uracil base (Hoang and Ferré-D'Amaré 2001; Pan *et al*. 2003).

Like in all other pseudouridine synthases, the catalytic aspartate is required for Ψ55 synthesis by TruB, but is not involved in RNA binding (Ramamurthy *et al*. 1999a). Several groups have determined the rate of pseudouridine formation by TruB with a k_{cat} reported to be between 0.12 and 0.7 s^{-1} (Gu *et al*. 1998; Ramamurthy *et al*. 1999b; Wright *et al*. 2011). Substrate binding was also proposed to occur in two phases, initial binding followed by a conformational change, with an overall rate of 6 s^{-1}. Additionally, it was observed that along with TruA and RluA, the catalytic step of pseudouridine formation (k_{Ψ}) by TruB occurs at a rate of 0.5 s^{-1} (Wright *et al*. 2011). These findings suggest that catalysis is uniformly slow for all pseudouridine synthases since they most likely share the same chemical mechanism. This rate reflects all steps of catalysis: glycosidic bond breakage, base rotation/flipping, and C-C bond formation. Interestingly, the first step of catalysis resembles the cleavage of the N-glycosidic bond in DNA by uracil-DNA glycosylases, which have been reported to have k_{cat} values between 4 and 200 s^{-1} (Duraffour *et al*. 2007; Liu *et al*. 2007). Thus the first step of catalysis could in theory be

faster than the rate reported by Wright *et al.* (2011), and it may be the subsequent base rotation/flipping or C-C bond formation that is the rate-limiting, slow step.

1.5 Methylation of Bacterial tRNAs

Methylation of tRNA is very diverse with many different nucleotide positions targeted as well as different atoms within the nitrogenous base or ribose sugar. In *E. coli*, methylated nucleotides can range from a simple, single methyl group addition to a complex modification requiring multiple enzymes. Simple methylations include the 2´-*O*-methylation of G18 in the D loop, N_7 methylation of G46 in the variable region, and the conserved C_5 methylation of U54 in the T-arm (Figure 1.2A). All three modifications are proposed to contribute to the stabilization and maintenance of the tertiary structure of tRNA (Motorin and Helm 2010). Within the anticodon loop, methylations are commonly part of more intricate modifications, such as 2-methylthio-N^6-isopentenyladenosine or 5-carboxymethylaminomethyl-2´-*O*-methyluridine.

Within the elbow region, the C_5 methylation of U54 is found in most sequenced tRNA species (Machnicka *et al*. 2012). This modification can also be found in rRNA. In *E. coli*, it is found in 23S rRNA at position U747 in the loop of helix 35 of domain II, as well as at U1939 in hairpin 70 in domain IV. These modifications are catalyzed by the SAM-dependent methyltransferases RlmC and RlmD, respectively (Agarwalla *et al*. 2002; Madsen *et al*. 2003). The presence of this modification at position 54 in the T-arm raises the melting temperature of *E. coli* initiator $tRNA^{Met}$ by 6°C and contributes to the overall stability of the tRNA (Davanloo *et al*. 1979; Horie *et al*. 1985; Motorin and Helm 2010).

In most Gram-negative bacteria m^5U54 is introduced by the SAM-dependent methyltransferase TrmA.

1.5.1 SAM-Dependent Methyltransferases

S-adenosyl-L-methionine (SAM)-dependent methyltransferases are ubiquitous and involved in biosynthesis, signal transduction, protein repair, chromatin regulation, and gene silencing (Schubert *et al*. 2003). Although they all share the same methyl group donor, there are five structurally distinct families of SAM-dependent methyltransferases (Classes I – V). The first methyltransferase structure was obtained for *E. coli* DNA methyltransferase HhaI in 1993 which has become a model example of Class I methyltransferases (Cheng *et al*. 1993). The *E. coli* enzyme TrmA is a class I methyltransferase and one of the subjects of this thesis (Figure 1.5). Members of class I are comprised of a seven-stranded β-sheet with a central "topological switch-point" and a reversed β hairpin at the C-terminus. The sheet is also flanked by α helices forming an open αβα sandwich, similar to the NAD(P)-binding Rossman-fold (Fauman *et al*. 1999). A conserved GXG motif is located at the end of the first β strand and is essential for SAM binding. The only other strongly conserved amino acid is an acidic residue located at the end of the second β strand that forms hydrogen bonds with SAM's ribose hydroxyl groups (Fauman *et al*. 1999). Although most Class I methyltransferases act as monomers, they can be found as homodimers or tetramers (Huang *et al*. 2000; Matsumoto *et al*. 2007). Along with the consensus structural core containing the SAM-binding motif, most methyltransferase enzymes have auxiliary domains for substrate recognition. The substrates for Class I methyltransferases range from nitrogenous bases, ribose sugars, and basic residues to small molecules such as catechol and large substrates like tRNA.

In archaea and eukaryotes, 2´-*O*-ribose methylation of ribosomal RNA can also be carried out by specialized ribonucleoprotein complexes, similarly to pseudouridine formation. In eukaryotes, the complexes localize to the nucleolus and are thus called small nucleolar RNPs (snoRNPs), whereas in archaea they are known simply as small RNPs (sRNPs). The guide RNA, referred to as C/D box RNA, contains two consensus motifs, the 5´ "box C" sequence of RUGAUGA (R is purine), and the 3´ "box D" sequence CUGA. Often guide RNAs contain a second set of these conserved sequences – the C´ and D´ boxes (Tollervey and Kiss 1997; Kiss-Laszlo *et al*. 1998). The guide RNA folds into a hairpin structure with a K-turn motif. Modification is directed through base pairing of the single stranded region between the C and D boxes with sequences flanking the site of modification in the substrate RNA. Methylation takes place always five nucleotides upstream of the conserved D box (Kiss-Laszlo *et al*. 1996; Kiss-Laszlo *et al*. 1998). In yeast, the C/D snoRNP is composed of the catalytic enzyme Nop1 (fibrillarin), as well as auxiliary proteins Nop56, Nop58, and the K-turn binding 15.5-kDa protein Snu13 (Galardi *et al*. 2002). A single protein Nop5 replaces both Nop56 and 58, and L7Ae binds the K-turn motif in archaea (Omer *et al*. 2002). Fibrillarin folds into a novel N-terminal domain connected to the C-terminus via a single short helix. The C-terminal domain folds into the common Rossman-like conformation of Class I methyltransferases and contains a Gly-rich motif for binding SAM (Wang *et al*. 2000).

Class II methyltransferases do not resemble Class I enzymes in overall architecture or SAM binding and instead target proteins (histones) for methylation. The active site domain is dominated by a long, central, antiparallel β-sheet flanked by groups of helices at either end. SAM is bound in a shallow groove along the edges of the β strands, where

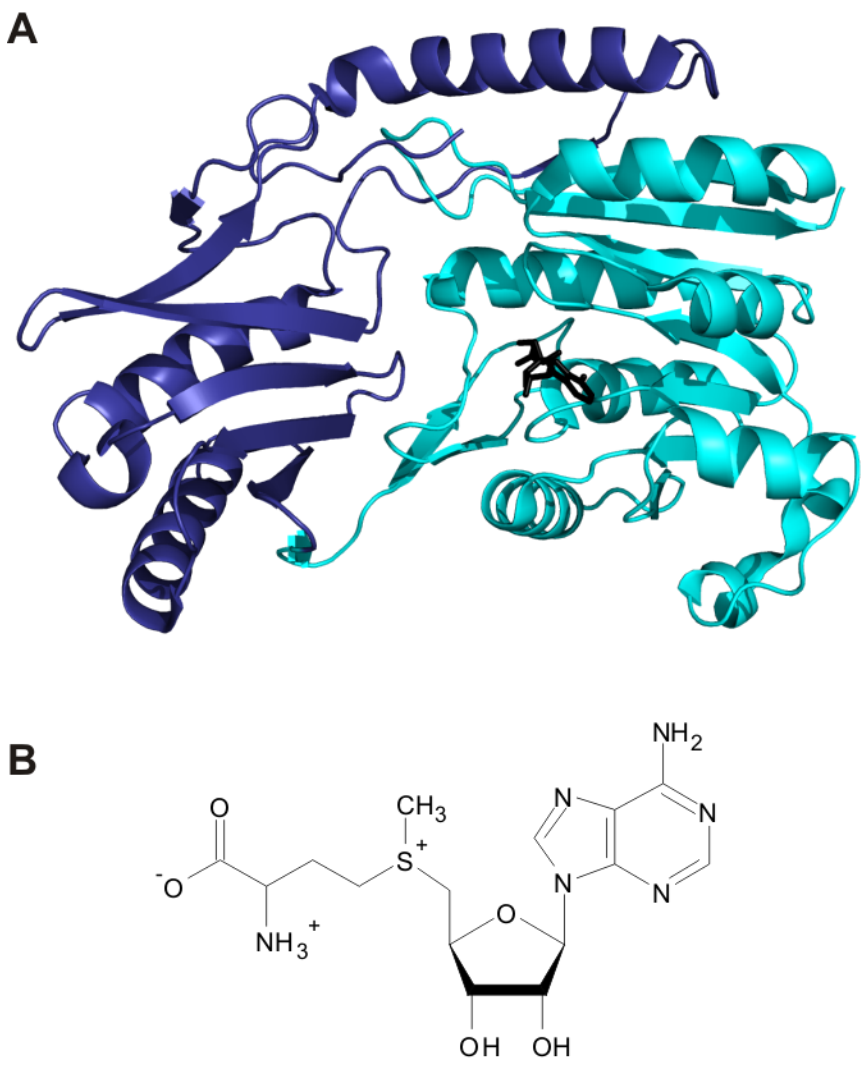

Figure 1.5. Model SAM-dependent methyltransferase TrmA. A) Crystal structure of TrmA (3BT7) from *E. coli* (Alian *et al*. 2008). RNA-binding domain proposed to interact with tRNA D-arm is dark blue. Catalytic domain (cyan) bound to SAH (black). B) *S*-Adenosylmethionine (SAM) ligand used as methyl group donor.

it forms hydrogen bonds to a conserved RXXXGY motif (Dixon *et al*. 1996; Jarrett *et al*. 1998). The third class of methyltransferases is characterized by the homodimeric CbiF methyltransferase, part of the cobalamin synthesis pathway (Schubert *et al*. 1998). The active site of this class in inserted into a cleft between two αβα domains. Similar to Class

I, a GXG motif occurs at the end of the first β strand, but is not involved in SAM binding; instead SAM is tightly bound between the two domains. Class IV contains the SPOUT family of methyltransferases, including the tRNA m^1G37 methyltransferase TrmD and rRNA G2251 2´-O-rRNA methyltransferase RlmB, both from *E. coli* (Anantharaman *et al*. 2002; Michel *et al*. 2002; Elkins *et al*. 2003). This family is unique as they include a six-stranded parallel β-sheet flanked by seven α-helices, and the active site is located near the homodimer interface. Interestingly, a significant proportion of the C-terminus is folded back into the structure making a "knot". Finally, the last class (V) is composed of the SET-domain enzymes. These methyltransferases are comprised of a series of eight curved β strands forming three small sheets. The C-terminus then tucks underneath the sheets forming a knot-like structure, like that of Class IV enzymes. SAM is bound in a kinked conformation to a concave surface near an invariant tyrosine residue. Members of this family are involved in histone methylation (Min *et al*. 2002; Zhang *et al*. 2002; Dillon *et al*. 2005).

Methylation can occur at nitrogen, carbon, and oxygen atoms in a variety of macromolecules. Recognition of nitrogen by Class I methyltransferases typically occurs through a conserved [D/N/S]PP[Y/F] motif at the C-terminal end of β4 (Gong *et al*. 1997; Goedecke *et al*. 2001). A charged methylamine intermediate results after methyl group transfer which is followed by β-elimination to facilitate product release. This recognition mechanism is not nucleotide specific, but instead selects for nitrogens conjugated to a planar system. Methylation at N7 of G46 occurs in several tRNA isoacceptors in both eukaryotes and prokaryotes (Machnicka *et al*. 2012). In yeast, this modification is catalyzed by the Class I Trm8-Trm82 complex, whereas in bacteria TrmB is responsible

(De Bie *et al*. 2003; Purta *et al*. 2005; Matsumoto *et al*. 2007). However, instead of the [D/N/S]PP[Y/F] motif, this family of enzymes has a conserved PDP[W/H] sequence at the C-terminal end of β strand four, which has been shown to be critical for catalysis (Purta *et al*. 2005). Conversely, the Class V SET-domain methyltransferases bind their target lysine nitrogen opposite to SAM in a small channel. The C-terminal pseudoknot forms a hydrophobic pocket for the substrate and contains a conserved tyrosine residue required for catalysis (Xiao *et al*. 2003).

Methylation of carbon is more difficult than modification at polarizable nitrogen. For TrmA and similar enzymes, when methylating C5 of uracil, the target nucleotide must first be activated by covalent-bond formation between a conserved cysteine thiol group in the methyltransferase and carbon C6 of the base (Wu and Santi 1987; Gu and Santi 1992; Kealey *et al*. 1994; Agarwalla *et al*. 2002). Class I DNA C_5-cytosine methyltransferases have a conserved Pro-Cys motif within the active site and a neighbouring aspartate residue to facilitate proton abstraction (Wu and Santi 1987). Similarly, the RNA C_5-uracil methyltransferases all have a conserved Cys-Asn motif as well as a glutamate residue within the active site (Gu and Santi 1992; Agarwalla *et al*. 2002; Lee *et al*. 2004; Lee *et al*. 2005; Alian *et al*. 2008).

Oxygen methylation can occur at either 2´ or 3´-hydroxyl groups of riboses, and Mg^{2+} appears to be important for coordinating the hydroxyl group for catalysis as observed for Class I catechol methyltransferase. However, the metal ion is not acting as a general base; instead a nearby lysine residue seems to deprotonate the substrate hydroxyl before attack by the SAM methyl group (Zheng and Bruice 1997).

1.5.2 Alternative Pathways to Methylation

Interestingly, not all methyltransferases utilize SAM the same way, or even at all. The radical SAM superfamily of enzymes includes some methyltransferases. These enzymes contain a characteristic [4Fe-4S] cluster coordinated by CX_3CX_2C motif with the fourth iron atom coordinated by bound SAM. The bacterial enzymes RlmN and Cfr, which methylate C_2 and C_8 respectively, of A2503 of 23S rRNA, utilize this mechanism. An active site non-cluster cysteine residue is methylated by the bound SAM. A second SAM substrate is then used to produce the 5´-deoxyadenosyl radical in order to activate the target for methyl group transfer from the methylated cysteine residue (Yan *et al*. 2010; Benítez- Páez *et al*. 2012; Shisler and Broderick 2012).

In Gram positive and some Gram negative bacteria, the conserved tRNA m^5U54 modification is formed by TrmFO, a folate/FAD-dependent methyltransferase (Urbonavičius *et al*. 2005; Yamagami *et al*. 2012). Similar to TrmA, TrmFO initiates catalysis through nucleophilic attack on U54 C_6 by a conserved thiol group. The C_5 carbon can then attack the methylene group of folate with the iminium ion acting as an electron sink. Proton abstraction from C_5 releases the covalent complex. The methylene group at C_5 is reduced by the oxidation of $FADH_2$ to FAD to form m^5U54. Finally, FAD is reduced to $FADH_2$ by NADPH to continue the cycle (Nishimasu *et al*. 2009).

1.5.3 tRNA m^5U Methyltransferase: TrmA

The near-universally conserved methylation of U54 in the T arm of tRNA is achieved through modification by members of the TrmA family (Trm2p in *S. cerevisiae*, TRMT2A in humans) (Ny and Björk 1980; Di Matteo *et al*. 1998; Nordlund *et al*. 2000). All

homologs belong to methyltransferase Class I and share many common features (Figure 1.5). Intriguingly, in Alpha- and Deltaproteobacteria, Cyanobacteria and Deinococci, a folate/FAD-dependent methyltransferase (TrmFO) is found instead of the SAM-dependent TrmA enzyme (Urbonavičius *et al*. 2005; Urbonavičius *et al*. 2007). In *Thermococcus* and *Pyrococcus* genera, both hyperthermophiles, 5-methyluridine is found at position 54, but is hypermodified to 2-thio-5-methyluridine, depending on growth temperature (Edmonds *et al*. 1991; Kowalak *et al*. 1994). Members of the *Methanococci* and *Halobacteria* classes have 1-methylpseudouridine at this position instead. The pseudouridylation is catalyzed by Pus10, whereas the methylation is completed by Class IV SAM-dependent methyltransferase TrmY (Gurha and Gupta 2008; Wurm *et al*. 2012).

In *E. coli*, point mutations in the *trmA* gene lead to a lack of m^5U54 formation *in vivo*, but the cells only show a mild reduction in growth rate (Björk and Isaksson 1970; Björk and Neidhardt 1975; Urbonavičius *et al*. 2007). In contrast, strains with an insertion relatively early in the *trmA* gene are nonviable (Persson *et al*. 1992). However, there is a *trmA* knockout strain available from the Keio collection that shows no growth phenotype which suggests that TrmA is not an essential protein as speculated previously (Baba *et al*. 2006). This is in agreement with findings in *S. cerevisiae*, where strains with either complete gene deletion or mutations within the TRM2 gene, are viable and exhibit no apparent phenotype (Hopper *et al*. 1982; Nordlund *et al*. 2000). Mutations in *S. cerevisiae* genes coding for tRNAs in combination with deletion of TRM2 induced lethality; however, the strains could be rescued by expression of a catalytically inactive Trm2p suggesting additional roles in tRNA maturation separate from m^5U formation (Johansson and Byström 2002). *E. coli* strains lacking m^5U in tRNA were outcompeted in

co-culture experiments suggesting a fitness advantage under non-ideal conditions (Björk and Neidhardt 1975).

The *E. coli* TrmA protein was first identified in 1962, and the gene was identified, cloned, and sequenced years later (Fleissner and Borek 1962; Gustafsson *et al*. 1991; Li *et al*. 1997). *E. coli* TrmA is a 42 kDa polypeptide and modifies all tRNAs in the cell (Greenberg and Dudock 1980). Several groups have reported that genomic-expressed *E. coli* TrmA can be purified with RNA as a higher molecular weight complex (Greenberg and Dudock 1980; Gu and Santi 1990; Gustafsson *et al*. 1991; Gustafsson and Björk 1993). Gustafsson *et al* (1993) identified that TrmA is in fact bound *in vivo* to two different RNA species: tRNA and a 3´-end fragment of 16S rRNA. Although the reason for the presence of these TrmA-RNA complexes is not known, it may be related to a secondary function of TrmA during RNA maturation as proposed previously (Persson *et al*. 1992; Johansson and Byström 2002). *E. coli* TrmA was overexpressed and purified without any bound RNA, but then crystallized in the presence of a 19-mer T-arm analog (Alian *et al*. 2008).

The catalytic mechanism of TrmA has been well studied (Santi and Hardy 1987; Kealey *et al*. 1991; Kealey and Santi 1991; Kealey *et al*. 1994). TrmA forms a covalent complex with tRNA via a Michael addition similar to thymidylate synthases (Lomax and Greenberg 1967; Armstrong and Diasio 1982). Methylation by TrmA begins with the thiol group of a catalytic cysteine attacking C_6 of U54 resulting in a nucleophilic centre at C_5. The methyl group from SAM is then transferred to C_5 with sulfur acting as an electron sink. Lastly, proton abstraction at C_5 by a basic residue (E358) releases the methylated product tRNA and TrmA via β-elimination (Kealey *et al*. 1991; Kealey and

Santi 1991; Kealey *et al*. 1994; Urbonavičius *et al*. 2007; Alian *et al*. 2008). The catalytic cysteine residue (C324) was identified by Kealey and Santi (1991) via isolation of a peptide fragment covalently bound to 5-fluorouracil substituted substrate tRNA and was later confirmed via site-directed mutagenesis (Urbonavičius *et al*. 2007). Substituting fluorine at position C_5 inhibits product release, but allows for methyl group transfer from SAM to the RNA. Kealey *et al* (1991) also demonstrated that methyl group transfer from SAM to C_5 occurs via a direct displacement reaction as shown by monitoring the stereochemistry of the methylated product RNA.

TrmA modifies position 54 in the T-arm of tRNA, but can modify T-arm analogs as short as 11 nucleotides; however, the 11-mer substrate had a reduction in k_{cat} of 20-fold and an increase in K_M of 6-fold compared to full-length substrate (Gu and Santi 1991). These findings suggest that the majority of recognition elements are contained in the T-arm stem loop, but the increase in catalytic efficiency and tighter binding of full length tRNA implies that other aspects of the structure of tRNA may be important for optimal activity. Analysis of all tRNA sequences in *E. coli* and T-arm nucleotide substitutions revealed that T-arm recognition is not sequence specific and requires only the presence of a 7-base loop structure closed by a CG base pair, as well as invariant positions U54, U55, and A58 (Gu and Santi 1991; Gu *et al*. 1996). Interestingly, TrmA can modify a 16S rRNA fragment *in vitro* as it shares the same consensus elements required for tRNA modification (Gu *et al*. 1994). However, the modified position U788 is not found to be modified *in vivo* (Madsen *et al*. 2003).

The crystal structure of TrmA bound to a 19 nucleotide T-arm analog revealed a similar substrate binding strategy as that observed in the rRNA m^5U methyltransferase RlmD

(Alian *et al*. 2008). In full-length mature tRNA, TrmA's target base U54 is buried inside the T loop, where it forms a reverse-Hoogsteen base pair with A58. TrmA flips U54 out of the loop into the active site, rotating bases G57 and A58 into the loop to form a nonsequential co-linear stack with G53, U55 and C56. This new base stacking is similar to the 23S rRNA substrate bases 1938-1942-1941-1940 when bound to RlmD. This refolding arrangement by these methyltransferases could be important for substrate selectivity (Lee *et al*. 2004; Lee *et al*. 2005; Alian *et al*. 2008).

1.6 Additional T-Arm Modifications

Although not present in *E. coli* tRNAs, A58 in the T-arm stem loop can be modified to 1-methyladenosine, which still forms the reverse-Hoogsteen base pair with U(m^5U)54. Methylation is completed by the SAM-dependent heterodimeric Trm6/Trm61 enzyme complex in *S. cerevisiae* and TrmI in eubacteria and archaea (Anderson *et al*. 1998; Droogmans *et al*. 2003; Roovers *et al*. 2004).

1.7 Variable Loop Modification Enzymes

While the focus of this study was on the modification of U54 and U55, tRNAs contain additional elbow region modifications as mentioned above. The methylation of G46 is catalyzed by the SAM-dependent Class I methyltransferase TrmB, forming 7-methylguanosine (m^7G) (De Bie *et al*. 2003). This modification occurs in the variable loop of 21 tRNA species in *E. coli* and forms a triple base interaction with C13 and G22 of the D-arm (Agris *et al*. 1986; Machnicka *et al*. 2012). In mature tRNA, this modification carries a positive charge possibly to alleviate the large concentration of negative charge surrounding the elbow region (Hurd and Reid 1979; Agris *et al*. 1986).

TrmB recognizes its target base through interactions with the T-arm and the size of the variable loop region, but does not require a full length tRNA substrate (Okamoto *et al*. 2004). The crystal structure of *E. coli* TrmB has been solved in the *apo* state, as well as bound to SAM and SAH, but not with an RNA substrate (Zhou *et al*. 2009). While the *E. coli* enzyme acts as a monomer, the *B. subtilis* protein functions as a homodimer (Zegers *et al*. 2006). Interestingly, in *S. cerevisiae* this modification is produced by the heterodimer complex Trm8-Trm82, with Trm8 containing the substrate binding and catalytic domains, whereas Trm82 functions to stabilize and promote the active conformation of Trm8 (Alexandrov *et al*. 2002). Similar to other modification enzyme knockout strains, *E. coli* lacking TrmB expression showed no growth phenotype compared to the wild type strain (De Bie *et al*. 2003). However, in *T. thermophilus*, this modification is required for cell viability at high temperatures, and the loss of TrmB resulted in tRNAs that were hypo-modified suggesting m^7G46 modification supports the introduction of other modifications critical for survival (Tomikawa *et al*. 2010).

In several *E. coli* tRNAs, 3-(3-amino-3-carboxypropyl)uridine is found at position 47 of the variable loop. Little is known about the incorporation of this modification into tRNA, but it has been shown that SAM serves as the propylamine donor during catalysis, although the enzyme responsible has yet to be identified (Nishimura *et al*. 1974). In humans and other eukaryotes, dihydrouridine (discussed below) is often found at this position in cytoplasmic tRNAs (Machnicka *et al*. 2012).

In *S. cerevisiae* and some thermophiles, 5-methylcytidine (m^5C) is found at position 48 or 49 of the variable loop in certain tRNAs. This modification is completed by the SAM-dependent methyltransferase Trm4 in both organisms (Motorin and Grosjean 1999;

Auxilien *et al*. 2007). Interestingly, when yeast are exposed to hydrogen peroxide, Trm4-mediated methylation of $tRNA^{Leu}$(CAA) at the wobble position increases, which causes selective translation of mRNA from genes enriched in the TTG codon, specifically ribosomal protein gene RPL22A (Chan *et al*. 2012). Though, how Trm4 changes its specificity to target the wobble position instead of the variable loop under oxidative stress is still unknown.

1.8 D-Arm Modification Enzymes

The formation of dihydrouridine (D) is abundant in tRNAs from all domains of life (Machnicka *et al*. 2012). The reduction of the C5-C6 double bond of specific uracil bases is catalyzed by the Dus family of enzymes. These flavin-dependent enzymes use NADH or NADPH to reduce their target uracil. NADH/NADPH bound to the enzyme transfers a hydride to the active site flavin prosthetic group, reducing the enzyme. The reduced enzyme then binds tRNA, and the target uracil is reduced, which then dissociates from the enzyme (Rider *et al*. 2009). In *E. coli*, DusA has been demonstrated to be specific for the modification of U20, whereas DusC is specific for U16. DusB has also been identified in *E. coli*; however its target has not been confirmed, but could either be U17 or U20a. Further, removal of all three Dus enzymes from *E. coli* did not result in an obvious growth phenotype, suggesting that the cellular role these modifications play is subtle under the conditions tested (Bishop *et al*. 2002; Byrne *et al*. 2015). Whereas pseudouridine modifications result in a local increase in RNA stability by rigidifying the RNA backbone, dihydrouridine modifications bring about a local increase in RNA flexibility. Instead of the typical C_3´-endo sugar conformation of A-type helical RNA, the

more flexible C_2'-endo conformation is preferred in RNAs with D modifications (Dalluge *et al*. 1996).

Modification of U8 to 4-thiouridine (s^4U) occurs in several prokaryotic tRNAs (Machnicka *et al*. 2012). In *E. coli*, two enzymes are required for catalysis: ThiI and IscS (Mueller *et al*. 1998; Kambampati and Lauhon 2000). IscS converts L-cysteine to L-alanine and sulfane sulfur, which is then sequentially transferred to ThiI and then tRNA in an ATP-dependent reaction. The minimal RNA substrate for ThiI activity was a 39 nucleotide truncated tRNA consisting of the acceptor-stem, a bulged loop, and the modified T-arm stem loop (Lauhon *et al*. 2004). The crystal structure of ThiI from *Thermotoga maritima* showed that RNA is mainly bound by the N-terminal ferredoxin-like domain and the THUMP domain of one subunit within the enzyme homodimer. This positions the target U8 base close to the catalytic centre in the pyrophosphatase domain of the other subunit. The tRNA 3´CCA end is recognized by the THUMP domain and acts as a molecular ruler specifying U8 for thiolation (Neumann *et al*. 2014). Unlike other tRNA modifications, the cellular role of 4-thiouridine has been established. When prokaryotes are exposed to near-UV light, a photochemically induced 2+2 cycloaddition occurs between s^4U8 and C13, which greatly reduces the ability of tRNA to interact with its aminoacyl synthetase (Favre *et al*. 1971; Bergstrom and Leonard 1972; Carre *et al*. 1974). This results in an arrest of bacterial growth in a manner similar to amino acid starvation (Ramabhadran and Jagger 1976).

Methylation of the 2´-hydroxyl group of guanosine (Gm) is found at position 18 in the D loop of 13 tRNA species in *E. coli* (Machnicka *et al*. 2012). Modification of G18 stabilizes the tertiary structure of tRNA by interacting with pseudouridine 55 in the T-

arm (Robertus *et al*. 1974). Enterobacteria also utilize Gm18 in tRNA to avoid detection by the host's immune system (Gehrig *et al*. 2012). The modification is introduced by class IV SAM-dependent methyltransferase TrmH in bacteria and archaea, and the homolog Trm3 in yeast (Persson *et al*. 1997; Hori *et al*. 1998; Cavaillé *et al*. 1999; Hori *et al*. 2002). Acting as a homodimer, TrmH will methylate D-stem loops of only 12 nucleotides and also has some flexibility on the target ribose, as it can methylate both G18 and G19 in *in vitro* transcripts (Hori *et al.* 1998). In mature tRNA, TrmH most likely utilizes the D-arm structure, conserved nucleotides in the elbow region, and an induced fit strategy to achieve target specificity (Ochi *et al*. 2010). In the *T. thermophiles* crystal structure, SAM is bound to one enzyme subunit while an arginine residue from the other subunit coordinates the phosphate and hydroxyl groups of G18 in the active site (Ochi *et al*. 2010).

1.9 Function of tRNA Elbow Modifications

It is expected that primary tRNA transcripts rapidly form the classic cloverleaf structure through Watson-Crick base pairing within the stem regions. Even without modifications, tRNA can fold into the canonical L shape structure observed in crystallography, but it always requires the presence of mono- or divalent cations to stabilize this conformation (Serebrov *et al*. 1998; Serebrov *et al*. 2001; Byrne *et al*. 2010). In fact, most unmodified tRNAs are functional in *in vitro* aminoacylation and translation experiments (Sampson and Uhlenbeck 1988; Harrington *et al*. 1993). The predominant, i.e. the most populated, conformation of tRNA is a direct result of both secondary and tertiary interactions, whereas modifications, specifically those within the elbow region, can directly affect the equilibrium between different conformations (folded, unfolded or misfolded). The

hydrogen bond network within the elbow region is complex (Figure 1.2). In brief, U8 (or s^4U8) forms a *trans* Watson-Crick/Hoogsteen base pair with the invariant A14, whereas a second *trans* Watson-Crick/Hoogsteen pair forms between T54 and A58 in the T loop. A *trans* Watson-Crick/Watson-Crick base pair occurs between semi-invariant positions R15 and Y48 and stacks with the U8:A14 base pair. Contacts between the D- and T-arms are maintained through the invariant G18G19 nucleotides of the D-loop and pseudouridine 55 and C56 in the T-loop. The G18:Ψ55 interaction occurs through hydrogen bonds between O4 of pseudouridine and N1 and N2 in G18. The G19:C56 interaction is a classic antiparallel *cis* Watson-Crick pair. In mature tRNA, the G18G19 segment interdigitates with R57A58, where R57 inserts itself between G18 and G19 of the D loop, and G18 intercalates between R57 and A58 (Holley *et al*. 1965; Klug *et al*. 1974; Robertus *et al*. 1974; Motorin and Helm 2010).

Formation of the canonical tertiary structure occurs rapidly in the presence of magnesium with both yeast and *E. coli* tRNAs folding within 2 ms (Stein and Crothers 1976; Serebrov *et al*. 2001). Melting of tRNA typically occurs in multiple steps with the first transition resulting from disruption of the tertiary interactions as well as the secondary interactions within the D-arm (Cole and Crothers 1972; Cole *et al*. 1972; Yang and Crothers 1972). Interestingly, Yang and Crothers found that the two *E. coli* tyrosine tRNA isoacceptors that differ by only two nucleotides in the variable region adopt a misfolded, non-cloverleaf state upon denaturation of tertiary interactions. Instead, four nucleotides in the variable region of $tRNA^{Tyr}$(I) base pair with the TΨC loop, whereas the variable loop of $tRNA^{Tyr}$(II) base pairs with the anticodon loop. These noncanonical interactions can prevent both of these tRNAs from properly forming their tertiary

interactions (Yang and Crothers 1972). The combined enthalpy for unfolding the tertiary and D stem of native *E. coli* $tRNA^{fMet}$ was found to be 52 kcal mol^{-1}, with tertiary interactions contributing approximately 30 kcal mol^{-1}. Complete unfolding of the molecule has an enthalpy of over 200 kcal mol^{-1} (Crothers *et al*. 1974). At the same magnesium concentration, unmodified yeast $tRNA^{Phe}$ has a melting temperature (T_m) almost 15°C lower than the native tRNA (Maglott *et al*. 1998). Taken together, tRNA modifications appear to play a critical role in overall stability and help drive the proper folding of tRNA in the cell. Some studies have also suggested that modifications may play an active role in shaping tRNA during maturation. Human mitochondrial $tRNA^{Lys}$ is unable to fold into the characteristic cloverleaf conformation when it lacks the m^1A9 modification (Helm *et al*. 1998).

The modifications in the anticodon loop have been shown to be important in reading frame maintenance, recognition by aminoacyl-tRNA synthetases, and expanding tRNA decoding capacity (Agris *et al*. 2007; Ranjan and Rodnina 2016). As discussed above, modifications within the elbow region of tRNA tend to serve a structural role rather than a functional one, acting to stabilize tertiary interactions between the variable, D- and T-arm stem loops. The loss of any one elbow modification typically does not result in a growth defect (Björk and Neidhardt 1975; Persson *et al*. 1997; Raychaudhuri *et al*. 1999; Gutgsell *et al*. 2000; Bishop *et al*. 2002; De Bie *et al*. 2003). In thermophilic eubacteria and archaea m^5U54 is further modified to 5-methyl-2-thiouridine (m^5s^2U) which increases the thermostability of the T-arm (Watanabe *et al*. 1976). In contrast, psychrophilic bacteria have increased levels of dihydrouridine modifications as these increase local flexibility, but an overall decrease in tRNA modifications compared to

mesophiles and thermophiles (Dalluge *et al*. 1997). In *E. coli,* loss of Gm18, m^5U54 and Ψ55 results in a reduced growth rate, especially at high temperatures, and an increase in frameshift errors (Kinghorn *et al*. 2002; Urbonavičius *et al*. 2002). Lack of the modifications formed by Pus1 (Ψ26-28, Ψ34, Ψ36, Ψ65) become essential when Pus4 (Ψ55), or the essential minor $tRNA^{Glu}$ are mutated in *S. cerevisiae* (Großhans *et al*. 2001). Deletion of pseudouridine synthase TruB (Ψ55) in the hyperthermophile *Thermus thermophilus* resulted in a severe growth defect at 50°C. It was found that along with missing Ψ55, levels of Gm18, m^5s^2U54 and m^1A58 in tRNA were abnormally increased, which resulted in an increase in the melting temperature of the tRNA and suggests that the tRNA structure may be too rigid to function properly at 50°C, and Ψ55 acts to ensure tRNA is not hypermodified at low temperatures (Ishida *et al*. 2011). A growth defect at high temperatures was observed for *T. thermophilus* when TrmB was deleted leading to impaired m^7G46 synthesis in tRNA, suggesting this modification is critical for survival at elevated temperatures. In addition to the lack of m^7G46, the presence of Ψ, m^2G, m^5U, m^6A, and m^1G were also decreased in tRNA. Together these findings suggest that there is a tRNA modification network, where m^7G46 has a positive effect on other modifications in this organism (Tomikawa *et al*. 2010).

Although tRNA modifications may be important for tRNA maturation and stability in and of themselves, it may also be valuable to express the modification enzymes responsible. *E. coli* strains lacking pseudouridine 55 synthase TruB are out-competed in co-culture assays by the wild type strain. However, it was demonstrated that it is not the formation of pseudouridine 55 in tRNA that provides this fitness advantage since expression of a catalytically inactive TruB variant could rescue this phenotype (Gutgsell *et al*. 2000;

Kinghorn *et al*. 2002). It was proposed that TruB could be functioning as an RNA chaperone in the cell, assisting in the correct folding of tRNA regardless of pseudouridine formation. RNA chaperones are not uncommon and are found throughout all domains of life. Hfq is an RNA binding protein found in bacteria and plays a role in the biogenesis of small noncoding RNAs (ncRNAs) by helping them identify their target mRNA during stress responses. Recently it has been proposed that Hfq may also play a role in tRNA maturation, binding to the elbow region of the tRNA (Lee and Feig 2008). The possibility exists that enzymes that modify tRNA, and thus have to bind to tRNA, are acting as tRNA chaperones *in vivo* and should be investigated.

1.10 tRNA Modifications and Disease

tRNA plays a critical role in the cell, therefore any mutations within genes associated with tRNA biosynthesis or the tRNA itself can give rise to severe functional abnormalities. Mutations in tRNA modification enzymes can result in neurological disorders. The human homolog of yeast TRM7, FtsJ, acts as a 2´-*O*-methyltransferase targeting positions 32 and 34 of $tRNA^{Leu}$, $tRNA^{Phe}$, and $tRNA^{Trp}$ (Feder *et al*. 2003). Mutations in the FtsJ gene result in nonsense-mediated mRNA decay and lead to a decrease in cognitive function (Freude *et al*. 2004). NSun2, which catalyzes the formation of 5-methylcytosine at position 34 of $tRNA^{Leu}$(CCA), as well as at positions 48, 49, and 50 in several tRNAs is linked to both intellectual disabilities and cancer (Frye and Watt 2006; Abbasi-Mohed *et al*. 2012; Khan *et al*. 2012; Hussain *et al*. 2013). Methyltransferase TRMT12, homolog of yeast Trm12, is part of the modification pathway for the formation of wybutosine 37 in $tRNA^{Phe}$ and has increased gene expression in breast cancer cell lines and tumors (Rodriguez *et al*. 2007). Overexpression

of TRMT2A, another methyltransferase, which targets U54 in the T-arm, correlates with an increase in cancer recurrence in HER2+ patients (Hicks *et al*. 2010). Links to the development of type 2 diabetes in mice has also been proposed for CDKAL1, which encodes a methylthiotransferase involved in the production of the hypermodified complex 2-methylthio-N6-threonyl carbamoyladenosine modification at position 37 in $tRNA^{Lys}$(UUU) (Wei *et al*. 2011). Mitochondrial disease can also arise from aberrant defects in tRNA modifications within the mitochondria. Mitochondrial myopathy, encephalopathy, lactic acidosis, and stroke-like episodes (MELAS) and myoclonus epilepdy associated with ragged-red fibers (MERRF) are two conditions that result from hypomodification of uridine 34 in mitochondrial tRNAs (Suzuki and Nagao 2011).

In some cases it has been reported that the lack of these modifications leads to unstable tRNA transcripts that are then degraded resulting in a decrease in certain tRNA species (Freude *et al*. 2004). Modifications in the anticodon loop, particularly at the wobble position, can result in the misreading of mRNA codons (Suzuki and Nagao 2011). Specific tRNA modifications enzymes are important during development. In particular it was previously demonstrated that *FTSJ* was expressed higher in fetal brain tissue, whereas in adults the expression was reduced in the brain, but higher in the heart and liver (Freude *et al*. 2004; Ramser *et al*. 2004). These findings indicate that *FTSJ1* expression in the developing brain is critical for normal development, but its role in adults is still undefined. Mutations in the elongator complex have been implicated in familial dysautonomia, and patients lack 5-methyoxycarbonylmethyluridine and 5-carbamoylmethyluridine in tRNA. This disease primarily affects neurons of the autoimmune system, resulting in the absence of sensory neurons and leads to premature

death. In neurons, a donor splice site in the elongator complex component *IKBKAP* gene leads to exon skipping and an introduction of an early stop codon and a decrease in tRNA modification. However in non-neuronal tissues, the low levels of wild type IKAP are sufficient to ensure cell survival. Animal models have suggested that the reason why sensory neurons are affected may be a combination of neurons being more sensitive than other cell types to perturbations in tRNA modification levels (Sarin and Leidel 2015). Several questions remain as to how aberrant tRNA modifications and mutant tRNA modification enzymes impact human health. In particular, are tRNA modifications involved in other complex human disorders that are currently unknown, and are the predicted human tRNA modification enzymes indeed carrying out their predicted role on tRNAs? Are aspects of the pathology tissue specificity due to expression of tRNA targets, modification enzymes, splicing differences, protein/RNA turnover, or metabolite levels? How does tRNA abundance, codon usage, or GC content contribute to the disorder? Abnormal RNA modification pathways may reroute metabolites and indirectly affect other pathways. Translation is most likely affected in many cases. Codon specific translation defects may lead to decreased production of individual proteins that are cell specific or required under stress conditions. Further analysis of human disorders and animal models is required to find the answers to these questions.

1.11 tRNA Degradation

Transfer RNA molecules are among the most stable RNAs in a cell, with half lives of several days (Phizicky 2010). This longevity is most likely due to the compact, highly folded structure and level of modification found within tRNAs. The degradation pathway of tRNA in bacteria is less well known compared to eukaryotes, but similarly changes

that affect tRNA stability or folding result in tRNA degradation in bacteria. Loss of ions due to altered membrane permeability results in a decrease in tRNA and rRNA stability and digestion by RNase I (Deutscher 2003). Additionally, precursor tRNAs that do not fold properly are polyadenylated and then degraded by PNPase and RNase R (Li *et al*. 2002; Chen and Deutscher 2005). In *E. coli*, colicin E5 and D cleave the anticodon loop of specific tRNAs and result in an arrest of protein synthesis (Masaki and Ogawa 2002). In eukaryotes, two tRNA turnover pathways have been reported that can act at the level of precursor or mature tRNA species. The first pathway involves the TRAMP complex and the nuclear exosome, whereas the second pathway utilizes cytoplasmic exonucleases. Cleavage of tRNAs can result in half tRNAs or shorter tRNA fragments of 15-25 nucleotides that can act to inhibit translation, induce RNA silencing or apoptosis (Megel *et al*. 2015).

The nuclear surveillance pathway was first identified in temperature-sensitive yeast strains lacking Trm6 or Trm61, the two subunits of the m^1A58 methyltransferase complex (Anderson *et al*. 1998; Anderson *et al*. 2000). It was shown that the lack of m^1A58 leads to rapid turnover of initiator $tRNA^{Met}$. The precursor tRNA lacking this modification is polyadenylated at its 3´ end by the TRAMP complex, specifically by Trf4, a poly(A) polymerase. The polyadenylated transcript is then degraded from the 3´ end by Rrp6, the 3´ exoribonuclease of the nuclear exosome (Kadaba *et al*. 2004; Kadaba *et al*. 2006). Atypical 3´ end maturation of pre-tRNAs can also lead to degradation by the TRAMP complex (Copela *et al*. 2008).

The rapid tRNA decay pathway was also identified in yeast strains lacking enzymes involved in tRNA modification. *S. cerevisiae* strains lacking both Trm8 and Trm4 show a

severe growth defect at high temperatures due to rapid degradation of $tRNA^{Val}$(AAC), which is deficient in 7-methylguanosine and 5-methylcytidine modifications (Alexandrov *et al*. 2006). This rapid tRNA degradation process was shown in yeast strains lacking a number of different tRNA modification enzymes, and it was therefore hypothesized that under normal conditions most tRNAs do fold correctly and are functional. However, under non-ideal conditions, such as increased temperature, the hypomodified tRNAs are destabilized and trigger this degradation pathway. However, it is not necessarily the modifications themselves, but the overall stability of the tRNA itself that triggers decay as fully mature tRNAs are also degraded by this pathway (Whipple *et al*. 2011). Unlike the nuclear surveillance pathway, rapid tRNA decay does not require the TRAMP complex for degradation. Instead two 5´-3´ exonucleases Rat1 and Xrn1 are implicated in this process (Chernyakov *et al*. 2008).

Once RNA is digested to individual nucleotides, they can be broken down further into their basic components. Purine derivatives GMP and AMP are eventually converted to xanthine, which in turn is oxidized to form uric acid. Alternatively both guanine and the adenine byproduct hypoxanthine can be recycled back to form GTP and ATP for further nucleic acid synthesis or other cellular processes. Pyrimidine catabolism results in cytosine, thymine and most uridine derivatives being converted to methylmalonyl-semialdehyde and finally to succinyl-CoA (Howland 1990). In bacteria, uracil can be directly converted to UMP by phosphoribosyltransferase or to uridine by uridine phosphorylase. Free cytidine can be converted to CMP via similar mechanism (Nyhan 2001; Nelson and Cox 2005). Modified nucleotides most likely undergo similar mechanisms of catabolism. Pseudouridine in *E. coli* was shown to be phosphorylated to

pseudouridine 5´-phosphate by YeiC, which is subsequently hydrolyzed to D-ribose-5-phosphate and uracil by YeiN. This enzyme has the unique ability to hydrolyze the C-C glycosidic bond of pseudouridine (Preumont *et al*. 2008; Thapa *et al*. 2014). In humans with malignancies, modified nucleosides are excreted in abnormal amounts in the urine and could potentially be used as a marker to test for tumors (Seidel *et al*. 2006).

1.12 RNA folding by RNA chaperones

RNA chaperones have been defined as proteins that aid in the process of RNA folding by preventing misfolding or by resolving misfolded species (Rajkowitsch *et al*. 2007). Some classical examples are bacterial Hfq, the S12 protein and the eukaryotic La protein. Hfq binds to many small noncoding RNAs (ncRNAs) in *E. coli* and assists in gene regulation by helping these ncRNAs identify and bind to their mRNA targets (Massé and Gottesmann 2002). The ncRNAs bind to the proximal surface of the homohexameric ring, whereas the poly(A) sequence of the target mRNA interacts with the distal face. Interestingly, Hfq has also been found to bind to tRNAs through the tRNA elbow region and may coordinate tRNA modification (Lee and Feig 2008). The *E. coli* S12 ribosomal protein facilitates proper folding of group I introns *in vivo* through nonspecific binding, but is only required for folding and not the catalytic step, thus acting as an RNA chaperone (Coetzee *et al*. 1994; Clodi *et al*. 1999). In eukaryotes, the nuclear La protein mainly binds to newly synthesized small RNAs, including tRNAs, pre-5S rRNA, U6 snRNA and 7SL RNA. Binding by the La protein protects the 3′ ends of these RNAs from exonuclease digestion, and La-mediated stabilization is required for the normal biogenesis of pre-tRNA, while also facilitating the assembly of small RNAs into functional RNP complexes (Wolin and Cedervall 2002). In yeast, La has also been shown

to be required for efficient folding of certain pre-tRNAs (Chakshusmathi *et al*. 2003). All of these RNA chaperones share the common features of binding RNAs nonspecifically and helping to fold or stabilize RNA conformations. Based on these findings the involvement of RNA chaperones in tRNA folding *in vivo* cannot be excluded evan though tRNAs are typically assumed to fold independently, in particular when studied *in vitro*.

Chapter 2 -
Objectives

The life cycle of a tRNA is a multifaceted process, and it is the subtle differences in tRNA sequence and structure that allow it to function in the cell. Although all tRNAs are composed of the same four nucleotides, it is the minute differences in sequence or their modification pattern that differentiate them from one another. Subtle aberrant changes to tRNA can result in misaminoacylation, decoding of noncognate codons, or degradation (Urbonavičius *et al*. 2002; Alexandrov *et al*. 2006; Agris *et al*. 2007; Ranjan and Rodnina 2016). Therefore, accurate tRNA biosynthesis is essential for cellular fitness and involves a multitude of proteins interacting with tRNA.

To gain a better understanding of this process and the role modifying enzymes play in tRNA biogenesis, it is the objective of this thesis to analyze two highly conserved tRNA modifying enzymes: TruB and TrmA. Both enzymes have homologs in almost all organisms and their respective modifications are found across all domains of life (Ny and Björk 1980; Nurse *et al*. 1995; Di Matteo *et al*. 1998; Nordlund *et al*. 2000; McCleverty *et al*. 2007; Gurha and Gupta 2008; Urbonavičius *et al*. 2008). Whereas this conservation across evolution would suggest a critical role for these modifications in the cell, neither is essential for growth (Björk and Neidhardt 1975; Gutgsell *et al*. 2000; Kinghorn *et al*. 2002; Urbonavičius *et al*. 2007). Conversely, lack of either modification can lead to a decrease in cellular fitness in co-culture. Ofengand and coworkers demonstrated that it is the modifying enzyme TruB itself, and not the resulting tRNA modification, that is indispensable for conveying a cellular advantage (Björk and Neidhardt 1975; Gutgsell *et al*. 2000; Kinghorn *et al*. 2002; Urbonavičius *et al*. 2007). Consequently already in 2000, TruB (and possibly other tRNA modification enzymes) was speculated to be an RNA chaperone *in vivo*.

Based on these earlier findings, I hypothesized that TruB is indeed an RNA chaperone and that this activity of TruB provides a fitness advantage. I will test this hypothesis *in vitro* and *in vivo* by assessing the impact of TruB on tRNA folding and aminoacylation as well as by analyzing the importance of tRNA binding by TruB for cellular fitness and TruB's role as a tRNA chaperone. Second, I will analyze the mechanism by which TruB gains access to its target uridine and provide a detailed kinetic mechanism of pseudouridine formation to gain a better understanding of tRNA folding/conformational changes facilitated by TruB. It is known that TruB binds to its target tRNA substrates by disrupting the elbow region tertiary interactions and flipping U55 into the active site of the enzyme as observed via crystallography (Hoang and Ferre-D'Amare 2001). However, this structure only shows TruB bound to a small T-arm analog and not full-length tRNA. Additionally, it has been suggested that TruB binds to the tRNA acceptor stem through interactions with its C-terminal PUA domain (Pan *et al*. 2003). Therefore, I will investigate the role of the PUA domain for substrate binding and catalysis, as well as TruB's proposed chaperone activity.

In addition, 5-methyluridine formation by TrmA will be investigated as the first step towards establishing whether TrmA could serve a similar RNA chaperone function *in vivo*. TrmA binds tRNA and SAM within the same active site and in close proximity (Alian *et al*. 2008). I will determine if this binding is cooperative and calculate the dissociation constants for initial substrate binding and covalent bond formation. Towards assessing whether TrmA has the potential of acting as a tRNA chaperone, I first need to analyze tRNA binding by TrmA in order to understand how TrmA may gain access to its buried target uridine by disrupting D- and T-arm interactions within the full-length

tRNA. Therefore, I will investigate the function of TrmA residues in different domains of the enzyme for tRNA binding and catalysis of methylation.

In summary, this thesis aims to answer the following questions:

1. TruB
    a. Is TruB an RNA chaperone?
    b. How does TruB gain access to its target base and how does this relate to TruB's chaperone activity?
    c. What is the function of TruB's PUA domain?
2. TrmA
    a. How does TrmA bind to its ligands and is it a cooperative process?
    b. How does TrmA gain access to its target base and what role does the "RNA binding" domain play?

Together, the studies described here will advance our knowledge of the mechanism and function of tRNA modification by universally conserved enzymes targeting the T arm of all tRNAs. This research will thereby contribute to our understanding of why tRNAs are so highly modified and why all cells invest significant energy in fine-tuning the chemical composition of tRNAs.

Chapter 3 – TruB is a tRNA Chaperone

A version of this chapter has been submitted as a manuscript for publication. The manuscript has been prepared jointly by Laura Keffer-Wilkes and Ute Kothe.

3.1 Introduction

While there is a wealth of information on RNA structure, we are just beginning to understand the RNA folding process which is often assisted by RNA chaperones (Rajkowitsch *et al*. 2007). In contrast to many protein chaperones, RNA chaperones are not ATPases, but instead facilitate unfolding and folding of RNA directly through their interactions with RNA. In addition, the vast majority of all RNAs, including mRNAs, are post-transcriptionally modified by a plethora of RNA modification enzymes (Machnicka *et al*. 2013). Very little is known about the interplay of RNA folding and modification, although it has been speculated that RNA modification enzymes may also act as RNA chaperones (Ishitani *et al*. 2008).

Despite the abundance of RNA modifications, their cellular functions are often unclear including their possible contributions to RNA structure and stability (Charette and Gray 2000). Interestingly, very few RNA modification enzymes are essential for the cell; however many of these enzymes are conserved. The most abundant RNA modification is the conversion of uridines to pseudouridines that are found in almost all cellular RNAs (Charette and Gray 2000; Carlile *et al*. 2014; Schwartz *et al*. 2014). Pseudouridine formation is catalyzed by stand-alone pseudouridine synthases in all domains of life. Additionally, pseudouridines are generated by H/ACA small ribonucleoproteins (H/ACA sRNPs) in eukaryotes and archaea (Hamma and Ferré-D'Amaré 2006). Remarkably, the only essential pseudouridine synthase is the eukaryotic enzyme Cbf5, the catalytic component of H/ACA sRNPs, whereas all known stand-alone pseudouridine synthases are non-essential (Kiss *et al*. 2010). Indeed, deletion of most stand-alone pseudouridine

synthases in *E. coli* (Gutgsell *et al*. 2000; Del Campo *et al*. 2001) or *Saccharomyces cerevisiae* (King and Lu 2014) does not impact cell growth under optimal conditions. Surprisingly, even an *S. cerevisiae* strain is viable that is expressing only a Cbf5 variant that is catalytically inactive, raising the question why cells invest so much energy into seemingly dispensable pseudouridine formation (Zebarjadian *et al*. 1999).

Here, we utilize the pseudouridine synthase TruB as a model enzyme to identify the cellular function and mechanism of pseudouridine synthases. *E. coli* TruB catalyzes the modification of U55 in the TΨC arm of all elongator tRNAs (Nurse *et al*. 1995) and is the homologue of the eukaryotic pseudouridine synthase Pus4 that modifies both tRNAs and mRNAs (Becker *et al*. 1997; Carlile *et al*. 2014; Schwartz *et al*. 2014). Several crystal structures of TruB bound to a TΨC arm fragment have revealed that TruB gains access to the target base by flipping three nucleobases (positions 55-57) out of the T loop and into the active site (Hoang and Ferre-D'Amare 2001; Pan *et al*. 2003). Superimposing the T-arm bound to TruB onto full-length tRNA indicates that tRNA binding by TruB disrupts the tertiary interactions between the T- and D-arm of tRNA. Kinetic studies in our lab have shown that tRNA binds quickly to TruB, but that catalysis of pseudouridine formation is surprisingly slow and rate-limiting (Wright *et al*. 2011). In fact, slow catalysis is a hallmark of all pseudouridine synthases studied in detail thus far (Wright *et al*. 2011; Kamalampeta and Kothe 2012; Kamalampeta *et al*. 2013). Deleting the *E.coli truB* gene does not impact growth under optimal conditions (Gutgsell *et al*. 2000). However, the pseudouridylation activity of TruB is important for temperature adaptation in *E.coli* (Kinghorn *et al*. 2002) and *Thermus thermophiles* (Ishida *et al*. 2011). *truB* knockout strains are outcompeted by wild type *E. coli* in co-culture at 37°C indicating

that TruB does contribute to bacterial fitness (Gutgsell *et al*. 2000). Surprisingly this fitness disadvantage of the *truB* knockout strain can be rescued by expressing a catalytically inactive variant of TruB (Gutgsell *et al*. 2000; Kinghorn *et al*. 2002). This finding suggests that the presence of the TruB protein itself is important for the cell, rather than pseudouridines that are formed by TruB. Therefore, Ofengand and coworkers speculated more than a decade ago that TruB might act as an RNA chaperone that facilitates tRNA folding (Gutgsell *et al*. 2000); however this hypothesis has not been experimentally tested.

3.2 Materials and Methods

3.2.1 Buffers and reagents

TAKEM$_4$ buffer: 50 mM Tris-HCl, pH 7.5, 70 mM NH_4Cl, 30 mM KCl, 1 mM EDTA, and 4 mM $MgCl_2$. [5-^{3}H]UTP was purchased from Moravek. T4 RNA ligase was purchased from New England Biolabs. All other enzymes and chemicals were obtained from Fermentas (Fisher Scientific). 2-aminopurine (2AP)-labeled 3′-half tRNA was purchased from Dharmacon.

3.2.2 Protein expression and purification

QuikChange® site-directed mutagenesis was used to mutate the *Escherichia coli* TruB protein coding region in the pET28a-EcTruB plasmid in order to encode the single amino acid substitutions R40E, K64E, K130E, and K176E (Table 3.1; Figure 3.1) (Wright *et al*. 2011). Two tandem stop codons were introduced at positions D244 and S245 to remove the C-terminal PUA domain. All proteins were expressed and purified as previously described using Ni^{2+}-affinity and size-exclusion chromatography (Wright *et al*. 2011).

Table 3.1. Primers used in TruB study. The first set of primers is used to generate full-length or 5′ half $tRNA^{Phe}$ whereas the second set of primers were used for site-directed mutagenesis of the *truB* gene.

Primer Name	Sequence
T7 promoter (tRNA – pCF0)	5′ – GCTGCAGTAATACGACTCACTATAG – 3′
Eco $tRNA^{Phe}$ antisense	5′ – mUmGGTGCCCGGACTCG – 3′
5′ half sense $tRNA^{Phe}$	5′ – GCGTAATACGACTCACTATAGCGCGGATAGCTCAGTCG – 3′
5′ half antisense $tRNA^{Phe}$	5′ – TCAATCCCCTGCTCTACCGACTGAGCTATCCG – 3′
5′ T7 shortened	5′ – GCGTAATACGACTCACTATAG – 3′
5′ half $tRNA^{Phe}$ antisense	5′ – mUmCAATCCCCTGCTCTACCGAC – 3′
TruBnoPUA sense	5′ – GCCAATGGACAGTCCAGCTTAGTAGTACCCGGGGGTGAATCTTCC GTT – 3′
TruBnoPUA antisense	5′ – AACGGAAGATTCACCCCCGGGTACTACTAAGCTGGACTGTCCATT GGC – 3′
TruBR40E sense	5′ – CGTATATATAACGCCAACGAGGCCGGGCATACGGGTGCGCTGG – 3′
TruBR40E antisense	5′ – CCAGCGCACCCGTATGCCCGGCCTCGTTGGCGTTATATATACG – 3′
TruBK64E sense	5′ – GCCGATTTGCCTGGGGGAAGCGACGGAGTTTTCCCAG – 3′
TruBK64E antisense	5′ – CTGGGAAAACTCCGTCGCTTCCCCCAGGCAAATCGGC – 3′
TruBK130E sense	5′ – CCCTTCGATGTATTCAGCACTCGAGTATCAGGGCAAAAAACTGTACG – 3′
TruBK130E antisense	5′ – CGTACAGTTTTTTGCCCTGATACTCGAGTGCTGAATACATCGAA GGG – 3′
TruBK176E sense	5′ – GGAGCTGGAAATTCACTGCAGCGAAGGCACTTATATCCGCACCATC – 3′
TruBK176E antisense	5′ – GATGGTGCGGATATAAGTGCCTTCGCTGCAGTGAATTTCCAGCTCC – 3′
$tRNA^{Phe}$ RT primer	5′ – TGGTGCCCGGACTCGG – 3′

Final protein preparations were >90% pure as judged by SDS-PAGE and were RNA free as determined by A_{260} and urea-PAGE analysis. Circular dichroism spectra of each TruB variant revealed no differences between the wild type and mutant enzymes (Figure 3.1).

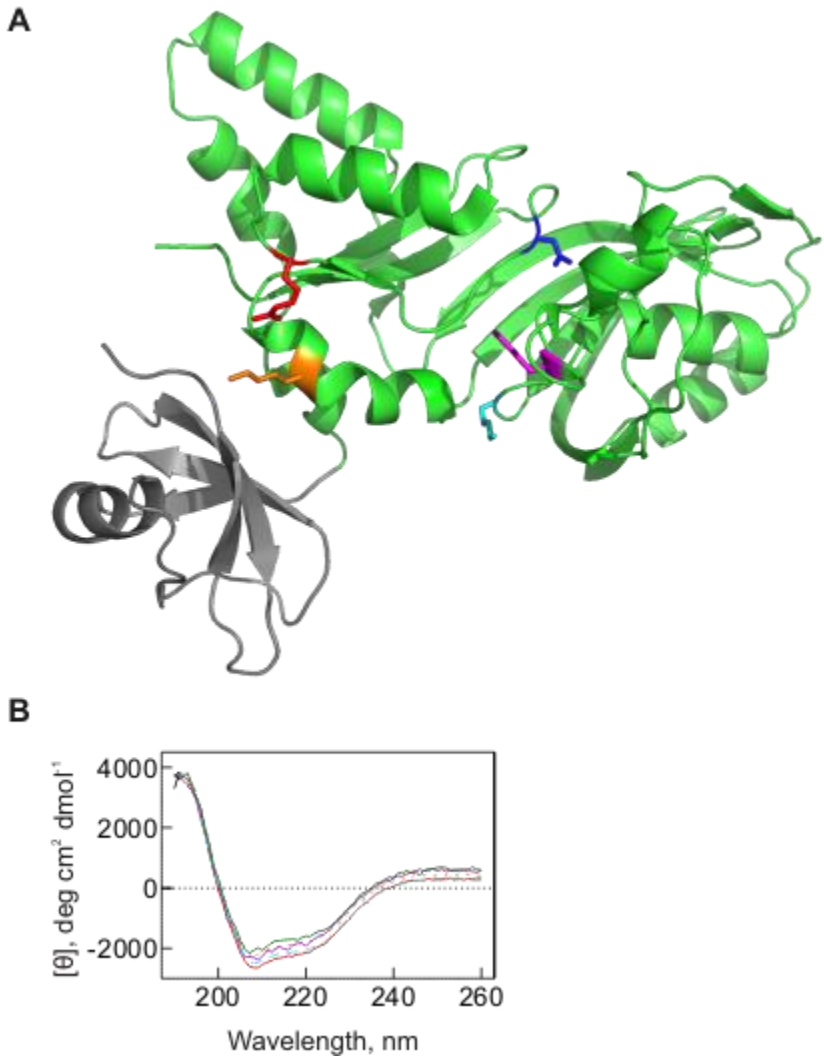

Figure 3.1. Preparation of TruB variants impaired in tRNA binding. A) The basic residues R40 (red), K64 (orange), K130 (purple), and K176 (cyan) were substituted with glutamate to impair tRNA binding to TruB. The catalytic residue D48 (dark blue) is also depicted whereas the C-terminal pseudouridine synthase and archeosine transglycosylase (PUA) domain is shown in grey. The figure was generated with PyMOL using PDBID: 1K8W (Hoang and Ferre-D'Amare 2001). B) Circular dichroism spectra of TruB variants. Proteins were diluted to 1 µM with 50 mM sodium phosphate buffer: TruB wild type (green solid line), TruB R40E (red solid line), TruB K64E (orange dotted line), TruB K130E (purple solid line), and TruB K176E (turquoise dotted line).

3.2.3 Measuring tRNA folding by aminoacylation

This method was adapted from Bhaskaran *et al*. (2012). $TAKEM_4$ buffer was used throughout the experiment. First, *in vitro* transcribed $tRNA^{Phe}$ was unfolded at 65°C as described previously, but was then immediately added to precooled 0°C reaction buffer containing 6 mM ATP, 1 mM DTT, 3 mM inorganic pyrophosphatase, 3 mM phosphoenolpyruvate, and 1% pyruvate kinase. The tRNA (680 nM) was allowed to refold at 0°C for 0, 2, 5, or 20 minutes in the absence or presence of 200 nM TruB, TruB D48N, TruB K64E, or TruBΔPUA. Following tRNA folding, [^{14}C]Phe and Phe-$tRNA^{Phe}$ synthetase were added to the reaction mixture to final concentrations of 40 µM and 20 µM, respectively. 10 µL samples taken at different times from the aminoacylation reaction were spotted onto 5% TCA presoaked Whatman paper disks. Disks were allowed to dry, then washed 3 times with 5% TCA and finally with 100% ethanol to remove free [^{14}C]Phe. Following a final drying step at 65°C, the amount of [^{14}C]Phe-$tRNA^{Phe}$ on the disks was quantified via scintillation counting. The aminoacylation time courses were fit with a single exponential function to determine the initial level of instantaneously aminoacylated tRNA (Y_0):

$$Y = Y_0 + (Y_{max} - Y_0)\,(1 - exp(-k \times t))$$

The initial level of folded and aminoacylated tRNA was then plotted against folding time. The resulting time courses were fit with the same exponential equation to obtain the rate of folding.

3.2.4 2AP-tRNA preparation

Full-length 2AP-labeled $tRNA^{Phe}$ was created by annealing two halves of the tRNA and ligating using T4 RNA ligase as described before (Friedt *et al*. 2014). The 5′-half tRNA was *in vitro* transcribed and the 3′-half was purchased from Dharmacon with 2-aminopurine at position 57.

3.2.5 Fluorescence spectroscopy and stopped-flow experiments

Equilibrium binding measurements were completed with 200 nM 2AP-tRNA in 1× $TAKEM_4$ buffer. 2AP was excited at 315 nm and the emission was measured from 340 to 400 nm at 5°C. The catalytic inactive variant TruB D48N (Wright *et al*. 2011) was titrated into the 2AP-tRNA and the resulting fluorescence changes were recorded after each addition of enzyme using a Quanta Master 60 fluorescence spectrometer (Photon Technology International). Similarly, TruB D48N was titrated into buffer alone, and the measured fluorescence intensity was subtracted from the titration with 2AP-tRNA. The concentration dependence of the relative fluorescence change at 365 nm was fitted with a hyperbolic function to determine the dissociation constant (K_D):

$$Y = B_{max} \times [protein] / (K_D + [protein])$$

Pre-steady state rapid kinetics binding experiments were completed using a KinTek SF-2004 stopped-flow apparatus. 2AP-tRNA (final concentration 0.3 µM) was rapidly mixed with TruB variants and excited at 325 nm at 20°C or 5°C. The resulting emission was monitored at wavelengths greater than 350 nm using a long-pass cut-off filter. Time courses at 20°C were fitted with a three-exponential function:

$$F = F_{max} + Amp1 \times \exp(-k_{app1} \times t) + Amp2 \times \exp(-k_{app2} \times t) + Amp3 \times \exp(-k_{app3} \times t)$$

where F_{max} is the fluorescence end level; *Amp* is the respective amplitude change of the fluorescence signal for each phase; *t* is time; and k_{app} represents the apparent rate for each respective phase (1 – initial binding, 2 – tRNA conformational change, and 3 – tRNA release that is rate-limited by pseudouridine formation, see results). At 5°C, only the two phases of fluorescence increase were observed within the first 20s; a subsequent slow fluorescence decrease was recorded, but it was difficult to distinguish it from photobleaching. Therefore, time courses with TruB wt at 5°C were fitted with a two-exponential function:

$$F = F_{max} + Amp1 \times \exp(-k_{app1} \times t) + Amp2 \times \exp(-k_{app2} \times t)$$

In order to determine the rate constants k_1 and k_{-1}, k_{app1} was plotted against the concentration of TruB and the resulting graph was fit to the following linear function:

$$k_{app1} = k_{-1} + k_1 \times [\text{TruB}]$$

To measure 2AP-tRNA dissociation, TruB variants were allowed to form a complex with 2AP-tRNA for 10 minutes at 37°C. This solution (2 µM TruB and 0.3 µM 2AP-tRNA after mixing) was then rapidly mixed with an excess of unlabeled tRNA (final concentration 8 µM) in the stopped-flow at both 5°C and 20°C. The data were fitted with a single-exponential function where the apparent rate corresponds to the rate constants k_{-2} for catalytically inactive TruB D48N and to $k_{release}$ for catalytically active TruB wild type. The tRNA conformational change is the second, slower step in a two-step equilibrium, (Fersht 1998) and therefore k_2 can be determined from k_{-2} and k_{app2} according to the equation

$$k_{app2} = k_{max} = k_2 + k_{-2}$$

3.2.6 [^{3}H]-labeled tRNA preparation

The *E. coli* $tRNA^{Phe}$ gene was PCR amplified from the pCF0 plasmid for *in vitro* transcription with 100 µM [5-^{3}H]UTP followed by purification with a Nucleobond PC100 column (Macherey-Nagel) as described previously (Wright *et al*. 2011).

3.2.7 Nitrocellulose membrane filter binding

10 nM [^{3}H]tRNA was incubated with increasing concentrations of TruB for 10 min at room temperature before filtering through a nitrocellulose membrane. The amount of [^{3}H]tRNA bound to TruB was determined by scintillation counting as described previously (Wright *et al*. 2011).

3.2.8 Tritium release assay

Tritium-labeled tRNA was refolded in 1× $TAKEM_4$, mixed with pre-warmed TruB and the amount of released tritium corresponding to the amount of pseudouridine formation was determined as described previously (Wright *et al*. 2011). Single-turnover experiments were analyzed by fitting with a single-exponential function:

$$Y = Y_{max} + Amp \times \exp(-k_{\psi} \times t)$$

yielding the apparent rate of pseudouridine formation (k_{app}), the maximal amount of pseudouridines formed (Y_{max}) and the amplitude (Amp).

In order to determine a Michaelis constant (K_M) for TruB K64E and TruB ΔPUA, the resulting apparent rates were plotted against enzyme concentration ([protein]) and the data fitted with the Michaelis-Menten function:

$$k_{app} = v_{max} \times [protein] / (K_M + [protein])$$

3.2.9 Co-culture competition assay

Parental *E. coli* strains Frag1 ("wild type") and the *truB* knockout strain MJF546 ($TruB^-$ Tet^R) as well as plasmids pTrc99a-mt (empty vector) and pTrc99a-TruB (plasmid with wild type TruB gene) were kindly provided by the Stansfield lab (Kinghorn *et al*. 2002). Quikchange site-directed mutagenesis as described above was utilized to produce plasmids pTrc99a-TruBK64E and pTrc99a-TruBΔPUA. The competition experiments were completed as described previously (Gutgsell *et al*. 2000; Kinghorn *et al*. 2002). In brief, growth of all *E. coli* strains was completed at 37°C in lysogeny broth (LB) without inducer as it has been previously shown that leaky expression occurs (Kinghorn *et al*. 2002). For the competition experiments, strains were first grown individually overnight. Samples containing 1 OD_{600} of each cell strain were mixed to start the competition. The numbers of viable cells were determined by plating dilutions on LB plates with and without tetracycline (25 μg mL^{-1}).

3.2.10 Pseudouridine detection in cellular tRNA by CMC modification

tRNAs were isolated from various *E.coli* strains by resuspension of a cell pellet in 6.2 M guanidine thiocyanate, 0.04 M sodium citrate, pH 7.0, 0.8% sarcosyl, 0.1 M β-mercaptoethanol, addition of 1/10 volume of 2 M sodium acetate, pH 4.0 and extraction with phenol:chloroform:isoamyl alcohol followed by two ethanol precipitations. 50 pmol RNA was reacted for 1 h at 37°C with 0.66 M CMCT in 50 mM bicine, pH 8.0, 7 M urea, 4 mM EDTA. Following ethanol precipitation, the RNA was resuspended in 50 mM Na_2CO_3 solution, pH 10.3, incubated at 50°C for 2 hours and again precipitated. The $tRNA^{Phe}$ RT primer was labelled with [^{32}P] using T4 polynucleotide kinase and incubated with RNA for 5 minutes at 65°C, and then an additional 10 minutes at 47°C.

Subsequently, reverse transcriptions were carried out with AMV reverse transcriptase for 45 min at 47°C, followed by 15 minutes at 70°C to heat inactivate the enzyme. Following precipitation, samples were separated on a 15% sequencing Urea-PAGE at 50 W (3000V) for 1.5 hours which was analyzed by phosphorimaging. This experiment was duplicated to detect pseudouridine formation in $tRNA^{Phe}$ showing that the presented results are reproducible. In a separate experiment, similar results were obtained for *in vivo* pseudouridine formation in $tRNA^{Cys}$ (data not shown). To estimate the relative level of pseudouridine formation, the Ψ55 band intensity was quantified using Image J software (NIH) and the intensity of the band at position 56 was subtracted to account for random stops during the primer extension. The percentage of pseudouridine formation at position 55 is estimated relative to the pseudouridines found in the wild-type strain which are set to 100%.

3.2.11 Circular dichroism spectroscopy

All proteins were diluted to a concentration of 0.05 mg/mL in 50 mM sodium phosphate buffer, pH 7.5 and analyzed in a Jasco J-815 CD spectrometer with a 1 mm path length cuvette. Spectra were recorded from 190 to 320 nm with 1 s digital integration time, 1 nm bandwidth, and a scanning speed of 50 nm/min. For each enzyme, eight individual spectra were accumulated and averaged. The mean ellipticity $[\theta]_{mrw}$ was calculated from the observed ellipticity (θ), path length (d), and protein concentration (c; mg/mL):

$$[\theta]_{mrw} = MRW \times \theta / (10 \times d \times c)$$

3.2.12 Preparation of fluorescein-labelled tRNA

Purified *in vitro* transcribed $tRNA^{Phe}$ was oxidized with 2 mM potassium periodate for 30 minutes. The reaction was stopped by the addition of ethylene glycol to a final concentration of 10 mM. Following an ethanol precipitation, the tRNA was incubated with 10 mM fluorescein-5-thiosemicarbazide (LifeTechnologies) in a 0.1 M sodium acetate solution for 16 hours in the dark at room temperature. The RNA was precipitated by the addition of 3 M sodium acetate, pH 5.2 and ethanol. The unbound dye was removed via phenol extraction. The tRNA was again precipitated in ethanol and finally resuspended in water. RNA concentration was estimated by absorbance at 260 nm. The dye concentration was determined by measuring the absorbance at 492 nm with the extinction coefficient of 80 000 $M^{-1}cm^{-1}$. The final labelling efficiency was determined by comparing the concentration of tRNA and dye.

3.3 Results

3.3.1 TruB folds tRNA *in vitro* independent of its modification activity

First, TruB's ability to bind to *in vitro* transcribed RNA was measured via nitrocellulose membrane filtration. While TruB can bind to its substrate tRNA with relatively high affinity (1.9 ± 0.7 µM), it is unable to bind to 23S ribosomal RNA or single-stranded RNA (Figure 3.2).

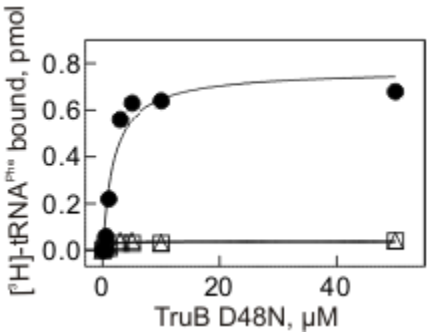

Figure 3.2. Assessing binding of TruB to different RNAs. Catalytically inactive TruB D48N was incubated with [^{3}H]-labelled RNAs and binding was analyzed by nitrocellulose filtration. The natural substrate *E.coli* tRNA^{Phe} (filled circles) was used as a positive control. No binding was detected with a short single-stranded RNA (open squares) or a structured, ~200 nt fragment of the 23S rRNA corresponding to the peptidyltransferase center (open triangles). In conclusion, while TruB is known to interact with all elongator tRNAs, it is not binding non-specifically to other RNAs.

To assess whether the pseudouridine synthase TruB is able to promote tRNA folding, we used aminoacylation of tRNA as the readout for the successful folding of tRNA into a biologically active conformation (Figure 3.3). It is well established that folded tRNA is rapidly aminoacylated whereas un- or misfolded tRNA is only slowly aminoacylated (Bhaskaran *et al*. 2012). Using a published assay to monitor tRNA folding, we first unfolded unmodified, *in vitro* transcribed *E. coli* tRNA^{Phe} through incubation at 65°C and subsequently allowed tRNA to slowly fold at 0°C in the presence or absence of TruB wild type or variants. At several time points, tRNA folding was analyzed by assessing aminoacylation of the tRNA (Figure 3.3). The fraction of folded tRNA was determined by recording the fraction of instantaneously aminoacylated tRNA (Bhaskaran *et al*. 2012). In the presence of TruB wild-type, the rate of tRNA folding was increased about twofold with twice as much tRNA folded at any given time point compared to the reaction without TruB (Figure 3.3); thus TruB assists in tRNA folding. Next, the

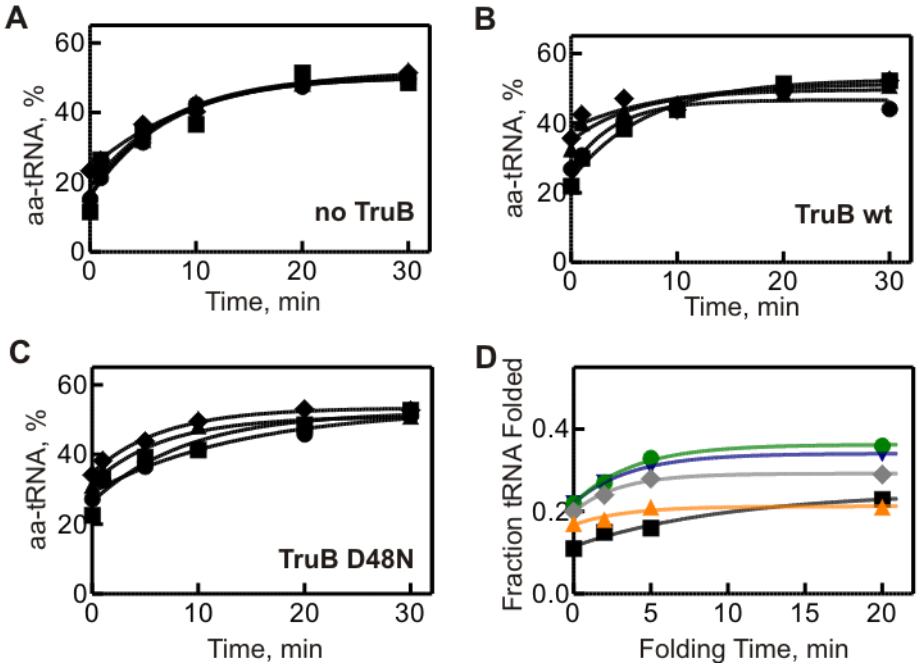

Figure 3.3. *in vitro* tRNA folding in the presence and absence of TruB as determined by tRNA aminoacylation time courses. tRNA was unfolded and then allowed to refold for 0 (squares), 2 (circles), 5 (triangles), or 20 minutes (diamonds) at 0°C prior to the start of the aminoacylation reaction. Figures A to C show representative time courses of aminoacylation reactions (A) without TruB, (B) with TruB wild type, or (C) with catalytically inactive TruB D48N. The initial fraction of aminoacylated tRNA reflects the proportion of correctly folded tRNA that is instantaneously aminoacylated in the presence of a large excess of Phe-tRNA^{Phe} synthetase (D). The remaining tRNA is only slowly aminoacylated because folding of these tRNAs is the rate-limiting step (Bhaskaran *et al*. 2012). tRNA was unfolded and then allowed to refold in the absence of TruB (black squares) or in presence of TruB wild type (green circles), catalytically inactive TruB D48N (blue inverse triangles), TruB ΔPUA (grey diamonds), or TruB K64E (orange triangles). At different times of the folding reactions, the aminoacylation reaction was started to determine the amount of folded and thus aminoacylatable tRNA (y-axis intercept of the aminoacylation time courses shown in A – C). Here the fraction of folded tRNA is plotted over time. Examination revealed a higher initial fraction of folded tRNA in the presence of TruB wt, TruB D48N, TruB ΔPUA (0.22 versus 0.12 in absence of TruB) as well as a higher rate of folding in the presence of TruB wt, TruB D48N , and TruB ΔPUA with 0.26 ± 0.05 min^{-1} in contrast to a rate of folding of 0.1 ± 0.07 min^{-1} in the absence of TruB or in the presence of TruB K64E.

experiment was repeated with the TruB D48N variant which is inactive in pseudouridine formation, but unaffected in tRNA binding (Wright *et al*. 2011). The catalytically

inactive TruB variant is able to fold tRNA at the same rate as TruB wild type, demonstrating that TruB's tRNA chaperone activity is independent of its tRNA modification activity. Completing the assay in the presence of TruB ΔPUA also increased the fraction of folded tRNAs in solution to a similar level as the wild type or D48N enzymes. TruB K64E was unable to assist in folding tRNA under these conditions as the fraction of folded tRNAs is similar to the level observed in the absence of enzyme (Figure 3.3D).

3.3.2 Molecular mechanism of tRNA interaction with TruB

To understand how TruB folds tRNA, we need to know how TruB binds tRNA, how it induces conformational changes in tRNA and how it dissociates from tRNA. To separately detect and analyze these steps, we utilized a previously described $tRNA^{Phe}$ that is labeled at position 57 in the T-arm with a fluorescent base analog, 2-aminopurine (2AP) (Friedt *et al.* 2014). Binding of the tRNA by TruB causes nucleotides 55-57 of the tRNA to flip into the catalytic pocket of the enzyme which is reflected by an increase in 2AP fluorescence. Interaction with TruB wild type results in a two-phase fluorescence increase reflecting tRNA binding and a subsequent conformational change followed by a slower fluorescence decrease due to tRNA dissociation after catalysis is completed (Figure 3.4). The first fluorescence increase likely reflects the encounter of TruB with tRNA, but it is fast and has a small amplitude, preventing a quantitative analysis. Therefore, we reduced the reaction rate by measuring TruB – tRNA interactions at a low temperature (5°C) that does not affect the affinity of TruB for tRNA (dissociation constants of 0.8 ± 0.1 µM and 0.5 ± 0.1 µM at 5°C and 20°C, respectively Figure 3.4D).

The kinetic mechanism of tRNA interacting with TruB was investigated by titrating 2AP-labeled tRNA with TruB wild type at both both 20°C and 5°C in stopped-flow experiments (Figure 3.4A, 3.5B-E). This experimental system also allowed us to directly observe dissociation of tRNA from TruB in fluorescent chase experiments where a pre-

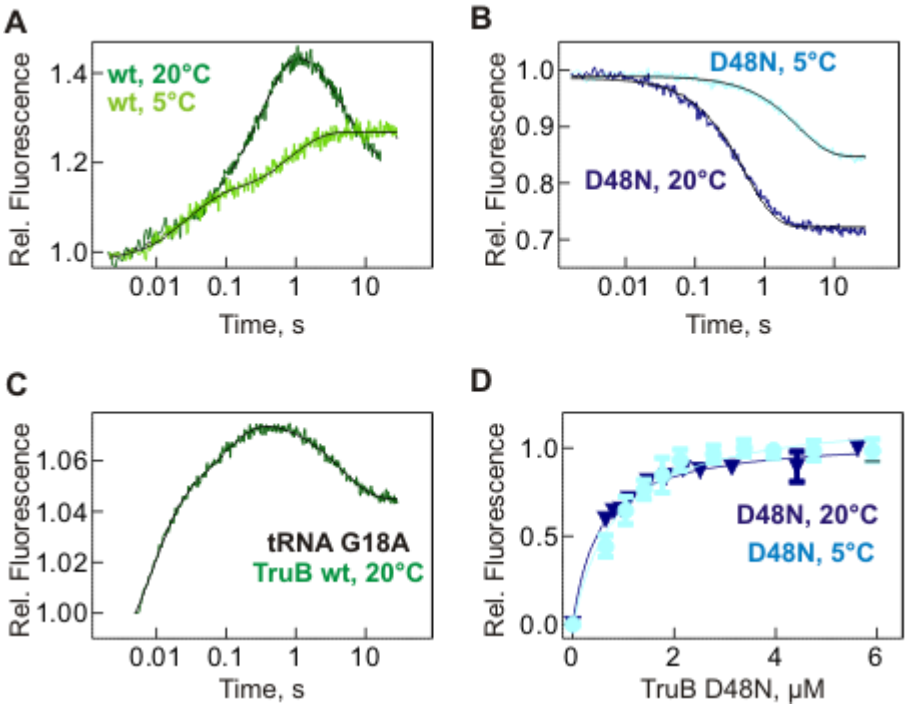

Figure 3.4. Determining the kinetic mechanism of the TruB - tRNA interaction. A) Time courses of TruB interacting with RNA^{Phe} containing a 2-aminopurine (2AP) at position 57 were monitored using a stopped-flow apparatus. 2AP-tRNA (0.3 µM final concentration) was rapidly mixed with TruB wild type (5 µM final concentration). Time courses were fitted with a 2-exponential function (wt, 5°C) or a three-exponential function (wt, 20°C). B) Dissociation of substrate tRNA from TruB was monitored by rapidly mixing TruB D48N in complex with 2AP-tRNA with an excess of unlabeled tRNA^{Phe} (for dissociation rates see Table 3.2). C) Rapid-kinetic stopped-flow analysis of 2-aminopurine-labeled tRNA^{Phe} G18A binding to TruB wild type at 20°C. Final concentrations were 1.5 µM tRNA and 5 µM enzyme. Fitting of the timecourse with a 3-exponential function (grey line) yielded the following apparent rates:k_{app1} = 123 ± 3 s^{-1}, k_{app2} = 10.5 ± 0.3 s^{-1} and k_{app3} = 0.22 ± 0.004 s^{-1}. D) Equilibrium fluorescence titrations of 200 nM tRNA^{Phe} containing a 2-aminopurine (2AP) at position 57 with increasing concentrations of TruB D48N obtaining a K_D of 0.5 ± 0.1 µM at 20°C and 0.8 ± 0.1 µM at 5°C.

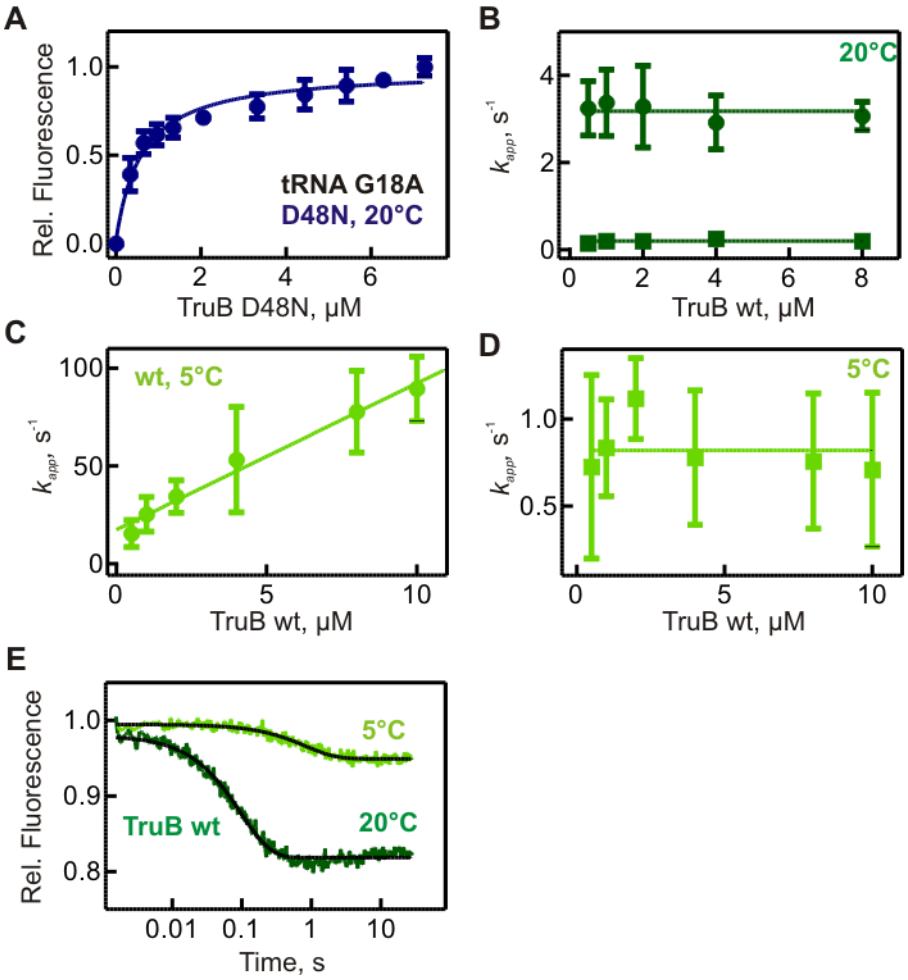

Figure 3.5. Rapid kinetic analysis of 2AP-tRNA binding to and dissociating from TruB. A) Equilibrium fluorescence titration of 2-aminopurine-labeled $tRNA^{Phe}$ G18A (final concentration of 200 nM) with increasing concentrations of TruB D48N at 20°C. The relative fluorescence change at 365 nm was plotted against enzyme concentration to determine a dissociation constant of 0.6 ± 0.3 μM. B) Apparent rates for the second (k_{app2}, circles) and third (k_{app3}, squares) phases of TruB – tRNA interaction at 20°C (Figure 3.4B). The apparent rates for the second phase (3.2 ± 0.1 s^{-1} at 20°C) are concentration independent consistent with a unimolecular conformational change in the tRNA. The fluorescence decrease observed at 20°C (k_{app3}) reflects release of modified tRNA, which is rate-limited by catalysis as described previously (Wright *et al*. 2011), and is concentration independent with an average apparent rate of 0.20 ± 0.01 s^{-1}. C) Apparent rates (k_{app1}) of tRNA binding to TruB at 5°C were plotted against enzyme concentration. Fitting to a linear equation determined k_1 and k_{-1} (Table 3.2). The apparent rates for the first phase increase linearly with the TruB concentration as expected for a bimolecular binding event allowing us to determine the association (k_1) and dissociation rate constants (k_{-1}) from the slope and y-intercept, respectively (Table 3.2). D) Apparent rates for second phase (k_{app2}) of TruB – tRNA interaction at 5°C were plotted against enzyme concentration. As reported for experiments performed at 20°C, the apparent rates

for the second phase (0.8 ± 0.1 s^{-1} at 5°C) are also concentration independent and therefore reflect the unfolding of the tRNA elbow region. E) Dissociation of product tRNA from TruB was monitored by rapidly mixing TruB wild type in complex with 2AP-tRNA with an excess of unlabeled $tRNA^{Phe}$ at 5°C (light green) and 20°C (dark green). The dissociation rate was determined by fitting the time course with a single-exponential function (smooth black line). The dissociation rate constant of substrate tRNA (Table 3.2) is significantly lower than the dissociation rate constant k_{-1} for the initial tRNA-TruB encounter at 5°C and therefore corresponds to the reversal of the conformational change in the second step of binding (k_{-2}). Knowing k_{-2} allows us to determine the forward rate constant k_2 (Table 3.2, Materials & Methods) (Fersht 1998).

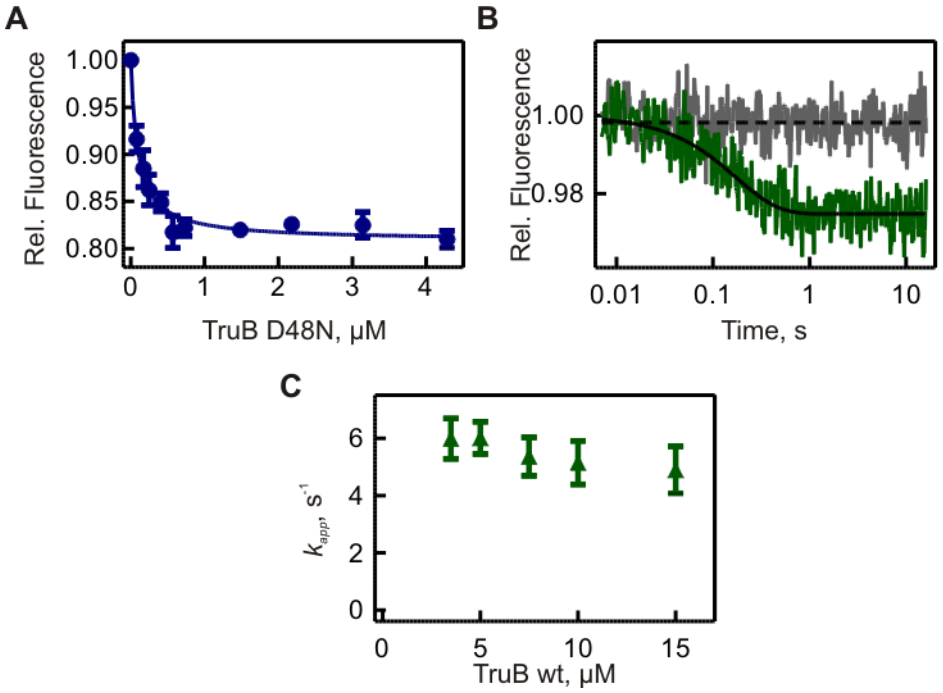

Figure 3.6. Interaction of TruB with tRNA labeled with fluorescein at its 3′ end. A) Equilibrium fluorescence titration of fluorescein-labeled $tRNA^{Phe}$ with TruB D48N. The relative fluorescence at 515 nm was plotted against enzyme concentration and fitted with a hyperbolic function to obtain the K_D of 0.10 ± 0.02 μM. B) TruB wild type (final concentration 5 μM; green) or TruB ΔPUA (final concentration 10 μM, grey) was rapidly mixed in a stopped-flow apparatus with fluorescein-labeled tRNA (final concentration 0.3 μM). Fluorescein was excited at 480 nm and emission was monitored using a LG-500 nm cutoff filter. The fluorescence change of TruB wild type was fitted with a single exponential function. C) Apparent rates of TruB wild type interacting with fluorescein-tRNA are plotted against enzyme concentration.

formed complex of TruB with 2AP-tRNA is rapidly mixed with excess unlabeled tRNA. By using catalytically inactive TruB D48N, the dissociation of unmodified substrate RNA can be followed (Figure 3.4B). Kinetic analyses of these time courses provide the rate constants for the initial encounter of tRNA and TruB (k_1 and k_{-1}), for the conformational change that TruB induces in tRNA to flip the target uridine into its active site (k_2 and k_{-2}) as well as for pseudouridine formation (k_ψ) as reported previously (Table 3.2).

Comparing these rate constants reveals that tRNA binding is rapid and reversible. However the subsequent disruption of the elbow region of tRNA to flip bases into TruB's active site is rather slow with a k_2 of only 1.3 s^{-1} at 20°C, and it is readily reversible since k_{-2} is rather large with 1.9 s^{-1}. Importantly, reversal of the unfolding of the tRNA elbow region is faster than actual pseudouridine formation (k_{-2} = 1.9 s^{-1} versus k_ψ = 0.2 s^{-1} at 20°C, Table 3.2). Therefore, upon binding to TruB, the tRNA is repeatedly unfolded and then rapidly refolded in the elbow region before the tRNA is eventually slowly modified by TruB.

Table 3.2. Summary of kinetic parameters for TruB wild type and TruB ΔPUA at 5°C, 20°C and 37°C.

	TruB wild type			TruB ΔPUA		
	5°C	20°C	37°C	5°C	20°C	37°C
k_1 (μM^{-1} s^{-1})	8 ± 1	ND	ND	2.0 ± 0.5	ND	ND
k_{-1} (s^{-1})	16 ± 5	ND	ND	ND	ND	ND
k_2 (s^{-1})	0.5 ± 0.5	1.3 ± 0.4	ND	(0.8 ± 0.3)[b]	(7.0 ± 0.5)[b]	ND
k_{-2} (s^{-1})	0.32 ± 0.04	1.9 ± 0.2	ND	ND	ND	ND
k_ψ (s^{-1})	ND	0.20 ± 0.02	0.5 ± 0.2[a]	ND	0.06 ± 0.01	0.02 ± 0.01
$k_{release}$ (s^{-1})	1.2 ± 0.1	10.6 ± 0.3	ND	0.9 ± 0.2	4.5 ± 1.2	ND

ND: not determined

[a] determined in (Wright *et al*. 2011)

[b] apparent rate (k_{app2}) for tRNA conformational change; k_2 for TruB ΔPUA will be slightly lower ($k_2 = k_{app} - k_{-2}$)

Since the previous experiments used folded wild-type tRNA (Figure 3.2A & B, 3.3B-E), we subsequently asked whether and how TruB interacts with a potentially mis- or partly unfolded tRNA. Therefore, we tested the interaction of TruB with 2AP-labelled tRNA harboring a G18A substitution in the D arm that affects the tertiary interaction of D and T arm (Figure 3.3C). The affinity of TruB for this tRNA is unchanged, and the kinetics of the interaction between TruB and tRNA G18A are similar to wild-type tRNA (Figure 3.3C & 3.4A). The most notable difference is an increase in the rate of base-flipping by about two-fold (k_{app2}) which is consistent with a disturbed tertiary structure in the elbow region of tRNA that allows TruB to gain access to the target uridine more easily. In conclusion, TruB does not discriminate between folded and partially folded tRNAs, but binds both folded and misfolded tRNAs followed by unfolding of the tRNA elbow region.

3.3.3 tRNA chaperone activity of TruB is critical for bacterial fitness

The data in Figures 3.2 and 3.3 show that TruB acts as a tRNA chaperone *in vitro*, but is TruB's tRNA chaperone activity important *in vivo*? If this were true, then bacterial fitness should be reduced when tRNA binding by TruB (but not its catalytic ability) is impaired. To test this hypothesis, single conserved, basic amino acid residues within the RNA binding surface of TruB (R40, K64, K130, and K176) were individually substituted with a negatively charged glutamate to impair tRNA binding (Fig. 3.1). In multiple-turnover tritium release assays, all of the TruB variants were significantly slower in pseudouridylation than the wild type (Figure 3.7A). Single-turnover pseudouridylation experiments (Figure 3.7B), revealed that the TruB K64E variant is most affected: 750-fold slower than the wild type enzyme (Table 3.3) (Wright *et al*. 2011; Kamalampeta *et*

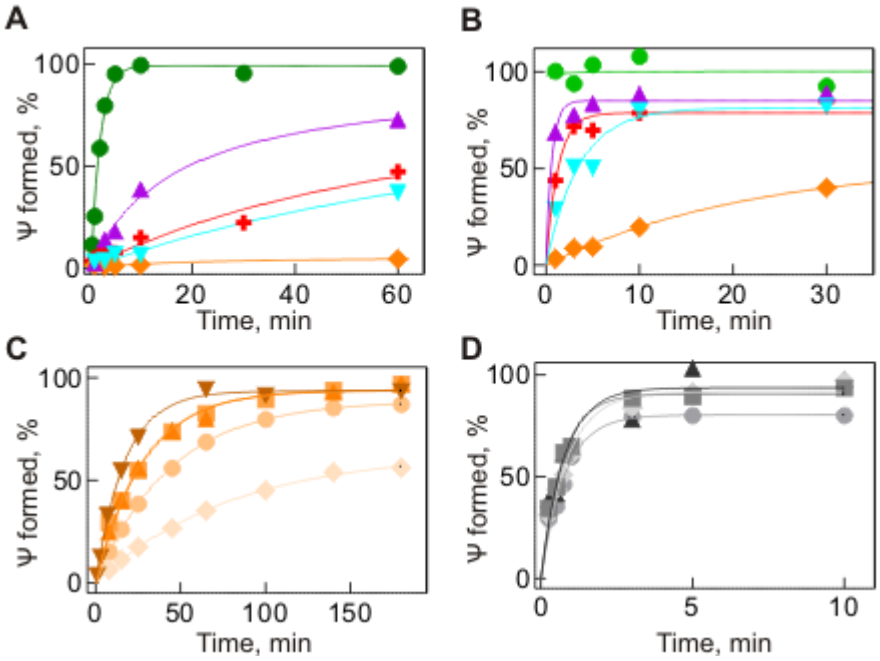

Figure 3.7. Pseudouridylation assays with TruB variants. A) Multiple-turnover pseudouridylation assays (600 nM tritium-labeled $tRNA^{Phe}$, 20 nM TruB) with TruB wild type (green circles), TruB R40E (red crosses), TruB K64E (orange diamonds), TruB K130E (purple triangles), and TruB K176E (turquoise reverse triangles). B) Pseudouridine formation by TruB variants with substitutions in the tRNA binding interface was monitored by a tritium release assay at 37ºC under single-turnover conditions (1 µM $tRNA^{Phe}$ with 5 µM TruB). Time courses were recorded for TruB wild type (green circles) and TruB variants as indicated in color in (A). C) Pseudouridine formation by TruB K64E under single-turnover conditions at several enzyme concentrations (from light to dark orange): 3 µM (diamonds), 5 µM (circles), 10 µM (squares), 15 µM (triangles), and 20 µM (reverse triangles). D) Single turnover tritium release assay at increasing TruB ΔPUA concentrations (from light to dark grey): 3 µM (diamonds), 5 µM (circles), 10 µM (squares), and 15 µM (triangles). Time courses in B and C were fitted with a single-exponential function to determine the apparent rate of pseudouridine formation (k_{app}).

Table 3.3. Apparent rates of pseudouridine formation by all TruB variants tested under single-turnover conditions (Figure 3.7B). The apparent rates were determined by fitting time courses with a single exponential function.

Enzyme	k_{app}, min^{-1}	Fold-decrease
TruB wild type*	30 ± 12	-
TruB R40E	0.8 ± 0.1	43
TruB K64E	0.04 ± 0.01	750
TruB K130E	1.6 ± 0.3	19
TruB K176E	0.3 ± 0.1	100

al. 2012). Therefore, all further experiments were conducted with the TruB K64E variant. We determined the Michaelis constant (K_M) in single-turnover tritium release assays (Figures 3.6C and 3.7A) since determination of a dissociation constant (K_D) for TruB K64E proved to be difficult as nitrocellulose filtration resulted in no signal change (Fig.3.8B). Compared to TruB wild type (K_D of 340 nM, K_M of 550 nM) (Wright *et al.* 2011), the K_M of TruB K64E is very high (28 ± 26 µM; Figure 3.8A) indicating that the

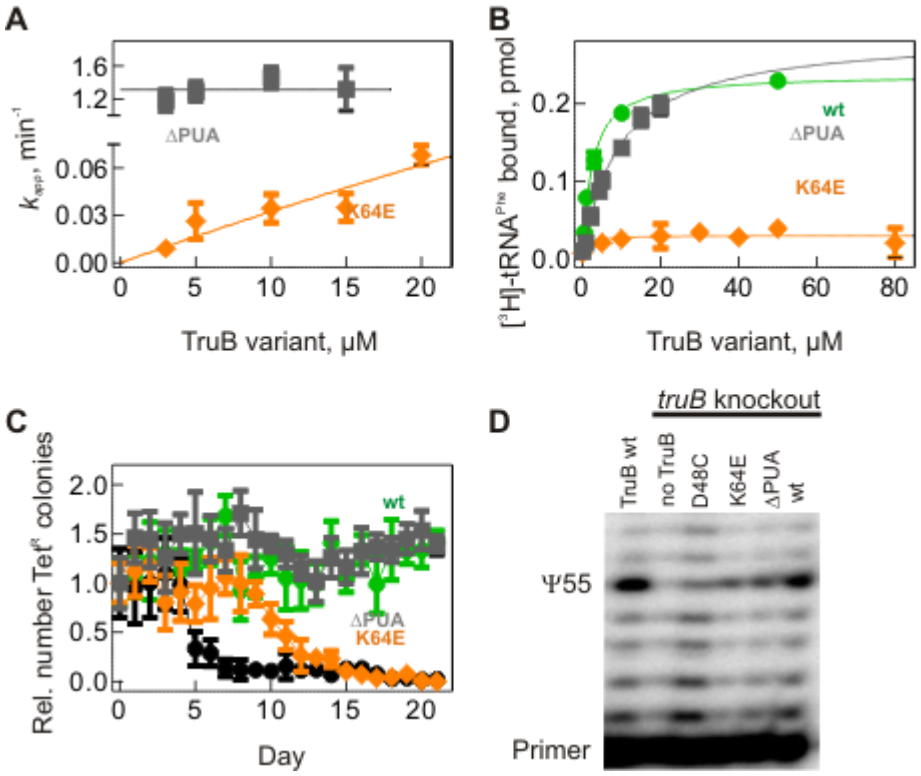

Figure 3.8. Bacterial fitness depends on tRNA binding by TruB. A) Apparent rates of pseudouridine formation (k_{app}) by TruB variants from single-turnover experiments (Figure 3.5C and D) were plotted against TruB concentration to determine the K_M. B) Binding of tritium-labeled tRNA (10 nM) to TruB was determined through nitrocellulose filter binding. Hyperbolic fitting yielded the K_D: 2.4 ± 0.3 µM for TruB wild type and 9 ± 1 µM for TruB ΔPUA. C) Co-culture competition assays between wild type *E. coli* and the *E.coli truB* knockout strain (black), the *truB* knockout strain expressing TruB wild type protein, TruB K64E or TruB ΔPUA. D) *in vivo* tRNA pseudouridine 55 formation in $tRNA^{Phe}$ assessed by CMCT modification in *E.coli* wild-type as well as *truB* knockout strains expressing TruB variants. Similar results were obtained with probing for pseudouridylation in $tRNA^{Cys}$ (data not shown).

affinity of TruB K64E for tRNA is strongly reduced. Next, we tested the impact of impaired tRNA binding by TruB K64E on bacterial fitness in co-culture competition assays with wild type (Gutgsell *et al*. 2000; Kinghorn *et al*. 2002). Notably, the *truB* knockout strain expressing TruB K64E was outcompeted by the *E.coli* wild type strain in about 15 days (Figure 3.8C). This result confirms that tRNA binding by TruB and in turn its tRNA chaperone activity are critical for cellular fitness. In contrast, the pseudouridylation activity of TruB is not important for cellular fitness as shown previously with the catalytically inactive TruB variant TruB D48C (Gutgsell *et al*. 2000). Notably, some pseudouridines were formed in $tRNA^{Phe}$ in the strain expressing TruB K64E (roughly 50% of wild-type) whereas essentially no pseudouridine was detected in presence of TruB D48C (Figure 3.8D). Residual pseudouridylation activity by TruB K64E is expected based on the low level of pseudouridylation activity observed *in vitro*. These findings further support the conclusion that tRNA binding and folding, in contrast to pseudouridylation, is the critical cellular function of TruB.

3.3.4 Functional role of the PUA domain of TruB for tRNA interaction

The TruB family of pseudouridine synthases contains a conserved catalytic domain and a C-terminal pseudouridine synthase and archeosine transglycosylase (PUA) domain which is predicted to interact with RNA (Hoang and Ferre-D'Amare 2001; Cerrudo *et al*. 2014). We hypothesized that the PUA domain is critical for tRNA binding and folding and in turn for cellular fitness. Initial studies with TruB ΔPUA lacking the PUA domain and tRNA labeled with fluorescein at the 3′CCA end suggested that the acceptor arm of tRNA interacts with the PUA domain of TruB, as no signal change is observed compared to the wild type enzyme (Figure 3.6B). Nitrocellulose filtration experiments with TruB

ΔPUA revealed only a 3-fold reduced affinity for [^{3}H]-tRNA^{Phe} with K_Ds of 9 ± 1 μM and 2.4 ± 0.3 μM for TruB ΔPUA and TruB wild type, respectively (Figure 3.8B). Single turnover pseudouridylation assays showed no concentration-dependence, but a 25-fold reduced rate of pseudouridylation by TruB ΔPUA (Figure 3.7D, 3.8A and Table 3.3). Surprisingly, this suggests that the PUA domain is more important for catalysis than for tRNA binding, possibly by positioning the substrate tRNA onto the TruB enzyme.

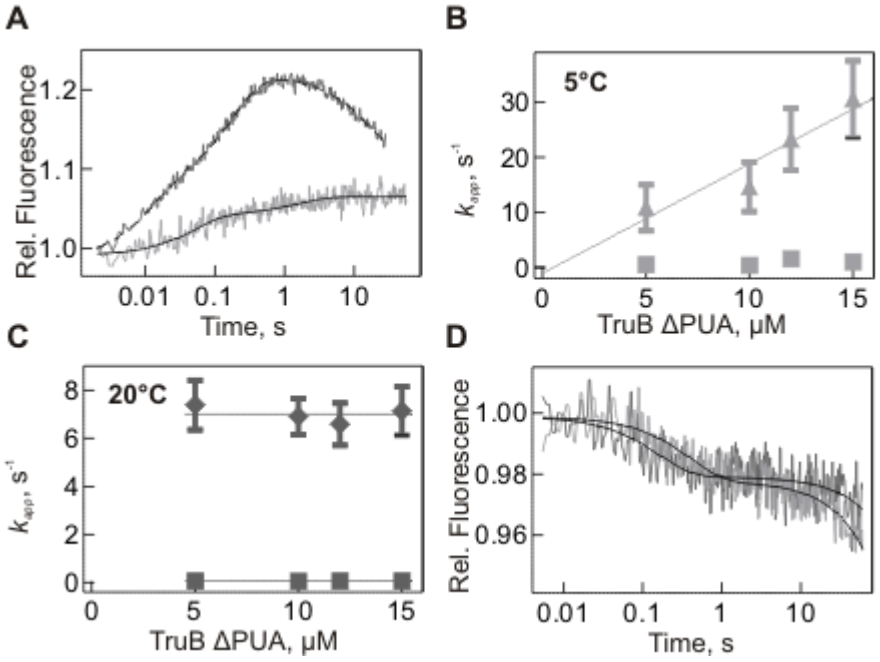

Figure 3.9. Rapid kinetic analysis of TruB ΔPUA interacting with tRNA. A) Time courses of 2AP-tRNA (0.3 μM final concentration) interacting with of TruB ΔPUA (10 μM final concentration) at 20°C (dark grey) and 5°C (light grey). The time courses were fitted with a three-exponential (20°C, dotted black line) and a two-exponential function (5°C, smooth black line), respectively. B) The apparent rates for the first phase (k_{app1}, triangles) and the second phase (k_{app2}, squares) of tRNA binding to TruB ΔPUA at 5°C were plotted against enzyme concentration. Linear fitting of (k_{app1}) yielded k_1 and k_{-1} (Table 3.2). C) Apparent rates for the second (k_{app2}, diamonds) and third (k_{app3}, squares) phases of TruB ΔPUA interacting with tRNA at 20°C. D) Dissociation of 2AP-tRNA•TruB ΔPUA complex was observed upon rapidly mixing with a large excess of unlabeled tRNA^{Phe}. Time courses at both 20°C (dark grey) and 5°C (light grey) were fitted with a single exponential plus linear function to determine the dissociation rate.

Therefore, we performed stopped-flow experiments with 2AP-tRNA to dissect the role of the PUA domain on the initial encounter versus the local unfolding of tRNA upon binding to TruB (Figure 3.9, Table 3.2). The association rate constant (k_1) at 5°C corresponding to tRNA binding by TruB is four-fold less for TruB ΔPUA than for TruB wild type (Table 3.2). In contrast, the unfolding of the tRNA elbow region (k_2 and k_{-2}) is minimally affected by the deletion of the PUA domain. The data indicate that deletion of TruB's PUA domain slows down the initial binding step between tRNA and TruB, but does not strongly affect the subsequent unfolding and refolding of tRNA. Thus, the PUA domain is likely not important for the tRNA chaperone function of TruB.

Lastly, we tested the cellular role of the PUA domain in co-culture competition assays where expression of TruB ΔPUA was able to overcome the fitness disadvantage of the knockout strain (Figure 3.8C). However, we observed fewer pseudouridines in cellular $tRNA^{Phe}$ than in the wild-type strain (Figure 3.8D), in agreement with the catalytic impairment of TruB ΔPUA. We conclude that the PUA domain of TruB contributes to tRNA binding, but is most important for accelerating pseudouridine formation. Notably, the PUA domain is not critical for TruB's tRNA chaperone activity. Accordingly, this domain is dispensable *in vivo*.

3.4 Discussion

We have combined biochemical, biophysical and cellular studies to verify the hypothesis that the model pseudouridine synthase TruB is a tRNA chaperone *in vitro* and *in vivo*. This is a proof-of-concept that during RNA maturation the modification and folding of RNA are linked, synergistic processes. As such, it is likely that other RNA modification enzymes are also RNA chaperones.

Besides proving that TruB is a tRNA chaperone that enhances tRNA aminoacylation (Figure 3.3), we characterized its molecular mechanism through rapid-kinetics experiments (Figure 3.4, 3.5 & 3.6). Importantly, following binding of tRNA, TruB induces the reversible unfolding of tRNAs in the elbow region such that tRNAs undergo multiple unfolding and refolding events before becoming eventually pseudouridylated and released. The ability of TruB to fold tRNA is critical for bacterial fitness as evident in co-culture competition assays (Figure 3.8) which indicates that this property of TruB has been selected for during evolution. Lastly, we clarified the function of the PUA domain of TruB as contributing to the initial binding of tRNA and to the catalysis of pseudouridine formation, likely by correctly positioning the tRNA (Figure 3.9). Moreover, the PUA domain is not involved in tRNA un- and re-folding and is dispensable for bacterial fitness (Figure 3.8).

To further discuss TruB's function as a tRNA chaperone, we use a definition for RNA chaperones that was proposed by Reneé Schroeder and coworkers: "A protein that binds transiently and non-specifically to RNA and resolves kinetically trapped, misfolded conformers. RNA chaperone activity entails the disruption of RNA-RNA interactions and the loosening of RNA structures. The interaction with the protein is needed for the unfolding of the RNA but not to maintain its structure. The protein does not require ATP binding or hydrolysis for its activity." (Rajkowitsch *et al*. 2007). First, does TruB "bind transiently and non-specifically to RNA"? As a multiple turnover enzyme, TruB clearly binds tRNA transiently (Nurse *et al*. 1995; Gu *et al*. 1998; Wright *et al*. 2011). TruB does not interact entirely non-specifically with RNA as it does not bind a single-stranded or a structured RNA (Figure 3.2). However, TruB does modify all elongator tRNAs in

bacteria in the TΨC arm and is therefore not specific to a single tRNA (Gu *et al*. 1998; Gutgsell *et al*. 2000). Together, these properties designate TruB as a tRNA chaperone rather than a general RNA chaperone. Second, as a tRNA chaperone, TruB must be able to "resolve kinetically trapped, misfolded conformers". We show that TruB increases the fraction of folded and aminoacylation-competent tRNAs. In this experiment, tRNAs were first unfolded and allowed to fold at 0°C in the presence or absence of TruB. Under these low temperature conditions, tRNA is likely to adopt an unfolded or mis-folded conformation and therefore correct tRNA folding is rate-limiting for aminoacylation. Clearly, TruB is able to accelerate the rate of folding and to increase the fraction of folded tRNA rendering it active for aminoacylation. Moreover, we have shown that TruB interacts similarly with a potentially mis- or unfolded tRNA G18A as with wild-type tRNA demonstrating its capability to act on misfolded tRNAs (Figures 3.4C & 3.5A). Third, we experimentally assessed TruB's activity in "the disruption of RNA-RNA interactions and the loosening of RNA structures". The crystal structures of TruB bound to the TΨC arm reveal that TruB disrupts interactions between the TΨC and the D arm of tRNA to gain access to the target uridine 55 (Figure 3.10) (Hoang and Ferre-D'Amare 2001; Pan *et al*. 2003).

Using tRNA with a 2-aminopurine base analog at position 57 allows us to observe the flipping of bases directly (Figure 3.4). This conformational change in tRNA loosens the tRNA structure in the elbow region which contains numerous tertiary RNA-RNA interactions. Importantly, this base-flipping and the associated conformational change can occur multiple times while tRNA is bound to TruB and before pseudouridylation occurs (Figure 3.9). Thus, TruB resembles a protein chaperone that can repeatedly unfold its

substrate, ensuring multiple chances to fold correctly (Kim *et al*. 2013). Indeed, pseudouridine formation may act as a timer and may have evolved to be slow in order to

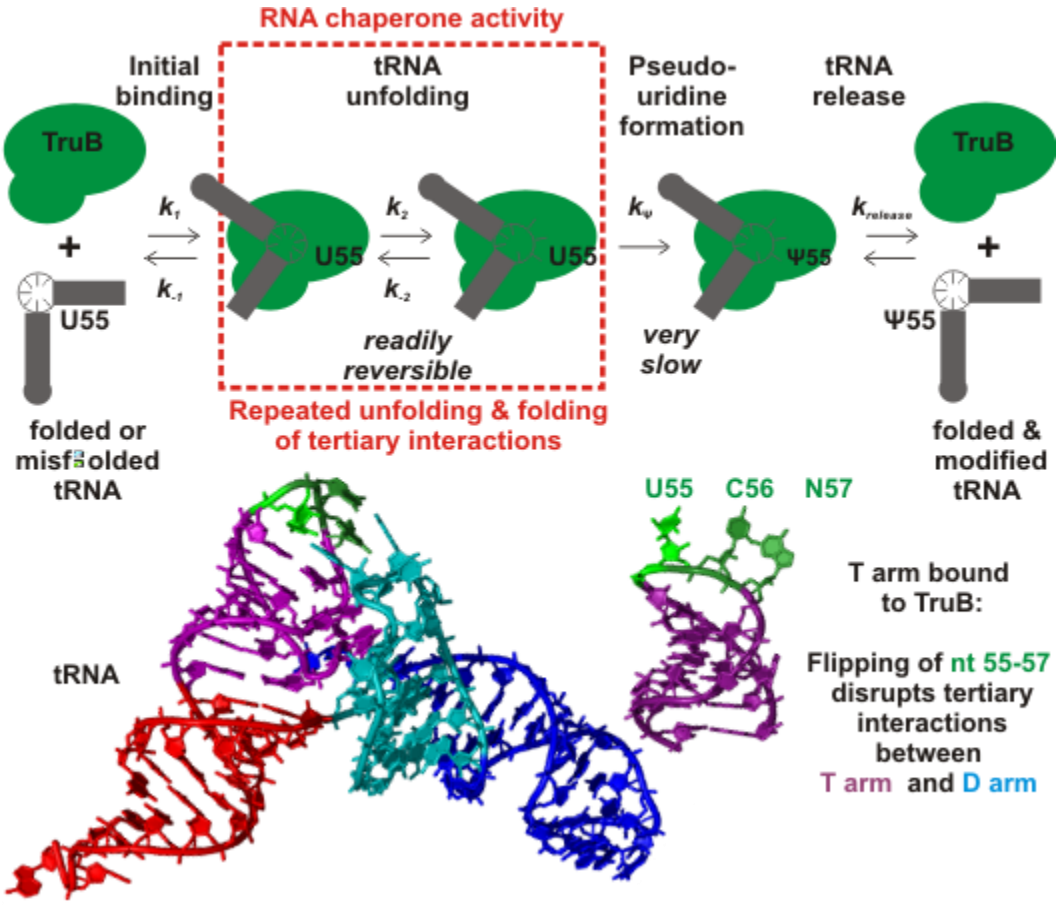

Figure 3.10. Mechanism of TruB acting as a tRNA chaperone while introducing pseudouridine 55. Rapid tRNA binding is followed by local tRNA unfolding in the elbow region which allows TruB to gain access to the modification site. By flipping out nucleotides 55-57 in the T arm (PDB: 1K8W), the tertiary interactions between T and D arm in tRNA (PDB: 4TRA) are disrupted (bottom) and the tRNA is unfolded. Since the reversion of the tRNA unfolding (k_{-2}) is faster than catalysis (k_{Ψ}) (Table 3.2), TruB allows the tRNA to repeatedly unfold and refold before becoming pseudouridylated. This repeated folding-unfolding transition in the elbow region of tRNA constitutes the tRNA chaperone activity of the pseudouridine synthase TruB.

facilitate this repeated conformational change (Wright *et al*. 2011). Fourth, the statement that "the interaction with the protein is needed for the unfolding of the RNA but not to maintain its structure. The protein does not require ATP binding or hydrolysis for its activity." is obvious for TruB. tRNA independently interacts with many other proteins

and the ribosome in the cell while maintaining its structure, and all TruB assays are conducted in the absence of ATP. In conclusion, our experimental evidence clearly demonstrates that TruB acts as a tRNA-specific chaperone.

Why is tRNA folding by TruB critical for cellular fitness? Under optimal growth conditions, TruB is dispensable suggesting that tRNAs can fold independently (Gutgsell *et al*. 2000). However, in nature bacteria typically grow under stress and in competition with other organisms. Under these conditions, tRNA binding by TruB, but not pseudouridine formation, would be important for cellular fitness. This is evident in comparing TruB K64E and TruB ΔPUA, which form similar levels of pseudouridine in tRNA (Figure 3.8D). Only the fitness of the strain expressing TruB K64E is impaired indicating that pseudouridylation is not the determining factor for cellular fitness (Figure 3.8C). Rather our *in vitro* data (Figure 3.7A) suggest that only a fraction of tRNAs will bind to TruB K64E and will be pseudouridylated, whereas a much larger fraction of tRNAs will not bind and will not benefit from the tRNA chaperone function of TruB. In contrast, a large proportion of tRNAs will interact with TruB ΔPUA (Figure 3.7B) and become correctly folded although only a small portion of these will be pseudouridylated due to the reduction of the catalytic rate (Figure 3.7A). This implies that there are kinetically trapped and misfolded tRNAs in the cell that benefit from TruB's tRNA chaperone activity.

Indeed there are several lines of evidence suggesting the presence of misfolded tRNAs and other potential tRNA chaperones in the cell. For instance, mutations in mitochondrial tRNAs are implicated in human diseases (Abbott *et al*. 2014), and one such mutation has been reported to result in tRNA misfolding (Jones *et al*. 2008). Similarly, mutations in

cytoplasmic $tRNA^{His}$ lead to tRNA misfolding and in turn reduced processing of precursor tRNAs (Levinger *et al*. 1995). In eukaryotes, the La protein functions as a tRNA chaperone that is important for pre-tRNA folding (Chakshusmathi *et al*. 2003). Moreover, the La protein functions redundantly with catalytically active Pus4, the yeast homolog of TruB, indicating that these proteins together contribute to tRNA folding and stability (Copela *et al*. 2006). The importance of Pus4 for tRNA stability and/or folding is also supported by a report of a genetic interaction between a $tRNA^{Ser}$ mutant and Pus4 (Johansson and Bystrom 2002). Lastly, several biochemical studies have addressed the folding of wild type tRNAs revealing intermediate structures and possible formation of misfolded structures (Serebrov *et al*. 2001; Bhaskaran *et al*. 2012; Li *et al*. 2013). In summary, misfolded tRNAs are present in cells, and TruB can thus enhance cellular fitness by accelerating tRNA folding and/or increasing the fraction of correctly folded tRNA.

It is astonishing that the PUA domain of TruB is not required for its tRNA chaperone function and consequently for bacterial fitness (Figure 3.7). Aligning 100 bacterial TruB sequences revealed that this domain is conserved, but absent in TruB proteins of *Chlamydia* species, which have a significantly reduced genome size compared to *E.coli*. Hence, *Chlamydia* may have lost the less-important PUA domain as TruB's catalytic domain alone can still support cellular fitness. Our biochemical studies demonstrate that TruB's PUA domain binds RNA (Figure 3.7B), as expected for this domain (Cerrudo *et al*. 2014). Superimposing the TruB-T arm structure (Hoang and Ferre-D'Amare 2001; Pan *et al*. 2003) with a full-length tRNA structure suggests a large binding interface between the PUA domain and the acceptor arm of tRNA which is supported by our

results with tRNA labeled at the 3′ end (Figure 3.5G). This is similar to the PUA domain in the TruB homolog Cbf5, which is in direct contact with the related 3′ACA motif of H/ACA guide RNA (Li and Ye 2006; Zhou *et al*. 2011). Our data suggest that this interaction contributes to tRNA binding, but is more important for catalysis. A plausible explanation is that the tRNA is positioned slightly differently on TruB ΔPUA since a significant portion of the interaction surface is lost.

Our findings show for the first time that the pseudouridine synthase TruB acts as a tRNA chaperone. Could this be a common phenomenon for RNA modification enzymes? The idea of a dual function for RNA modification enzymes is not new (Ishitani *et al*. 2008). Similar to Ofengand's fitness studies with TruB (Gutgsell *et al*. 2000), the yeast tRNA methyltransferase Trm2, which forms m^5U54 adjacent to pseudouridine 55, has been shown by genetic interaction to stabilize tRNA independent of its catalytic activity and could thus also act as a tRNA chaperone (Johansson and Bystrom 2002). Despite these supporting genetic studies, to the best of our knowledge direct mechanistic evidence for an RNA modification enzyme acting as an RNA chaperone has been lacking. Many RNA modification enzymes have been proposed or demonstrated to utilize a base-flipping mechanism to gain access to the target nucleotide for modification (Hoang *et al*. 2006; Dunkle *et al*. 2014; Hamdane *et al*. 2014), but base-flipping alone may not represent an RNA chaperone function. Rather, we hypothesize that RNA rearrangements, such as base-flipping, that are coupled to tertiary interactions such as in the elbow region of tRNA, could be the hallmark of the RNA chaperone activity by RNA modification enzymes.

A fine-tuned relationship between RNA folding and modification or binding by proteins may have arisen during the transition from an RNA world to a ribonucleoprotein world and could thus be an ancient and general mechanism. Proteins may enhance RNA structure and function not just by permanently associating with RNAs to form ribonucleoprotein complexes, but also by acting as RNA chaperones, which transiently interact with RNA and induce unfolding of incorrect RNA structures. Therefore, the finding that TruB acts as a tRNA chaperone simply by binding and rearranging tRNA structure prompts us to change how we think about RNA-protein interactions in general. It is possible that some of the more than thousand RNA-binding proteins also have a second function in acting as RNA chaperones with significant consequences for RNA biology.

In conclusion, we provide the first direct evidence that an RNA modification enzyme also acts as an RNA chaperone *in vitro* an *in vivo*. This alters our understanding of RNA maturation as modification and folding can no longer be considered as separate processes. Instead it is likely that more examples of enzymes with dual modification and chaperone activities will be identified. Apparently, evolution has selected an efficient mechanism that integrates seemingly different events: RNA modification to expand the repertoire of chemically distinct ribonucleotides and RNA folding to adopt the biologically active conformation.

Chapter 4 – Characterization of TrmA Ligand Binding

4.1 Introduction

The formation of the near universally conserved 5-methyluridine modification found at position 54 in tRNA is catalyzed by the *S*-adenosylmethionine-dependent methyltransferase TrmA in *E. coli*. However, as only a crystal structure of TrmA with a short tRNA fragment is available (Alian *et al*. 2008), it remains unknown how exactly TrmA interacts with its two ligands, tRNA and *S*-adenosylmethionine (SAM). Therefore, in this study, I aimed to identify specific amino acid residues that play a role in ligand binding and catalysis by TrmA.

TrmA belongs to the largest class of methyltransferase enzymes (Class I). These enzymes all have a Rossmann-like fold consisting of a seven-stranded β sheet connected to alpha helices that make up the conserved catalytic domain of the enzyme. The crystal structure of the *E. coli* catalytically inactive variant TrmA E358Q in complex with a 19 nucleotide T-arm analog revealed an enzyme with two domains – a SAM-binding catalytic domain and an RNA-binding domain (Alian *et al*. 2008). The catalytic domain contains the two amino acid residues absolutely required for 5-methyluridine formation, Cys324 and Glu358, as well as several residues that help position the target nucleotide and coordinate the T-arm stem loop. In mature folded tRNA, U54 makes a reverse-Hoogsteen base pair with A58 which is not present in the TrmA-bound T-arm substrate. Instead U54 is flipped out of the stem loop into the active site making a covalent bond via carbon 6 with the thiol group of Cys324. Additionally, the bases of G57 and A58 are rotated and form a nonsequential stack with G53, U55 and C56 in the T arm. Residues Gln190, Asp299, and Glu358 of TrmA form hydrogen bonds with the target base in this flipped out position.

Van der Waals and aromatic stacking interactions between residues Phe188 and Phe351 also help to stabilize U54 within the active site of TrmA (Figure 4.1).

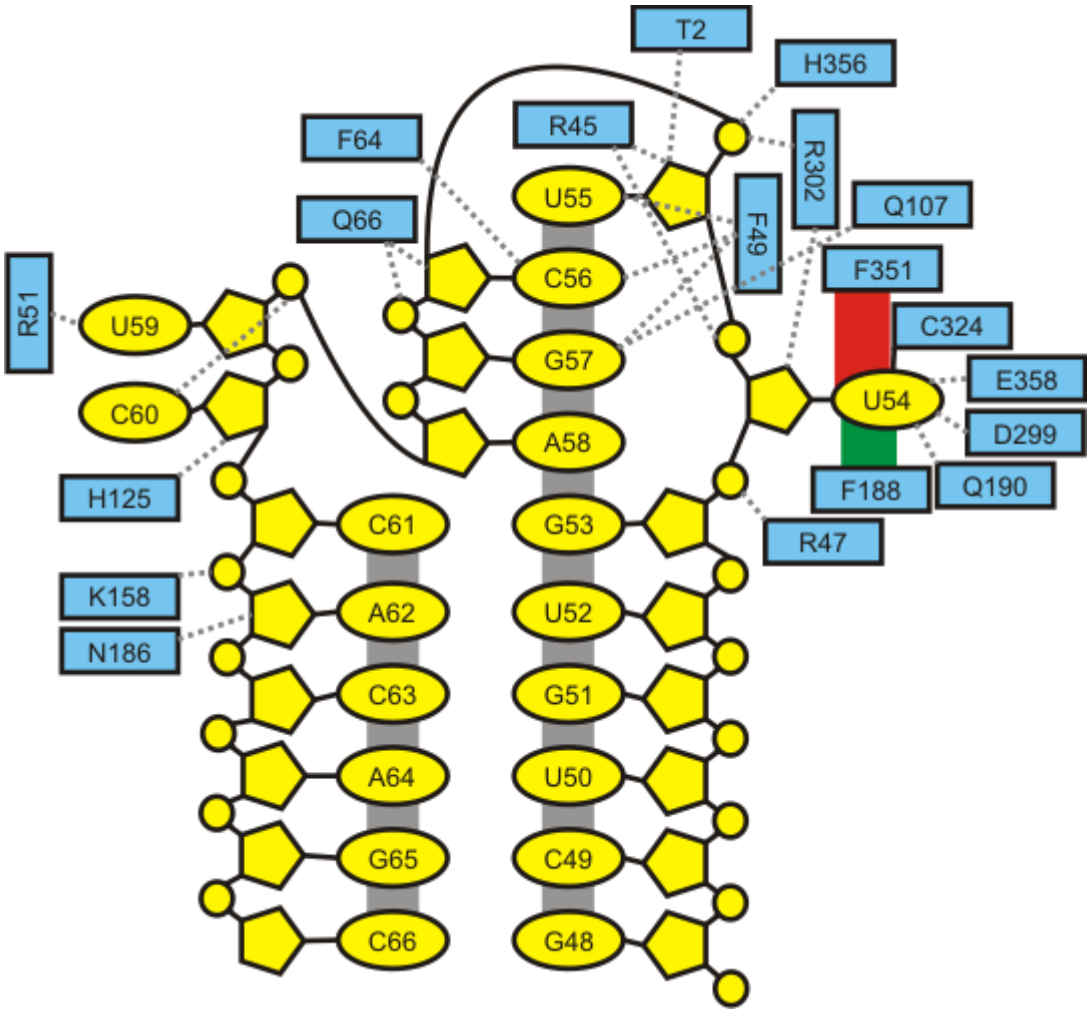

Figure 4.1. TrmA – RNA interactions. The depicted interactions were observed in the co-crystal structure (Alian *et al*. 2008). The T-arm 19-mer analog is shown in yellow with TrmA amino acids in blue. Face-to-face base stacking is depicted in grey. Edge-to-face stacking is in red and Van der Waals interaction is in green. Hydrogen bonds are shown as dotted grey lines.

TrmA locks onto its target stem loop within the catalytic cleft through several basic residue interactions. Residues Arg45, Arg47 and His356 all make hydrogen bonds to the RNA backbone, in addition to those described above. But in order to bind to the T-arm in

the catalytically active conformation with the flipped out target U54 nucleotide as observed in the crystal structure, TrmA must first break numerous tertiary interactions within the elbow region of tRNA. Unfortunately, no structural information on TrmA bound to full-length tRNA is available; therefore using the bound stem loop as a guide, the mature tRNA was docked into the TrmA crystal structure (Alian *et al*. 2008). It was proposed that clashes between residues Phe64 and Ile62 with tRNA nucleotide C56 and residue Arg51 with nucleotides G57 and G18 would help to destabilize D- and T-arm interactions in the full-length substrate. Additionally, residue Arg51 could potentially intercalate between G18 and G19 in the tRNA D-arm, thereby substituting for G57 in the canonical A58-G18-G57-G19 nucleotide stack of mature tRNA. Furthermore, TrmA residues Trp53, His54 and Phe106 could possibly make hydrophobic or aromatic stacking interactions with nucleobases U17, G18 and G19 of the D-arm, allowing the T-arm to refold within the active site. Finally, residue His125 was suggested to pack against the phosphate of G18 with its imidazole ring (Figure 4.2) (Alian *et al*. 2008).

Along with the tRNA, TrmA must also bind to the methyl group donor, SAM, within the catalytic pocket. The conserved β sheet contains a deep cleft where SAM binds to the conserved GlyXGlyX motif (Motif I) located at the end of the first β strand. This motif coordinates the methionine portion of SAM, while a conserved negatively charged residue (Glu239) in Motif II makes hydrogen bonds with the ribose hydroxyl groups (see Appendix I for alignments) (Schubert *et al*. 2003; Lee *et al*. 2004; Alian *et al*. 2008). Some investigations have been performed on bacterial phospholipid methyltransferase and SAM binding, but to our knowledge little is known about SAM-binding by bacterial

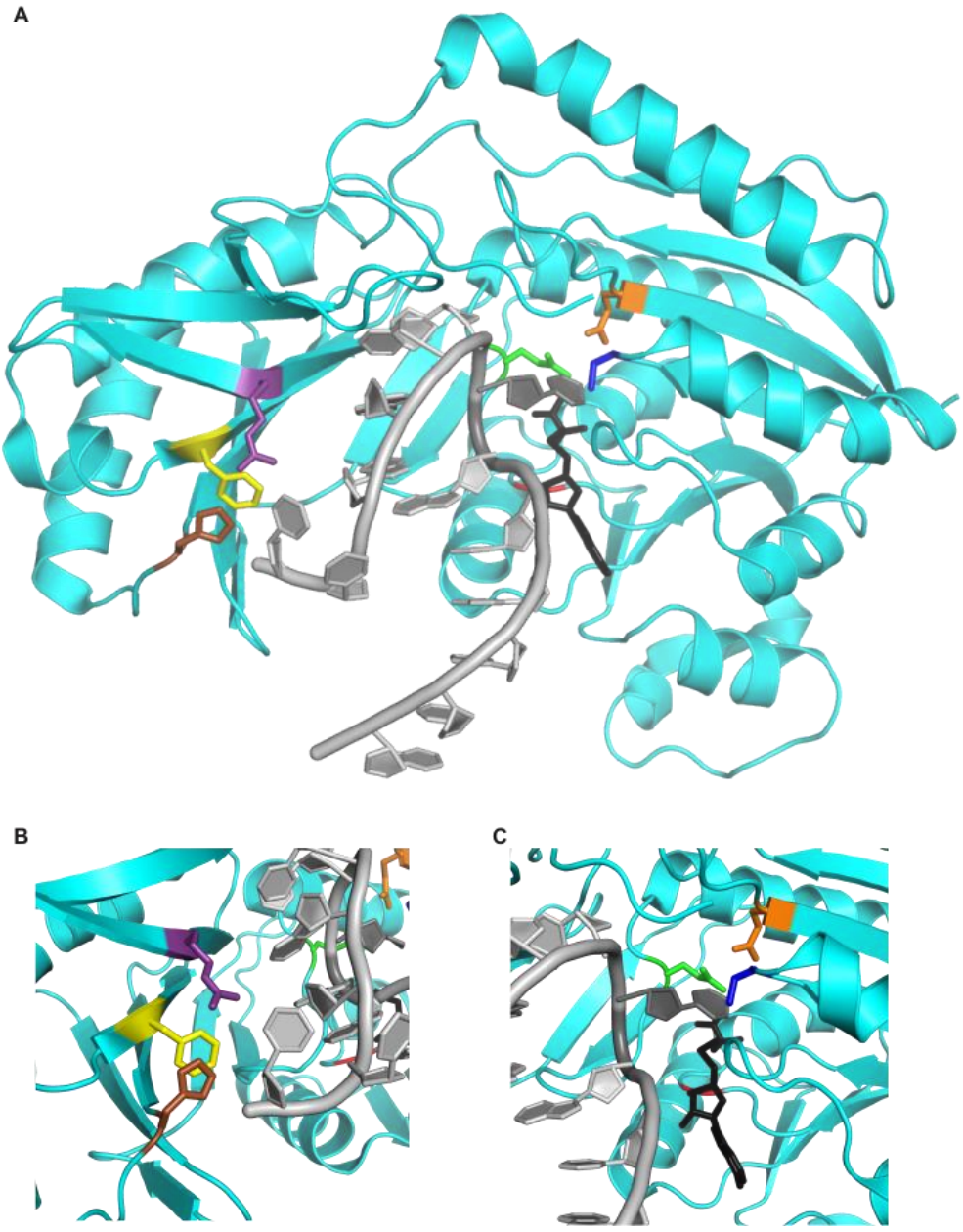

Figure 4.2 Position of residues TrmA variants analyzed with respect to catalysis and tRNA binding. A) Crystal structure (PDB 3BT7) of TrmA (cyan) in complex with 19-mer T-arm (grey) analog with SAH (black) positioned using RlmD structure as reference (PDB 2BH2) (Lee *et al.* 2004; Alian *et al.* 2008). Catalytic centre amino acids Cys324 and Glu358 are shown as line structures in blue and orange, respectively. Coordinating amino acids Gln190 (green) and Gly220 (red) are also shown as line structures. Proposed D-arm binding amino acids Arg51 (purple), Phe106 (yellow), and His125 (brown) are on the opposite side of the RNA fragment. Close-ups of the RNA binding site and the catalytic site are shown in panels B and C, respectively.

tRNA methyltransferases (Aktas *et al*. 2011). The TrmA crystal structure did not have electron density corresponding to SAM suggesting that it binds with low affinity, and can easily diffuse out of the crystal (Alian *et al*. 2008). Although no electron density was observed for SAM in the TrmA crystal structure, modeling the position of SAH (*S*-adenosyl-L-homocysteine) bound to RlmD (formerly RumA), a related *E. coli* rRNA methyltransferase, as well as comparing amino acid sequences to other methyltransferases allowed prediction of the SAM-binding surface in TrmA (Lee *et al*. 2004; Alian *et al*. 2008). In TrmA, Motif I is located in a loop region between β11 and α6, the canonical glycine-rich region (GXGX) observed in other SAM-dependent methyltransferases is made up of amino acids Gly220, Asn221, Gly222, and Asn223. SAM-binding in TrmA is likely further stabilized by aromatic stacking interactions between Tyr218 and the adenine ring of the cofactor. Unlike in other SAM-dependent methyltransferases, there seems to be no additional packing interactions on the opposite side of SAM and it remains solvent exposed in TrmA, which might explain why it wasn't bound with high occupancy in the crystal structure (Alian *et al*. 2008).

TrmA binds to tRNA in at least two steps, the first being the reversible formation of a noncovalent complex as depicted in Scheme I, with forward and reverse rate constants of k_1 and k_{-1}, respectively. This initial interaction most likely occurs through a number of basic amino acids in the RNA-binding domain and the tRNA sugar-phosphate backbone as well as hydrophobic interactions with aromatic amino acids and tRNA nucleobases, as described above. Following this initial binding event, TrmA flips the target nucleotide U54 into the catalytic site of the enzyme where the thiol group of cysteine 324 attacks carbon 6 of the uracil base forming a reversible covalent complex (complex 2 in scheme

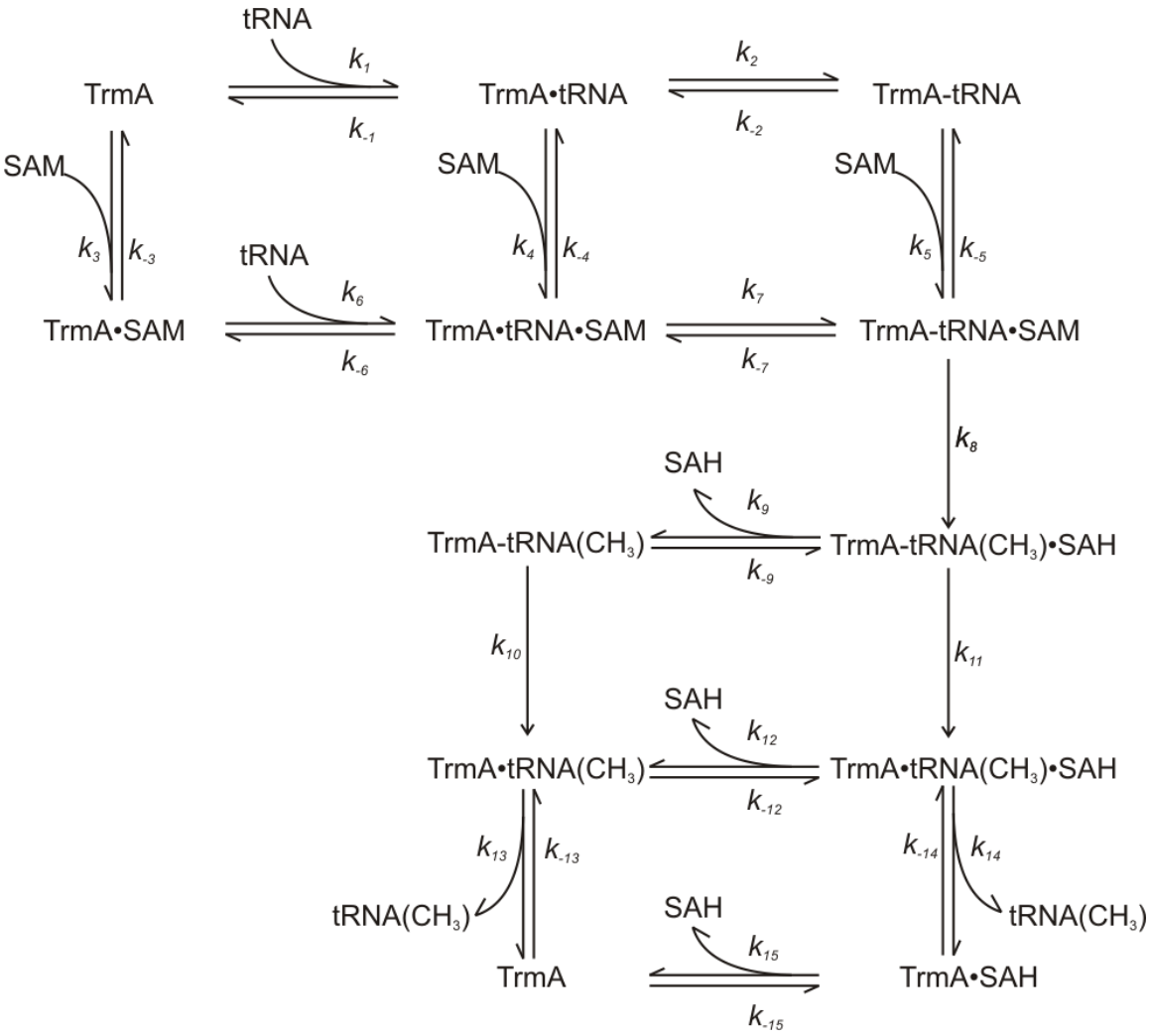

Scheme 1. Kinetics of 5-methyluridine formation by TrmA. Binding of tRNA and SAM occurs nonsequentially as both ligands can bind without the other present. However, when both are available for binding, the order of binding is unknown and therefore can proceed through multiple pathways.

I) with rate constants of k_2 and k_{-2} (Gu and Santi 1992). As described by Alian *et al*. (2008), the SAM binding site is open to the solvent, and even with full-length tRNA modelled into the structure, it seems likely that SAM can bind to TrmA after tRNA is bound. Nothing to date is known about the order of ligand binding, but previous studies have indicated RNA 5-methyluridine transferases undergo random sequential binding of the two ligands (Purich 2010). Once both ligands are bound, catalysis can proceed through the transfer of a methyl group from SAM to carbon 5 of the uracil base. To

resolve the covalent product complex, E358 in TrmA acts as a general base to abstract the proton from C5, releasing Cys324 from carbon 6 (Kealey *et al*. 1994a).

Previous studies have reported on the requirements of tRNA to be a target for TrmA methylation (Gu and Santi 1991; Gu and Santi 1992). TrmA is more active on full-length tRNA, but will modify T-arm stem loop analogs as short as 17 nucleotides. The only sequence characteristics absolutely required for activity are the conserved nucleotides U54, U55, C56, and A58, along with a loop-closing CG base pair (Gu and Santi 1991). Less is known about the amino acids required for efficient catalysis by TrmA. Therefore the amino acid substitutions in TrmA presented here were designed in order to gain a better understanding of 5-methyluridine formation in tRNA.

4.2 Materials and Methods

4.2.1 Buffers and reagents

TAKEM$_4$ buffer: 50 mM Tris-HCl, pH 7.5, 70 mM NH_4Cl, 30 mM KCl, 1 mM EDTA, and 4 mM $MgCl_2$. [5-^{3}H]UTP used in radioactive *in vitro* transcriptions was purchased from Moravek. Q5 DNA polymerase was purchased from New England Biolabs (NEB). Fluorescein-5-thiosemicarbazide fluorescent dye was purchased from LifeTechnologies. All other enzymes and chemicals were obtained from Fisher Scientific. Ecolite™ scintillation cocktail was from MP Biomedicals.

4.2.2 Protein expression and purification

QuikChange® site-directed mutagenesis (Stratagene) was used to mutate the *Escherichia coli* TrmA gene using NEB Q5 High-Fidelity DNA polymerase. The pCA24N(GFP

minus)-TrmA plasmid (JW3937) of the National Bioresource *E. coli* Project ASKA (Kitagawa *et al*. 2005) strain was used in mutagenesis reactions to construct single amino acid substitutions R51A, F106A, H125A, Q190A, G220D, C324A, and E358Q using overlapping primers (Table 4.1). All reactions were carried out using a MyCycler™ thermo cycler with conditions used in Table 4.2. The new plasmid pCA24N(GFP minus)-TrmA C324A was subsequently used as a template to generate double substitutions R51A C324A, F106A C324A and H125A C324A.

Table 4.1: Primers used for TrmA site-directed mutagenesis.

Primer Name	Sequence
TrmAQ190A sense	5′–GTAGAAAACAGCTTTACGGCGCCGAACGCGGCGATG–3′
TrmAQ190A antisense	5′–CATCGCCGCGTTCGGCGCCGTAAAGCTGTTTTCTAC–3′
TrmAG220D sense	5′–GGCGATTTACTCGAGCTGTACTGCGACAACGGTAAC–3′
TrmAG220D antisense	5′–GTTACCGTTGTCGCAGTACAGCTCGAGTAAATCGCC–3′
TrmAC324A sense	5′–GTATCCGCGTATTTTGTACATCAGCGCTAACCCGGAAACGTTATGCAAG–3′
TrmAC324A antisense	5′–CTTGCATAACGTTTCCGGGTTAGCGCTGATGTACAAAATACGCGGATAC–3′
TrmAE358Q sense	5′–CCTACACGCACCACATGCAGTGCGGCGTATTAC–3′
TrmAE358Q antisense	5′–GTAATACGCCGCACTGCATGTGGTGCGTGTAGG–3′
TrmAR51A sense	5′–GGAGTTCGCCATATGGCACGATGGCGATG–3′
TrmAR51A antisense	5′–GTGCCATATGGCGAACTCCGCGCGCATCC–3′
TrmA F106A sense	5′–CACAAGCTTGCCCAGATTGATTACCTCAC–3′
TrmA F106A antisense	5′–AATCTGGGCAAGCTTGTGGCGCAGAACGG–3′
TrmA H125A sense	5′–CTATACGCTAAGAAGCTTGATGATGAGTGG–3′
TrmA H125A antisense	5′–TCAAGCTTCTTAGCGTATAGCAGGGAAACC–3′

Table 4.2: PCR conditions for engineering TrmA variants.

Step	Temperature (°C)	Time, Cycles
Initial denaturation	98	30 seconds, 1 cycle
Denaturation	98	10 seconds, 20 cycle*
Annealing and Extension	72	9 minutes, 20 cycles*
Final extension	72	9 minutes, 1 cycle*

* For variant TrmAR51A denaturation, annealing and extension were completed for 30 cycles. Additionally, the annealing and extension step was 3 minutes and 30 seconds.

All proteins were expressed and purified as previously described using Ni^{2+}-affinity and size-exclusion chromatography (Wright *et al*. 2011). Final protein concentrations were determined through absorbance readings at 280 nm (molar extinction coefficient of 36 000 M^{-1} cm^{-1} for TrmA) and by sodium dodecyl sulphate-polyacrylamide gel electrophoresis (SDS-PAGE) followed by ImageJ (NIH) analysis. Final protein preparations were >90% pure as judged by SDS-PAGE and were RNA free as determined by A_{260}:A_{280} ratios and urea-PAGE analysis.

4.2.3 Circular dichroism spectroscopy

Enzymes were diluted to 1 µM in 50 mM sodium phosphate buffer (pH 7.5) and kept on ice prior to measurements. A Jasco J-815 CD spectrometer was initialized following a standard protocol according to Kelly *et al.* (2005). Using a 1 mm cuvette, each sample was scanned eight times, with a 1 nm band width, from 190 nm to 320 nm. To ensure correct concentration, samples were analyzed by SDS-PAGE following CD analysis.

4.2.4 tRNA preparation

Tritium-labeled $tRNA^{Phe}$ for use in activity and binding assays was prepared as described in Chapter 3. Nonradioactive tRNA was purified using a 5mL Bio-Scale Mini DEAE anion exchange column (Easton *et al*. 2010). The tRNA was eluted from the column using a gradient from 100% Buffer A (50 mM sodium phosphate pH 6.5, 150 mM sodium chloride, 0.2 mM EDTA) to 100% Buffer B (50 mM sodium phosphate pH 6.5, 2 M sodium chloride, 0.2 mM EDTA) as described in Easton *et al*. (2010). Peak fractions were analyzed by 15% urea-PAGE, pooled and ethanol precipitated. The tRNA concentration was determined photometrically by measuring the absorbance at 260 nm using the extinction coefficient of 5×10^5 M^{-1} cm^{-1}. The specific activity of the radiolabelled tRNA was determined through scintillation counting (Tri-Carb 28010TR). Absorbance measurements at 260 nm and scintillation counting were used to quantify the concentration and specific activity of the tRNA.

Table 4.3: PCR protocol for amplification of $tRNA^{Phe}$ gene.

Step	Temperature (°C)	Time, Cycles
Initial denaturation	95	5 minutes, 1 cycle
Denaturation, annealing and extension	1) 95 2) 45 (increase 1°C each repeat) 3) 72	1) 30 seconds, 6 cycles 2) 30 seconds, 6 cycles 3) 20 seconds, 6 cycles
Extension	1) 95 2) 50 3) 72	1) 30 seconds, 29 cycles 2) 30 seconds, 29 cycles 3) 20 seconds, 29 cycles
Final extension	72	11 minutes, 1 cycle

4.2.5 Tritium release assay

Tritium-labeled tRNA (1 µM) was refolded in 1× $TAKEM_4$ by heating to 65°C for 5 minutes followed by slow cooling to room temperature. The folded tRNA was added to

pre-warmed reaction mix (including enzyme and 50 µM S-adenosylmethionine (SAM)) to start the reaction. Samples were taken at select time points and the amount of released tritium corresponding to 5-methyluridine formation was determined through scintillation counting as described in Chapter 3 and previously (Lomax and Greenberg 1967; Armstrong and Diasio 1982; Wright *et al*. 2011). Single-turnover experiments were analyzed by fitting with a single-exponential function to determine the apparent rate of catalysis (k_{app}):

$$Y = Y_{max} + Amp \times \exp(-k_{app} \times t)$$

A KinTek quench-flow apparatus was used to measure pre-steady-state kinetics, where 1 µM (final concentration) [^{3}H]-tRNA^{Phe} was rapidly mixed with TrmA (final concentration 2.5 – 15 µM) preincubated with SAM (final concentration 50 µM) in TAKEM$_4$ buffer at 37°C. The reaction was quenched by the addition of 0.1 M HCl. The amount of total [^{3}H]-tRNA^{Phe} in the quenched sample was determined by scintillation counting. The amount of free tritium was quantified by subjecting a defined volume (165 – 245 µL) of the quenched sample to the tritium release assay as described above. The percentage of 5-methyluridine formation was determined as the fraction released tritium to the total radioactivity present for each time point. The resulting time courses were fit to a one exponential function to determine the apparent rate, k_{app}:

$$F = F_{\infty} + A \times \exp(-k_{app} \times t)$$

4.2.6 Methylation assay using [^{3}H]-SAM

In vitro transcribed tRNA^{Phe} was refolded as described above. The folded tRNA was then added to reaction mixture that included enzyme and 50 µM [^{3}H]-SAM. During the time

course, 40 µL aliquots were removed and spotted on 5% trichloroacetic acid (TCA) presoaked Whatman paper disks. Disks were allowed to dry, then washed 3 times with 5% TCA and finally with 100% ethanol to remove free [^{3}H]-SAM. The amount of tritium-labeled tRNA on the filters was quantified using scintillation counting.

Pre-steady-state [^{3}H]-methyl-group incorporation was examined using a quench-flow apparatus, similar as described above. Time courses were completed using tRNA^{Phe} (final concentration 1 µM) and 50 µM [^{3}H]-SAM with 5 µM TrmA wild type or TrmA E358Q. Whereas the tritium release quench-flow analysis examines the proton abstraction step, this experimental set-up measures the methyl-group transfer step. Following quenching, 260 µL of the reaction mix was spotted on Whatman paper and washed as described above. For each time point 25 µL of the reaction mix was also counted directly. Time courses were fitted with a single exponential function.

4.2.7 Nitrocellulose membrane filtration assay

To measure tRNA binding, a low constant concentration of [^{3}H]-tRNA^{Phe} (50 nM) was incubated with increasing concentrations of enzyme (0 – 60 µM) for 10 minutes in TAKEM$_4$ at room temperature to allow binding. Tritium-labeled tRNA^{Phe} was first refolded as described above. This titration was repeated in the presence of 10 µM SAM. The reaction mixture was filtered through a nitrocellulose membrane. The membrane was then washed immediately with 1 mL ice cold TAKEM$_4$ buffer and dissolved in 10 mL scintillation cocktail for 30 minutes. Similar conditions were used to measure SAM binding. Here, 50 nM [^{3}H]-SAM was incubated with increasing enzyme concentrations with and without tRNA (5 µM) present. The level of radioactive ligand binding was

determined through scintillation counting. The dissociation constant (K_D) was calculated by plotting the fraction of bound ligand against protein concentration and fitting the data to a hyperbolic function:

$$Bound = Bound_{max} \times [protein] / (K_D + [protein])$$

4.2.8 Measuring tRNA folding by aminoacylation

$TAKEM_4$ buffer was used throughout the experiment. First, *in vitro* transcribed $tRNA^{Phe}$ was unfolded at 65°C as described previously and was immediately added to precooled 0°C reaction buffer containing 6 mM ATP, 1 mM DTT, 3 mM inorganic pyrophosphatase, 3 mM phosphoenolpyruvate, and 1% pyruvate kinase. The tRNA (680 nM) was allowed to refold at 0°C for 0, 2, 5, or 20 minutes in the absence or presence of 200 nM TrmA or TrmA C324A and 50 µM SAM. Following tRNA folding, [^{14}C]Phe and Phe-$tRNA^{Phe}$ synthetase were added to the reaction mixture to final concentrations of 40 µM and 20 µM, respectively. 10 µL samples taken at different times from the aminoacylation reaction were spotted onto 5% TCA presoaked Whatman paper disks. Disks were dried, then washed 3 times with 5% TCA and finally with 100% ethanol to remove free [^{14}C]Phe. Following a final drying step at 65°C, the amount of [^{14}C]Phe-$tRNA^{Phe}$ on the disks was quantified via scintillation counting. The aminoacylation time courses were fit with a single exponential function to determine the initial level of instantaneously aminoacylated tRNA (Y_0):

$$Y = Y_0 + (Y_{max} - Y_0)\,(1 - exp(-k \times t))$$

The initial level of aminoacylated tRNA (folded tRNA) was then plotted against folding time. The resulting time courses were fit with the same exponential equation to obtain the rate of folding.

4.3 Results

In this study, specific amino acid residues of TrmA were altered with the intention of dissecting the roles they play in ligand binding and/or catalysis. To inhibit covalent complex formation, the catalytic residue Cys324 was changed to alanine, while changing Glu358 to Gln prevents proton abstraction (Kealey *et al*. 1994b). Within the SAM-binding motif, Gly220 was mutated to Asp as this change was reported to inhibit m^5U54 formation (Urbonavičius *et al*. 2007). To disturb U54 coordination within the active site, Gln190 was also mutated to alanine (Alian *et al*. 2008). In order to examine which residues are potentially important in disrupting D and T-arm interactions Arg51, Phe106 and His125 were all individually and in combination with the C324A mutation changed to alanine (Alian *et al*. 2008). Proteins containing an N-terminal hexahistidine tag were expressed from the pCA24N(GFP-) plasmid available from the AKSA database (Kitagawa *et al*. 2005). Following affinity and size exclusion chromatography, protein purity and concentration were determined as described previously (Wright *et al*. 2011). Finally, overall secondary structure was examined by CD spectroscopy to ensure amino acid substitution had no negative effect on enzyme folding (Figure 4.3).

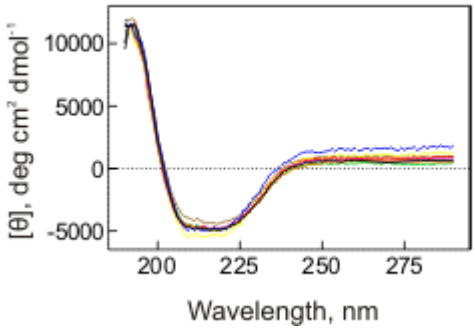

Figure 4.3. Circular dichroism spectroscopy of TrmA variants. No substantial changes in structure for the TrmA variants compared to wild type were revealed as ellipticity remained relatively unaffected between wild type and all variants. TrmA wild type (solid black line), C324A (blue), E358Q (orange), Q190A (green), G220D (red), R51A (purple), F106A (yellow), and H125A (brown) were diluted in 50 mM sodium phosphate buffer, pH 7.5, to 1 µM prior to being scanned.

4.3.1 Affinity for SAM and tRNA

In order to assess the impacts these mutations have on TrmA's ability to bind to its ligands, the wild type enzyme was examined along with all the variants using radioactive nitrocellulose filter binding assays. To measure tRNA binding, tritium-labeled tRNA substrate (50 nM) was incubated with increasing concentrations of enzyme (0 – 60 µM) in the presence and absence of SAM cofactor (50 µM). The wild type enzyme binds substrate tRNA with an affinity of 20 ± 10 nM which reflects a combination of both noncovalent (k_1) and covalent (k_2) complexes formed between TrmA and tRNA (Figure 4.4A; Scheme 1). This affinity decreased approximately 30-fold upon the addition of SAM to the reaction mix as the enzyme proceeds through catalysis, therefore reflecting TrmA's binding dissociation constant for m^5U-containing product tRNA instead (Table 4.4). Similarly, 10 nM of tritium-labeled SAM was incubated with increasing enzyme concentrations in the presence or absence of unlabeled tRNA (5 µM). For TrmA wild

type, [^{3}H]-SAM binds with a low affinity of approximately 17 µM (Alian *et al*. 2008). Interestingly, this affinity does not improve with the addition of tRNA to the reaction mix (Figure 4.4B; Table 4.4).

The C324A TrmA variant, which is unable to form a covalent complex with tRNA, has more than a 50-fold higher affinity for tRNA in the presence of SAM than for tRNA alone, 0.03 ± 0.02 vs 1.08 ± 0.16 µM (Figure 4.4C; Table 4.4). Unlike the wild type enzyme, the dissociation constant for SAM binding also decreases in the presence of tRNA from 24 µM to 150 nM, suggesting that having both ligands present results in tighter binding of each substrate (Figure 4.4D).

The TrmA E358Q variant results in an enzyme that can undergo covalent complex formation as well as methyl-group transfer, but cannot undergo proton abstraction (Figure 4.7A). Measuring the affinity for tRNA revealed very tight binding of tRNA to TrmA in the presence and absence of SAM, 0.011 ± 0.007 and 0.07 ± 0.04 µM, respectively (Figure 4.4E; Table 4.4). Comparable to the C324A variant, TrmA E358Q binds to tritium-labeled SAM with a dissociation constant of approximately 14 µM which decreased considerably upon addition of tRNA (Figure 4.4F; Table 4.4).

In order to methylate U54, TrmA flips its target base out of the T-arm stem loop into its active site. Residue Q190 forms hydrogen bonds with U54 in the flipped out conformation, thereby most likely helping to stabilize and coordinate the base for catalysis. When Q190 is mutated to alanine in TrmA, the affinity for tRNA is reduced 14-fold compared to the wild type enzyme (Figure 4.4G; Table 4.4). Upon the addition of SAM, like the wild type enzyme, the affinity for tRNA also decreases compared to tRNA

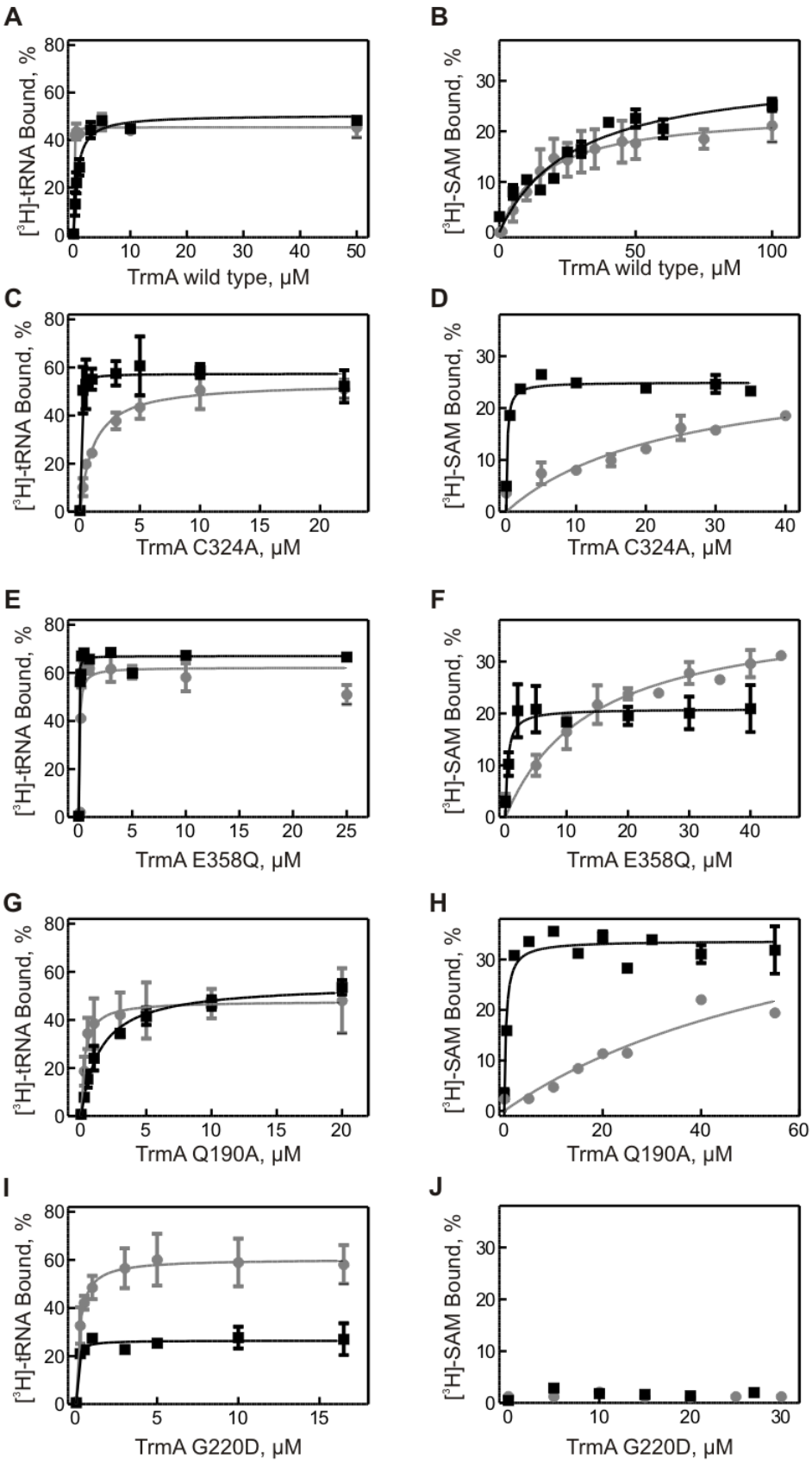

Figure 4.4 A complete figure legend can be found on the next page.

Figure 4.4. Ligand binding analysis of TrmA wild type and active site variants. Nitrocellulose filter binding assays were completed with 50 nM ^{3}H- tRNA (left panels: A, C, E, G, I) or 50 nM ^{3}H-SAM (right panels: B, D, F, H, J). Increasing concentrations of enzyme were titrated into the radioactive ligand either in the presence (black squares) or absence (grey circles) of the other ligand. Different TrmA variants were tested: TrmA wild type (A & B), TrmA C324A (C & D), TrmA E358Q (E & F), TrmA Q190A (G & H), and TrmA G220D (I & J). Following a short incubation, reaction mixtures were filtered and washed with cold buffer. The retained radioactivity was quantified via scintillation counting. The percentage of bound substrate was plotted against enzyme concentration and fitted with a hyperbolic curve (smooth lines). The dissociation constant for each enzyme is reported in Table 4.4.

Table 4.4. Dissociation constants for TrmA variants binding to (unmodified) tRNA and/or SAM as determined through nitrocellulose filtration.

	K_D, µM			
TrmA variant	**[^{3}H]-tRNA**	**[^{3}H]-tRNA + SAM**	**[^{3}H]-SAM**	**[^{3}H]-SAM + tRNA**
Wild type	0.02 ± 0.01	0.66 ± 0.11*	17 ± 2	27 ± 6
C324A	1.08 ± 0.16	0.03 ± 0.02	24 ± 11	0.15 ± 0.06
E358Q	0.07 ± 0.04	0.011 ± 0.007	14 ± 3	0.38 ± 0.21
Q190A	0.28 ± 0.10	1.5 ± 0.2*	75 ± 52	0.39 ± 0.15
G220D	0.22 ± 0.05	0.06 ± 0.03	no binding	no binding
R51A	0.14 ± 0.07	1.15 ± 0.34*	9 ± 3	6 ± 3
R51AC324A	2.8 ± 0.7	0.16 ± 0.06	17 ± 5	0.78 ± 0.70
F106A	1.0 ± 0.4	2 ± 1*	6 ± 2	2 ± 1
F106AC324A	18 ± 7	6 ± 2	56 ± 34	10 ± 7
H125A	4 ± 3	6 ± 2*	20 ± 5	2 ± 1
H125AC324A	47 ± 27	3 ± 1	13 ± 9	5 ± 2

*TrmA variants that are active in tRNA methylation will form methylated tRNA when incubated with both tRNA and and excess of SAM. In these cases, the binding of methylated tRNA, i.e. the product of TrmA, is observed rather than binding of unmodified substrate tRNA.

alone, by about 5-fold to 1.5 ± 0.2 µM. Like the C324A and E358Q variants, TrmA Q190A has a very low affinity (75 ± 52 µM) for SAM when tRNA was not present which increased dramatically when tRNA was included in the reaction mixture (Figure 4.4H; Table 4.4).

The substitution of aspartate for glycine at position 220 in TrmA was the most dramatic residue change in TrmA, but did not result in any major changes to protein structure as observed by molar ellipticity (Figure 4.3). This alteration takes place in the conserved SAM-binding GXGX motif common to SAM-dependent methyltransferases. When TrmA G220D was titrated into tritium-labeled tRNA alone, the affinity of TrmA to tRNA was determined as 220 ± 50 nM, which became tighter upon the addition of SAM to 60 ± 30 nM (Figure 4.4I; Table 4.4). Measuring SAM-binding directly using tritium-labeled SAM revealed only background level counts with or without tRNA present, thus suggesting that SAM binding is greatly reduced by this amino acid change as predicted (Figure 4.4J).

TrmA R51A showed a similar trend to TrmA wild type, where the affinity for tRNA alone was 140 ± 70 nM which decreased to approximately 1 µM when SAM was present (Figure 4.5A; Table 4.4). Of note is the endlevel for this TrmA variant; although the dissociation constants are similar to other variants, only 20% saturation was reached which is half of the endlevel observed with wild type enzyme or its corresponding double mutant R51A C324A. Conversely, the endlevel for SAM binding was similar to wild type, and SAM binding did not change when tRNA was included in the titration with dissociation constants of 9 ± 3 µM without tRNA and 6 ± 3 µM with tRNA (Figure 4.5B; Table 4.4). In contrast to the single R51A variant, the catalytically inactive variant TrmA R51A C324A had the same trend as the single substitution variant TrmA C324A, where tRNA affinity increased from 2.8 ± 0.7 µM to 160 ± 60 nM in the presence of SAM, while SAM affinity also increased from 17 ± 5 µM to 800 ± 700 nM in the presence of tRNA (Figures 4.5C and D; Table 4.4).

For the TrmA F106A variant, neither tRNA nor SAM affinity change significantly upon the addition of the other ligand (Figure 4.5E: Table 4.4). However, tRNA binding is reduced when compared to the wild type enzyme. While the F106A variant can still form a covalent bond, the F106A C324A variant cannot and reflects the ability of TrmA to form noncovalent complexes with tRNA and SAM. TrmA F106A C324A binds to tritium-labeled tRNA with an extremely low affinity of almost 18 μM, an 18-fold reduction compared to the single substitution C324A variant (Figure 4.5G; Table 4.4). Unlike TrmA C324A, the affinity for tRNA did not greatly improve with the addition of SAM, as TrmA F106A C324A has a tRNA affinity of approximately 6 μM. SAM binding by TrmA F106A C324A is reduced compared to TrmA F106A, but does become tighter when tRNA is added, although the affinity is still 3-fold lower than for TrmA F106A and 60-fold lower than for TrmA C324A (Table 4.4).

The affinity for tRNA binding to TrmA H125A does not change (within standard deviation) when SAM is included in the titration (Figure 4.5I; Table 4.4). However, SAM affinity increased when both ligands were present (Figure 4.5J: Table 4.4). The double substitution variant TrmA H125A C324A has the greatest effect on tRNA binding with an affinity of 47 μM in the absence of SAM (Figure 4.5K; Table 4.4). When SAM was added, the tRNA affinity improved to approximately 3 μM, which is similar to the H125A variant but more than a 100-fold reduction compared to the C324A variant (Table 4.4). The affinity for SAM remained relatively unchanged whether tRNA was present or not (Figure 4.5L; Table 4.4).

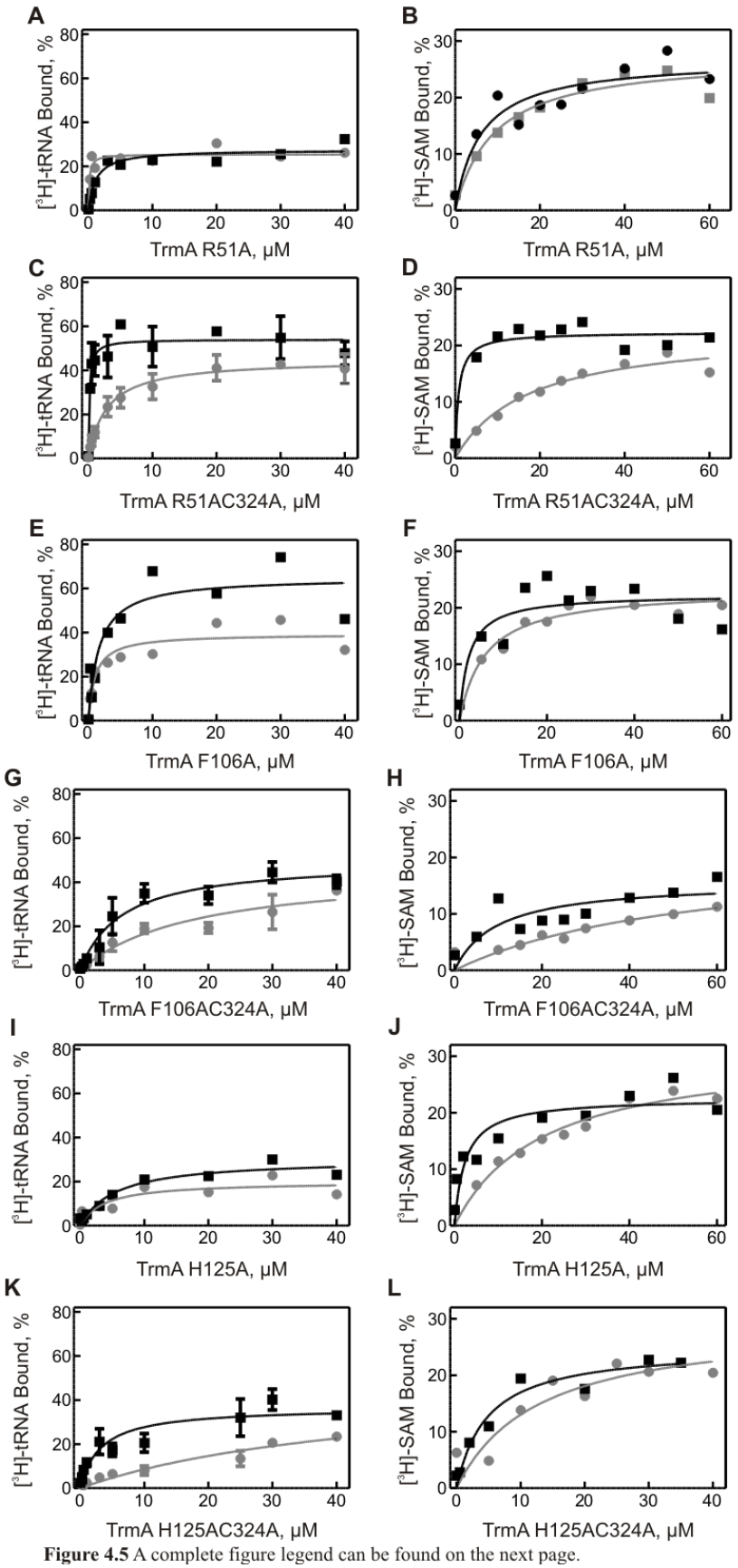

Figure 4.5 A complete figure legend can be found on the next page.

Figure 4.5. Analysis of ligand binding by TrmA variants proposed to be impaired in tRNA binding. Nitrocellulose filter binding assays were completed with 50 nM ^{3}H-tRNA (left panels) or 50 nM ^{3}H-SAM (right panels). Increasing concentrations of enzyme were titrated into the radioactive ligand either in the presence (black squares) or absence (grey circles) of the other ligand. TrmA variants tested were: TrmA R51A (A & B), TrmA R51A C324A (C & D), TrmA F106A (E & F), TrmA F106A C324A (G & H), TrmA H125A (I & J), and TrmA H125A C324A (K & L). Data was fitted with a hyperbolic curve and dissociation constants for each variant can be found in Table 4.4.

4.3.2 Steady-state 5-methyluridine formation

Since methylation of U54 occurs at position C_5, the tritium release assay was used to monitor the level of modification in tRNA similarly to measuring pseudouridine formation (Lomax and Greenberg 1967; Armstrong and Diasio 1982; Santi and Hardy 1987; Wright *et al*. 2011). Briefly, tritium-labeled tRNA is incubated with enzyme and upon methyl-group addition to C5, the tritium label at this position is abstracted and released into the supernatant where it can be isolated and counted. Increasing levels of tritium reflect the increase in modification over time. First, TrmA wild type was analyzed under multiple-turnover conditions and compared to the well characterized pseudouridine synthase enzyme TruB. Since all uridines within the tRNA are labeled with tritium at position C_5, I can detect both methylation and pseudouridine formation within the same tRNA. By themselves, both enzymes are active in forming their respective modifications as observed by the increase in tritium released over time (Figure 4.6A). TrmA (20 nM) appears to be slower than TruB (20 nM) under these conditions as TruB reaches 100% tritium release (pseudouridine formation) in approximately 10 minutes, while TrmA only reaches ~50% tritium release (methylation) in the same time frame. Neither enzyme exceeds 100% tritium release (within error) when used individually in the assay; however when the enzymes are both included in the reaction mix, tritium release reaches more

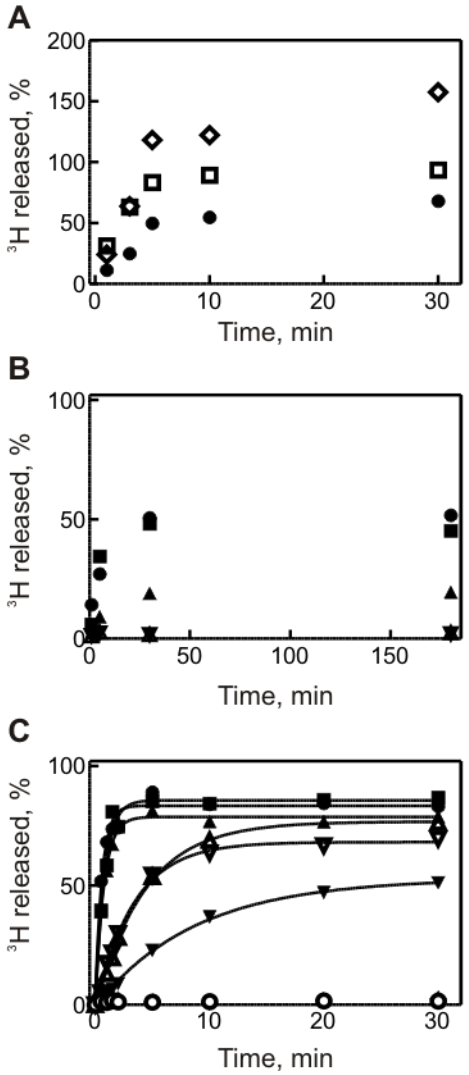

Figure 4.6. Tritium release assays to detect 5-methyluridine formation by TrmA. Tritium-labeled tRNA was incubated with enzyme in the presence of excess methyl group donor SAM (50 µM). For multiple-turnover assays (A & B), 20 nM enzyme was incubated with 600 nM substrate. Single-turnover conditions (5 µM enzyme vs. 600 nM substrate) were used for determining methylation activity rates for TrmA variants (C). Samples were taken at the indicated time points, quenched in 0.1% HCl and the released tritium extracted and quantified (see Materials and Methods for details). A) Activity of TrmA wild type and TruB wild type acting on tRNA substrate. TrmA catalyzed U54 methylation (circles) and TruB U55 pseudouridylation (open squares) is shown. Both can act on the same tRNA when incubated together (open diamonds). TrmA variants were assessed under multiple (B) and single-turnover conditions (C): TrmA wild type (circles), TrmA Q190A (triangles), TrmA G220D (inverted triangles), TrmA R51A (squares), TrmA F106A (open triangles), TrmA H125A (open inverted triangles), TrmA C324A (open circles), and TrmA E358Q (diamonds). Double substitution versions of TrmA R51A C324A, F106A C324A, and H125A C324A are not shown but were inactive in both single- and multiple-turnover assays. The data from single-turnover assays were fitted with a single-exponential function to determine a k_{app} for each enzyme (Table 4.5).

than 150% after 30 minutes indicating that both enzymes are active on the same tRNA, but are specific to their target base (Figure 4.6A).

To characterize the TrmA variants, both multiple- and single-turnover tritium release assays were completed. Only three variants were active under multiple-turnover conditions (20 nM enzyme vs 600 nM [^{3}H]-tRNA). TrmA wild type and TrmA R51A, which reached approximately 50% methylation in 30 minutes, plus TrmA Q190A which was considerably slower and only reached 20% tritium release even after 180 minutes (Figure 4.6B). Under single-turnover conditions, where a large excess of enzyme catalyzes a single round of methylation on a small pool of tRNA, I can detect activity in some of the other variants (Figure 4.6C; Table 4.5). The single-turnover time courses were fitted with a single exponential equation to determine a rate for each variant. Predictably, both TrmA C324A and E358Q variants, as well as the double substitution variants: R51A C324A, F106A C324A, and H125A C324A, were inactive in the tritium release assay regardless of enzyme concentration as they were designed to be impaired at different steps along the catalytic pathway preventing product formation (Figure 4.7A). TrmA Q190A, which was designed to potentially impair U54 recognition and stabilization, showed near wild type behavior (Figure 4.6C). TrmA R51A shows a similar level of activity as both Q190A and the wild type enzymes (Figure 4.6C).

The remaining TrmA variants all had reduced catalytic activity compared to the wild type. TrmA G220D, which was intended to disrupt SAM binding, has a rate almost 50-fold slower than the wild type at only 0.002 s^{-1}.The remaining variants TrmA F106A and TrmA H125A have rates of 0.004 ± 0.001 and 0.005 ± 0.001 s^{-1}, respectively (Figure

4.6C). These two variants were designed to impair TrmA's ability to disrupt D- and T-arm interactions within the tRNA.

Table 4.5. Rate of U54 methylation by TrmA variants under single-turnover conditions. Rates were determined by fitting tritium release time courses with an single exponential function.

TrmA variant	rate, min^{-1}	Fold change
Wild type*	5.4 ± 0.6	-
C324A	not active	-
E358Q	not active	-
Q190A	1.33 ± 0.09	-
G220D	0.11 ± 0.01	49
R51A	1.28 ± 0.13	-
R51AC324A	not active	-
F106A	0.23 ± 0.01	23
F106AC324A	not active	-
H125A	0.30 ± 0.02	18
H125AC324A	not active	-

*Rate determined from quench-flow analysis

4.3.4 Rapid kinetics analysis of 5-methyluridine formation

Quench flow kinetic analysis of TrmA catalysis allows us to dissect the individual steps along the reaction pathway under pre-steady-state conditions. Using tritium-labeled tRNA (1 μM), SAM (50 μM) and the wild type enzyme (2.5, 5, and 10 μM), the proton abstraction step could be observed directly. Using a modified version of the tritium release assay, the level of tritium in the supernatant following rapid mixing and quenching, corresponds to the level of proton abstraction and indirectly methylation. All three TrmA concentrations examined have a similar rate of tritium release when the data was fitted with a single-exponential function (average rate of 0.09 ± 0.01 s^{-1}) (Figure 4.7B).

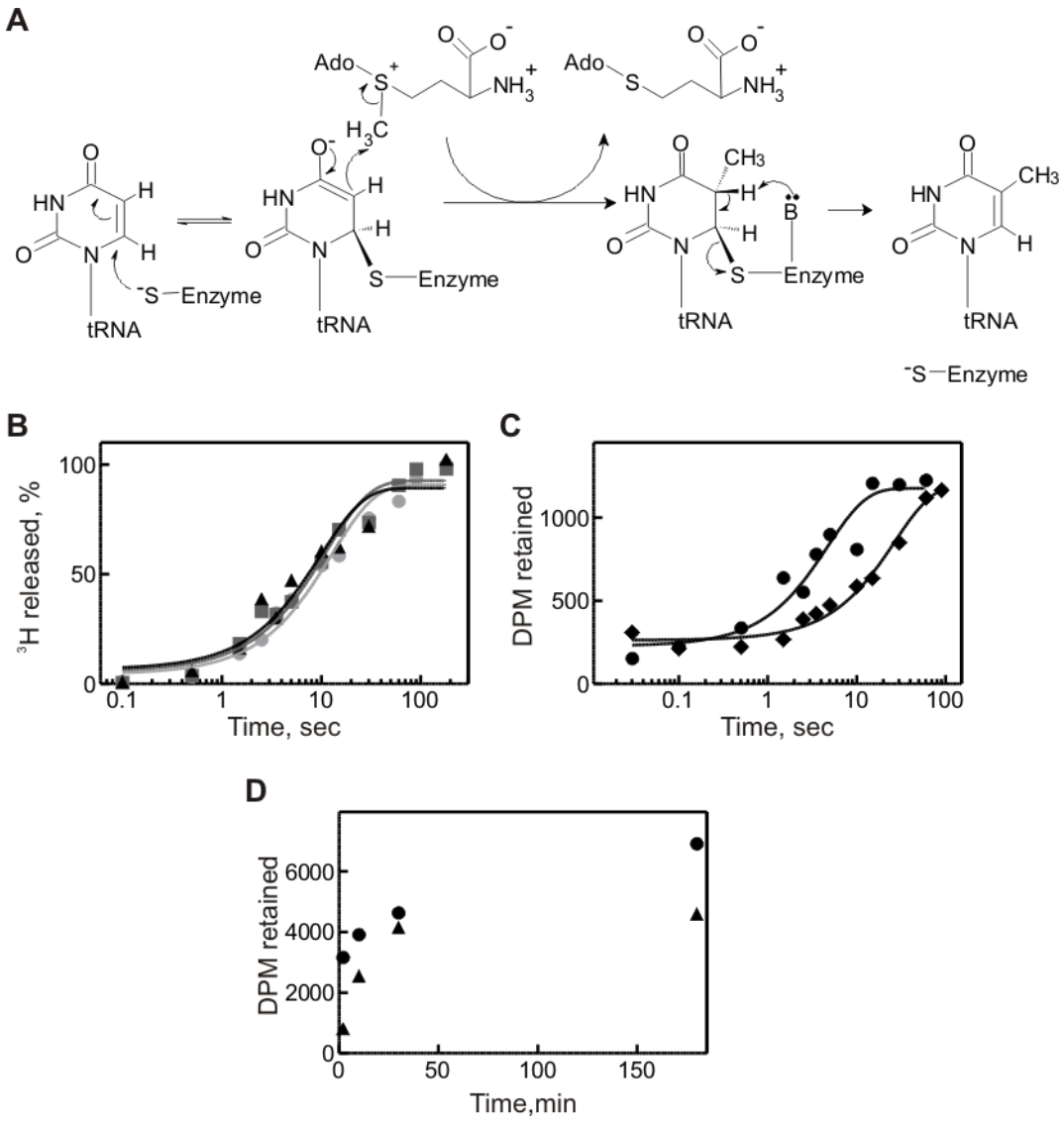

Figure 4.7. Dissecting U54 methylation in tRNA^{Phe} by means of pre-steady-state kinetics. A) The chemical mechanism of 5-methyluridine formation by TrmA has been reported previously (Kealey *et al.* 1994; Alian *et al.* 2008). The first step involves the thiol group of a cysteine (C324) residue attacking carbon 6 of the target uracil creating a covalent bond and a nucleophilic centre at carbon 5. The methyl group of SAM is then transferred to carbon 5 and following β-elimination via proton abstraction by an aspartate (E358) residue, the product tRNA is released from the enzyme. B) Pre-steady-state conditions were used to assess the rate of product formation by TrmA using quench flow. Tritium-labeled tRNA (final concentration 1 µM) was rapidly mixed with 2.5 (light grey circles), 5 (dark grey squares), and 10 µM (black triangles) TrmA wild type (preincubated with 50 µM cold SAM) for a defined amount of time before being quenched with HCl. The amount of released tritium was quantified via scintillation counting and plotted against time. The resulting data was fitted with a single exponential function to ascertain a k_{app}. C) Quench flow experiments were completed with TrmA wild

type (circles) and TrmA E358Q (diamonds) to examine the methyl-group transfer step. Unlabeled tRNA (final 1 μM) was rapidly mixed with enzyme (final 5 μM concentration) which was preincubated with tritium-labeled SAM cofactor (final concentration 50 μM). Following quenching, the incorporated radioactive methyl group was quantified by spotting on TCA soaked Whatman paper as described in Materials and Methods. The retained level of radioactivity was plotted against time and fitted with a single exponential function. D) Methylation reactions were completed under multiple- (20 nM TrmA; triangles) and single-turnover (5 μM TrmA; circles) conditions using 600 nM cold tRNA and 50 μM [^{3}H]-SAM.

The rate of methyl group transfer was measured using tritium-labeled SAM (50 μM) and unlabeled tRNA (1 μM) under the same quench flow conditions. Once samples were rapidly mixed and quenched, they were spotted on TCA-soaked Whatman paper and the incorporated radioactive methyl group was quantified using scintillation counting (see Materials and Methods for details). Using both the wild type enzyme and TrmA E358Q (final concentration of 5 μM), the rate of methylation was determined by fitting the time courses with a single exponential equation (Figure 4.7C). The wild type had a rate of 0.21 ± 0.06 s^{-1}, while the E358Q variant had a rate approximately 6-fold slower at 0.037 ± 0.006 s^{-1}. Product formation was analyzed under steady-state conditions as well using 20 nM and 5 μM TrmA wild type incubated with 600 nM tRNA and 50 μM [^{3}H]-SAM (Figure 4.7D).

4.3.5 TrmA increases fraction of folded tRNA *in vitro* independent of catalytic activity

It has already been established that aminoacylation of correctly folded tRNA occurs rapidly *in vitro*, followed by slower aminoacylation as un- or misfolded tRNAs fold (Bhaskaran *et al.* 2012). Therefore, TrmA's ability to promote tRNA folding was examined using aminoacylation as an indirect readout (Figure 4.8). *In vitro* transcribed $tRNA^{Phe}$ was unfolded and allowed to refold for a predetermined time in the absence or

presence of TrmA or catalytically inactive TrmA C324A. The fraction of instantaneously aminoacylated tRNA was plotted against folding time and revealed that the fraction of tRNAs active in aminoacylation increased with either enzyme over the no enzyme

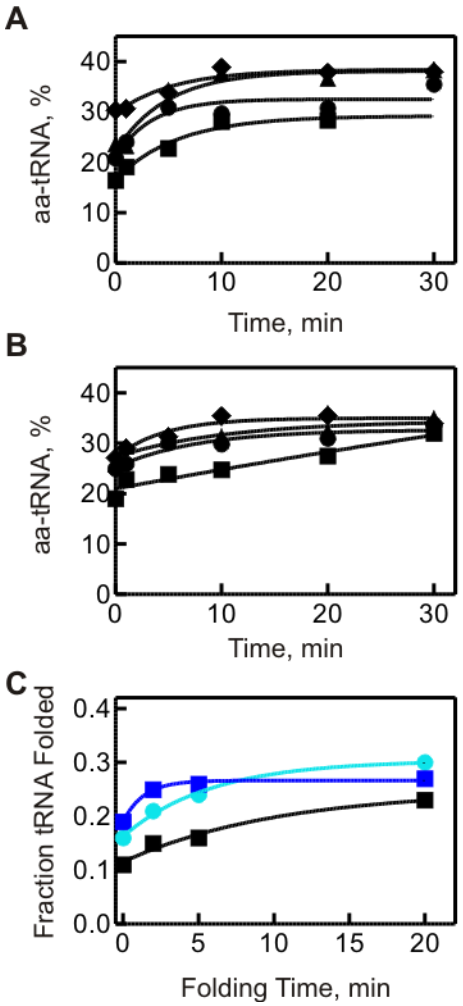

Figure 4.8. Aminoacylation assays to indirectly measure tRNA folding in the presence and absence of TrmA. *In vitro* transcribed tRNAPhe was unfolded and then refolded for 0 (squares), 2 (circles), 5 (triangles), or 20 minutes (diamonds) at 0ºC, then used as substrate in aminoacylation reactions. Figures A and B demonstrate representative time courses of the aminoacylation reactions following tRNA refolding in the presence of TrmA wild type (A) or TrmA C324A (B). The initial fraction of aminoacylated tRNA was plotted against folding time to demonstrate the increase in tRNAs that were instantaneously aminoacylated when either enzyme was included during the refolding step (C). The data for no enzyme control (black squares), TrmA wild type (blue circles), and TrmA C324A (dark blue squares) were fitted with an exponential function to determine the rate of folding.

control, suggesting that TrmA is indeed assisting in tRNA folding regardless of 5-methyluridine formation.

4.4 Discussion

This investigation describes the quantitative biochemical characterization of ligand binding and catalysis by *E. coli* tRNA 5-methyluridine methyltransferase TrmA. Although this enzyme shares many structural elements and conserved motifs with other Class I methyltransferases, this is the first study to biochemically identify amino acids that are important for tRNA binding within TrmA which can further our understanding of the evolution of this enzyme family. Through mutagenesis and subsequent thermodynamic and kinetic analysis, I confirm that TrmA undergoes random sequential binding of its two ligands and demonstrate that binding is cooperative. Additionally, I corroborated the roles of amino acids within the RNA binding domain of TrmA and their importance for interactions with the D-arm and positioning of the tRNA.

TrmA ligand binding is random and cooperative

Scheme I describes binding, catalysis, and release steps involved in 5-methyluridine formation by TrmA. By altering specific amino acids within the active site of TrmA, I have been able to provide evidence that TrmA is a random bi-bi enzyme that undergoes random sequential binding of its two ligands (Cleland 1973). Filter binding assays revealed that TrmA is able to bind to both ligands, tRNA and SAM, independently of each other. All four catalytic cleft variants, C324A, E358Q, Q190A, and G220D, were able to bind to tRNA in the absence of SAM with affinities ranging from 70 nM to 1 µM, compared to the wild type with an affinity of 20 nM (Table 4.4). TrmA wild type,

C324A, E358Q, and Q190A were also able to bind SAM when tRNA was not present although with much lower affinity (14 to 75 μM). These findings indicate that TrmA does not require binding of both substrates simultaneously, or a preferential order to binding and supports the random sequential binding mechanism. It is unknown whether the closely related *E. coli* rRNA 5-methyluridine transferases also share this ligand binding mechanism; however other types of methyltransferases do, such as the rRNA adenine-N^6-methyltransferases and the mRNA 2′-O-methyltransfereases (Purich 2010).

TrmA wild type, E358Q, Q190A, and G220D form covalent complexes with tRNA, whereas TrmA C324A provides a means of evaluating noncovalent binding of the substrates. Additionally, the C324A substitution permits measurement of tRNA binding in the presence of SAM without product formation and vice versa. Analysis of TrmA C324A reveals that ligand binding is in fact cooperative and does not require the formation of a covalent bond between tRNA and enzyme. TrmA C324A's affinity for tRNA in the presence of SAM increases 30-fold compared to tRNA alone, while the affinity for SAM also increases 160-fold with the addition of tRNA. Comparing the two tRNA titrations for TrmA C324A with and without SAM, I can speculate on the effects of SAM binding on the dissociation constants, K_1 and K_6 (Scheme I). One possibility is that tRNA binding (k_6) is increased (compared to k_1) when SAM is bound first. Alternatively or in combination to an increase in k_6, the reverse rate k_{-6} may decrease compared to k_{-1}, which is supported by the increase in the observed endlevel in the filter binding assay (Figure 4.4C). By binding to SAM before binding to tRNA, the enzyme may undergo some conformational change within the active site that renders TrmA more accessible for tRNA, perhaps by shielding the tRNA from acidic amino acids lining the

SAM-binding interface (Lee *et al*. 2004; Lee *et al*. 2005; Alian *et al*. 2008). Additionally, the active site may be stabilized by SAM and therefore U54 can be flipped out to create a more stable ternary noncovalent complex that is less likely to dissociate (Lee *et al*. 2004; Lee *et al*. 2005). Both scenarios would result in an increase in affinity for tRNA by TrmA C324A. This synergistic effect was also observed for SAM binding by TrmA C324A. Here the increase in SAM affinity in the presence of tRNA could be simply due to a closure of the active site, thus slowing down SAM diffusion (decrease in k_{-4}). In the RlmD (RumA) crystal structure, the adenine moiety of SAM is sandwiched between an aromatic residue and adenine base of the substrate rRNA (Lee *et al*. 2005). While TrmA also packs against the adenine ring of its cofactor with tyrosine 218, there are no aromatic residues or substrate bases that could flip into the SAM-binding site and pack against the other side (Alian *et al*. 2008). Therefore the exact method of SAM stabilization in the presence of tRNA remains unknown.

Comparing the TrmA C324A data to that of TrmA E358Q I can assess the effects of covalent complex formation on tRNA affinity. Since the K_D for tRNA binding by TrmA C324A in the absence of SAM is equal to K_1, this value can be substituted into the K_D equation for TrmA E358Q in order determine a value of 0.06 for K_2. This indicates that the equilibrium for this step lies towards the formation of the covalent complex. Additionally, TrmA E358Q's affinity for tRNA alone is comparable to wild type (70 nM vs 20 nM) as they both can proceed through covalent complex formation and would most likely have a similar rate of covalent complex formation. The addition of SAM during the TrmA E358Q tRNA titration had much less impact on tRNA binding than that observed for TrmA C324A, only increasing the affinity by approximately 7-fold. These findings

suggest that covalent bond formation and not the cooperative binding of SAM has a greater impact on tRNA binding, which is not surprising as discussed above, the tendency would be to form covalent binary complex as shown by K_2.

Within the active site, Gln190 helps to coordinate U54 for methylation. Interestingly, TrmA Q190A is active in both multiple and single-turnover assays (Figures 4.6B & C). While much lower in activity compared to the wild type under multiple-turnover conditions, TrmA Q190A has a rate comparable to wild type in the single-turnover assay. These findings indicate that Gln190 is dispensable for activity in contrast to earlier suggestions (Urbonavičius *et al*. 2007). In the TrmA crystal structure, Gln190 forms bidentate hydrogen bonds to N_3 and O_4 of U54. Additionally, Gln190 can hydrogen bond to Asp299 as well as U54 O_2 through a water bridge, all interactions that were lost with the alanine substitution (Lee *et al*. 2005; Alian *et al*. 2008). The data presented here suggest that these interactions are not crucial for catalysis by TrmA which is in contrast to findings with RlmD since the corresponding RlmD Q265A variant was 830-fold slower than the wild type enzyme under multiple-turnover conditions (Lee *et al*. 2005). Comparison of the substrate tRNA titrations (no SAM present), revealed that the Q190A mutation resulted in 14-fold reduction in affinity relative to the wild type substrate tRNA affinity. In the wild type enzyme this amino acid coordinates the positioning of the target nucleotide U54 in the active site, along with Phe188, Phe351, and Asp299 (Alian *et al*. 2008). These interactions allow for the attack of uracil C_6 by the thiol group of Cys324 and hydrogen bonding to Glu358 for later proton abstraction. I hypothesize that initial tRNA binding, represented by k_1 and k_{-1}, is unaffected by this amino acid change, as most contacts between tRNA and TrmA remain the same as in the wild type. If this assumption

is true, then the change in affinity would be due to changes of k_2 and k_{-2}. By introducing alanine at this position the tRNA could potentially be in a less stable position, or not anchored correctly in the active site, therefore resulting in a reduction in the rate of stable covalent complex formation (k_2) and thus a reduction in the rate of catalysis for covalent bond formation as observed under multiple-turnover conditions.

Both TrmA wild type and TrmA Q190A can form product when both ligands are present in the filter binding assay. Consequently both enzymes bind to 5-methyluridine-containing tRNA with reduced affinity relative to substrate tRNA, a 33-fold reduction for wild type and a 5-fold reduction for TrmA Q190A. Since the tRNA titration with SAM had such a large SAM excess, catalysis was able to be pushed forward to product formation, similar to conditions used during single-turnover activity assays. However, in the SAM titration, where tRNA was included albeit at concentrations significantly lower than the SAM concentration, complete product formation with respect to SAM turnover was not possible. Therefore, I observe SAM binding directly in the presence of tRNA like with TrmA C324A, and the increased affinity in presence of both ligands suggests again the cooperative binding between the two ligands.

The G220D mutation in TrmA was initially observed over 40 years ago (Björk and Neidhardt 1975). The authors isolated *E. coli* strains lacking 5-methyluridine in tRNA transcripts and this mutation was later further analyzed by Urbonavičius *et al.* (2007). Based on sequence alignments and structural analysis, G220 is a part of Motif I, the conserved GXGX SAM-binding motif of Class I SAM-dependent methyltransferases (Urbonavičius *et al*. 2007; Alian *et al*. 2008). This TrmA variant was not able to form 5-methyluridine *in vivo*, nor was it able form stable covalent complexes (Urbonavičius *et*

al. 2007). As reported here, TrmA G220D has considerably reduced activity under single-turnover tritium release conditions with a rate 15-fold slower than the wild type, and has undetectable activity under multiple-turnover conditions (Figures 4.6B). However, we were able to detect tRNA binding using radiolabeled substrate and nitrocellulose filter binding assays (Figure 4.4I). Compared to the wild type, the affinity of TrmA G220D for tRNA in the absence of SAM is reduced more than 10-fold. This could be due to the replacement of a small uncharged amino acid close to the tRNA binding site with a large negatively charged aspartate residue that electrostatically repels the tRNA, affecting k_1 and k_{-1}. As expected, the G220D substitution results in the most severe effect on SAM binding, and we are in fact unable to detect SAM binding by TrmA G220D under these conditions regardless of whether tRNA was also present. This result is unsurprising, but the first biochemical evidence of the importance of the conversed Motif I in SAM binding by TrmA. Similarly, PmtA, a bacterial SAM-dependent lipid *N*-methyltransferase also has nearly undetectable SAM binding when Motif I is mutated (Aktas *et al*. 2011). Based on the filter binding data we suggest that TrmA G220D activity is greatly reduced due to its inability to bind to SAM effectively. Under single-turnover conditions and at high concentrations, enough SAM can bind to TrmA allowing it to complete one round of catalysis, but even under these conditions the enzyme could be rate-limited by SAM binding.

TrmA wild type will bind substrate tRNA in the absence of SAM and also will bind SAM without tRNA being present. Gu and Santi previously reported TrmA's affinity for tRNA to be between 49 and 80 nM, which is in good agreement with our results. But this study is the first to report a SAM dissociation constant for TrmA (Gu and Santi 1992). From

the TrmA C324A data we show that binding of both ligands simultaneously to TrmA increases the affinity for each individual ligand. TrmA E358Q demonstrated that covalent complex formation was the major contributor to tRNA affinity. Additionally, the affinity for product tRNA as observed for TrmA wild type and Q190A was reduced compared to substrate tRNA. Lee *et al.* (2005) postulated that product release from RumA may be facilitated by unfavorably close contact between the main chain oxygen of P364 (P300 in TrmA) and the carbon of the methyl group on the target nucleotide U1939. This residue is part of Motif IV and is conserved both sequentially and spatially in TrmA. Since both enzymes adopt a similar fold of their RNA target stem loops and have almost identical catalytic sites, such an interaction could explain the decreased affinity of TrmA for methylated tRNA. Substitution Q190A did not have quite the predicted effect on tRNA binding or catalysis and the loss of its interactions may be compensated by other amino acids within the active site. TrmA G220D confirmed the importance of Motif I for SAM binding and its impact on methyltransferase activity.

Amino acid residues within RNA binding domain are essential for disrupting tRNA tertiary interactions

To identify the roles of amino acid residues within the RNA-binding domain of TrmA, R51, F106, and H125 were mutated to alanine. These residues were proposed to help induce the correct positioning of the T-arm within the active site by interacting with the D-arm of tRNA through breaking RNA tertiary interactions and stabilizing the bound substrate (Alian *et al*. 2008). Unlike the above catalytic cleft amino acid residues, R51, F106 and H125 are not conserved in either *E. coli* rRNA methyltransferase RumA or RumB. Whereas the target stem loops of TrmA, RumA and RumB share similar qualities,

the surrounding environment of the RNA outside the target site is quite different, thus requiring different methods of accessing RNA (Lee *et al*. 2004; Urbonavičius *et al*. 2007; Alian *et al*. 2008).

Under multiple and single-turnover conditions during tritium release assays, TrmA R51A is the most active TrmA variant analyzed here and has similar tRNA and SAM binding characteristics to the wild type. Like the wild type and Q190A variant, TrmA R51A can likely form product tRNA during the incubation time when SAM was included in the filter binding titrations. While TrmA R51A can still form covalent complex, the double substitution variant TrmA R51A C324A can only form the noncovalent complex and is inactive in activity assays. Compared to the single C324A variant, the affinity of TrmA R51A C324A for tRNA alone decreased by almost 3-fold, whereas the affinity for tRNA in the presence of SAM decreased roughly 5-fold. These results suggest that R51 could be slightly contributing to tRNA binding prior to covalent complex formation, but may not be a crucial contact between tRNA and TrmA, as opposed to F106 and H125 (see below). Comparable to the single C324A variant, TrmA R51A C324A bound to SAM with a higher affinity upon the inclusion of tRNA in the titration and also demonstrates the cooperative ligand binding described above.

Although both TrmA F106A and H125A can form covalent complexes with tRNA, the affinity of these enzymes for this substrate is greatly reduced compared to the wild type, regardless if SAM is included in the titration. The activity of TrmA F106A is reduced 23-fold, while H125A's activity is reduced 18-fold compared to the wild type under single turnover conditions, similar to those used for filter binding. Most likely the reduced apparent rate of catalysis reflects a reduction in the rate of tRNA binding for these TrmA

variants, but further kinetic characterization such as Michael-Menten titrations or pre-steady-state analysis is required to confirm this hypothesis. Together these results allow us to draw conclusions of the F106A and H125A substitutions on binary complex formation by TrmA. The difference in tRNA affinities between wild type and these variants is most likely due to a decrease in k_1 and/or an increase in k_{-1}; however additional effects on k_2 and k_{-2} cannot be ruled out. TrmA F106A's tRNA affinity was reduced by more than 50-fold compared to the wild type, while the H125A substitution resulted in a reduction of almost 190-fold. The additional C324A mutation to either single substitution variant only further reduced the tRNA affinity by 11- to 18-fold. Therefore, it appears that the loss of covalent bond formation by the double mutant only slightly exacerbates the already poor tRNA binding by TrmA F106A or H125A. These single amino acid changes most likely impair tRNA binding significantly, resulting in only marginal covalent complex formation, thus the tRNA affinity is affected less by the C324A substitution.

The *in vitro* aminoacylation assay would verify the role of Arg51, Phe106, and His125 in tRNA folding/binding. This assay demonstrated that TrmA can help to refold tRNA regardless of catalytic activity or the ability to form a covalent bond, as seen by an increase in the fraction of instantaneously aminoacylated tRNAs. Therefore, the next step would be to complete the assay in the presence of a TrmA variant impaired in tRNA binding.

This is the first biochemical evidence evaluating the importance of the RNA-binding domain of *E. coli* TrmA and conserved residues therein. Alian *et al.* (2008) speculated based on the TrmA crystal structure that R51, F106 and H125 could be disrupting the D-

and T-arm interactions of full-length tRNA. Specifically R51 was predicted to hydrogen bond to C60 of the 19-mer T-arm RNA oligomer in the TrmA structure, but was also proposed to be well positioned to intercalate between RNA bases G18 and G19 of the D-arm, substituting for G57 of the refolded T-arm. I demonstrate here that changing this position to alanine had little effect on tRNA binding or catalysis, implying that this residue is in fact not critical for disrupting tRNA tertiary interactions. Conversely, both F106A and H125A substitutions have severe consequences on TrmA tRNA binding and therefore indirectly on methylation activity. F106 was proposed to make hydrophobic or aromatic stacking interactions with G18, while H125's imidazole ring interacted with G18's phosphate group. Both of these residues appear to be central to efficient and effective tRNA binding by TrmA. Breaking the tertiary interactions of G18-U55 and G19-C56 is critical to gaining access to the target nucleotide U54. We know that tRNAs lacking these base pairs have approximately 10-fold higher k_{cat}/K_M values than the wild type tRNA due to an increase in k_1 (Kealey *et al*. 1994b). Together, these findings support the assumption that tRNA tertiary interactions are disrupted prior to gaining access to U54 by TrmA, and residues F106 and H125 are essential for this step. Sequence alignment of bacterial TrmA amino acid sequences revealed complete conservation of all three residues examined here. However, alignment of TrmA sequences from yeast and higher eukaryotes revealed that these organisms typically have large N-terminal extensions compared to the bacterial TrmA proteins that may be important for tRNA binding. Therefore, without further structural information we are unable to determine if these amino acids are conserved across other domains of life or whether the mechanism of tRNA binding is preserved between organisms.

Rates of proton abstraction and methyl group transfer by TrmA

Here I report the enzymatic activity of TrmA using both steady-state and pre-steady-state conditions. Quench flow analysis was completed with tritium-labeled tRNA and increasing TrmA wild type concentrations under single-turnover conditions. These experiments allowed us to measure the final proton abstraction step and resolution of TrmA-tRNA(CH_3) covalent complex which is concentration independent and nonreversible. This rate which corresponds to k_{10} or k_{11} (depending on the order of SAM dissociation, which is unknown) occurs within the TrmA-tRNA complex and therefore would not depend on enzyme concentration. All three TrmA concentrations tested here resulted in similar time courses with an average rate of 0.09 s^{-1}, which is in good agreement with previous reports (Gu and Santi 1991; Gu and Santi 1992; Kealey *et al*. 1994a). These findings also suggest that catalysis is not limited by initial substrate binding as I would have observed an increase in the rate with an increase in enzyme concentration.

When rapid kinetics analysis was used to measure the methyl-group transfer step (k_8), a rate of 0.21 s^{-1} was found for the wild type enzyme. The rate for methyl-group transfer is reduced by almost 7-fold compared to wild type in the TrmA E358Q variant for which no tritium release is detected under either multiple- or single-turnover conditions. The *E. coli* rRNA methyltransferase RumA E424Q variant also displayed a reduced rate of methyl transfer compared to the wild type enzyme (Lee et al. 2005).

Kealey, Gu, and Santi (1991, 1992, 1994) have shown that substrate tRNA binding is rapid, and I observed no rate increase with increasing enzyme concentration that would

suggest binding is limiting. The previously reported k_{cat} of 0.09 s^{-1} also suggests that product release is at least as fast as the proton abstraction step measured here. Since the rate of methyl group transfer discussed above is greater than the rate of proton abstraction, I can now propose that proton abstraction is the rate limiting step for 5-methyluridine formation by TrmA.

In summary, I provide evidence to support the roles that conserved catalytic amino acids play during methyl-group transfer, as well as show for the first time the importance of amino acids within the RNA-binding domain for disrupting tertiary tRNA interactions. Specifically, through examination of TrmA C324A and E358Q variants I found that ligand binding is cooperative but random, and I was able to determine values for K_1 and K_2. Furthermore, although conserved across all domains of life, I found that Q190 was dispensable for substrate binding and catalysis, whereas the G220D substitution severely impaired SAM binding and consequently methylation activity. I identified two amino acid residues within the RNA-binding domain that almost certainly play a critical role in tRNA binding. Finally, I measured the rates for both the methylation and proton abstraction steps directly and found that the resolution of the enzyme-product tRNA covalent bond is the rate-limiting step of 5-methyluridine formation by TrmA. In combination with previous findings on T-arm stem loop rearrangement and base flipping, we can start to understand how TrmA gains access to its inaccessible target nucleotide in a full-length folded tRNA substrate. These findings can help future analysis of other tRNA elbow targeting modification enzymes to clarify whether this strategy of tertiary interaction disruption is a common feature.

Chapter 5 -
Conclusions

tRNA biogenesis is a multi-step, multi-enzyme requiring complex process, and despite decades of research many questions remain unanswered. Do tRNAs fold first and then become modified? Are some modifications occurring early in tRNA maturation? Do modifications help in tRNA folding? What roles do modifying enzymes play in this process? It was proposed many years ago that tRNA modifying enzymes could be potentially acting as RNA chaperones *in vivo* (Gutgsell *et al.* 2000; Kinghorn *et al.* 2002). Ofengand and coworkers demonstrated that expression of the pseudouridine 55 synthase TruB can rescue the fitness disadvantage of the *trub* knockout strain when grown in co-culture, but it was not the formation of pseudouridine 55 in the T-arm stem loop that was critical. Rather, just the expression of the enzyme, even catalytically inactive, was enough to help recover the knockout phenotype (Gutgsell *et al*. 2000). However, they failed to demonstrate that tRNA folding by TruB was the critical factor in rescuing these knockout phenotypes which is required to prove that TruB is indeed acting as a tRNA chaperone in the cell. As unequivocal evidence for TruB's tRNA chaperone activity, I show here that TruB increases the fraction of folded tRNA that can be rapidly aminoacylated *in vitro*. In addition, tRNA binding by TruB is essential for rescuing the knockout phenotype, whereas pseudouridylation is not. Homologs of TruB are found across all domains of life and target the universally conserved U55 in the T-arm of tRNAs. This conservation suggests that this modification, and this modifying enzyme, are providing a fitness advantage by acting as a tRNA chaperone, are critical for survival and are therefore retained during evolution. Hypothetically, the methyltransferase TrmA could also be a tRNA chaperone. While I have not tested this (yet), I am here providing a detailed characterization of tRNA and SAM binding by TrmA. Most importantly, this

study identifies crucial interactions between TrmA and the elbow region that could contribute to tRNA unfolding similar to the described tRNA chaperone mechanism of TruB.

The biogenesis of tRNA involves many different modifying enzymes, acting at different positions of the polynucleotide strand. Potentially any of these RNA modifying enzymes could be functioning as a tRNA chaperone. All of these enzymes must bind the tRNA and in doing so often cause local unfolding of the tRNA structure. Possibly the process of tRNA modification could be functioning as a timer to provide sufficient time for the tRNA structure to establish its proper conformation. Potentially, pseudouridine formation is inherently slow catalytically in order to allow for rearrangement within the tRNA substrate (Wright *et al*. 2011). In addition, enzyme binding and modification may act as a checkpoint to mark correct folding of the tRNA structure and to signal that the tRNA is ready for subsequent steps in the tRNA maturation pathway such as other modifications. In the case of TruB, the T-arm can undergo repeated local unfolding and refolding steps, as demonstrated by fluorescence stopped-flow analysis. This fine-tuning of tRNA structure during biogenesis could be critical for tRNA interactions during its lifetime, as tRNA needs to bind to elongation factors, aminoacyl synthetases, and the ribosome. The subtle changes these modifications and modifying enzymes contribute to tRNA structure and stability could constitute a critical difference in cell survival, especially under stressful conditions. In particular, the two enzymes discussed in this thesis, TruB and TrmA, need to gain access to their target nucleotide by breaking tertiary interactions within the elbow region of the tRNA, and flipping out their target uridine into the enzyme active site. In doing so, at least TruB and potentially also TrmA, gives the tRNA a second

(or third, etc.) chance to fold into its functional conformation, ensuring the correct long-range interactions within the tRNA are established and maintained. Additionally, by binding to the T-arm stem loop during tRNA maturation, these enzymes may be acting to prevent aberrant interactions from forming prior to mature tRNA folding into its canonical L-shape structure. Similarly, although untested, modifying enzymes that target the D-arm stem loop could disrupt tertiary interactions and act in a similar manner to establish proper tRNA folding. Furthermore, since the energy of folding for the D-arm is less than the other stems, enzyme binding could protect it from endonuclease digestion, stabilize it while the rest of the tRNA folds, or help bring it together with the T-arm to form the proper tertiary interactions (Crothers *et al*. 1974).

As demonstrated in this thesis, tRNA binding by TruB is the critical, cellular characteristic enabling its chaperone activity. In order to establish if this is a common feature for other tRNA modifying enzymes, similar experiments would need to be repeated. It has already been demonstrated that an *E. coli* strain lacking m^5U54 modifications is outcompeted by the wild type strain in co-culture assays; however it was not confirmed whether tRNA binding by the TrmA could rescue this phenotype. Therefore, in order to establish whether TrmA is also acting as a tRNA chaperone *in vivo*, expression of a catalytically inactive variant, such as TrmA C324A, in the knockout strain will determine if this enzyme can rescue the fitness disadvantage. Further, to ensure it is tRNA binding that is essential for this hypothesized role, a TrmA variant defective in tRNA binding would be required for testing as well, which should not rescue the knockout phenotype if TrmA is truly acting as a tRNA chaperone. This thesis outlines the beginning of this process and demonstrates that TrmA binds both of its ligands in a

cooperative manner, whereas tRNA binding can be impaired by substituting amino acid residues within the RNA-binding domain. From the analysis described here substitutions of F106A or H125A in combination with C324A would be good candidates for these competition experiments; potentially residues F106 and H125 could be substituted with glutamate as in the case of TruB. TruB was also shown to increase the fraction of tRNA that could be aminoacylated after complete unfolding of the tRNA, suggesting a positive effect on tRNA folding *in vitro*. This same experiment could be repeated with TrmA to again establish its role in tRNA folding. Other tRNA modifying enzymes, such as the Dus enzymes, TrmB, or TrmH, that all target the elbow region of tRNAs are also likely tRNA chaperone candidates and could be evaluated in a similar manner. Possibly tRNA modifying enzymes that target the anticodon loop may also serve as tRNA chaperones, as co-culture competition assays revealed a fitness disadvantage for a RluA knockout strain compared to the wild type strain (Raychaudhuri *et al*. 1999). However, it is unclear whether it is tRNA or rRNA binding and/or modification by RluA that is contributing to the fitness advantage which would need to be investigated further.

The tRNA modifying enzymes discussed here share features of RNA chaperones as they often bind RNAs semi-specifically and may help to fold and/or stabilize their target RNAs. TruB and most likely other tRNA modifying enzymes are acting as multifunctional enzymes, whereby RNA modification is possibly only a secondary function compared to tRNA binding and tRNA folding. Since TruB (and TrmA in many cases) binds all tRNA isoacceptors in the cell, this may be a common checkpoint across all tRNAs to ensure proper folding of the T-arm and elbow region. RNA modifying enzymes targeting other species of RNA could also be acting as RNA chaperones, such

as the Pus enzymes from yeast that target spliceosomal RNA (Motorin and Grosjean 1999; Newby and Greenbaum 2001). Potentially, by binding snRNAs these modifying enzymes are preventing incorrect base pairing or stabilizing secondary structure motifs prior to or during the modification process. RNA chaperone activity is also most likely important during ribosome assembly, in order to ensure that the ribosomal RNA does not become trapped in nonnative conformers. Several ribosomal proteins have been demonstrated to have RNA chaperone activity *in vitro* and could potentially contribute to the dynamic rearrangement of the ribosome during translation (Semrad *et al*. 2004). Most likely, RNA modifying enzymes targeting the ribosome are also acting as RNA chaperones, similarly preventing the formation of misfolded regions of rRNA or actively facilitating RNA folding and establishing tertiary interactions.

The appearance of nonspecific RNA binding peptides could have arisen billions of years ago in the transition from the RNA world to the RNA/protein world. These peptides possibly provided a fitness advantage in a primitive RNA world by rescuing RNAs from kinetic traps, aiding in folding, and helping RNAs explore more diverse structural landscapes. From Renée Schroeder's description of RNA chaperones, enzymes must meet certain criteria to fit into this category of biological tools. First, they must bind transiently and nonspecifically to RNA. Whereas TruB, TrmA and the other RNA chaperones discussed above certainly meet this standard, other RNA binding proteins do not, such as proteins involved in forming relatively stable ribonucleoprotein complexes. Second, RNA chaperones must be able to resolve kinetically trapped or misfolded RNAs. While I have shown this for TruB, other modifying enzymes that require a pre-existing conformation for binding will not fulfill this stipulation. Thirdly, RNA chaperones must

be able to loosen or disrupt RNA-RNA interactions. Both enzymes discussed in this thesis must be able to disrupt tertiary interactions within the elbow region of all tRNAs in order to gain access to their target bases. I have also shown that TruB is able to facilitate local unfolding and refolding within the T-arm. Finally, RNA chaperones are not ATP-dependent or require any energy input to perform their function and are not required for maintaining the RNA structure once properly folded. Although TruB, and most likely TrmA fit all these criteria, other tRNA binding enzymes do not. Whereas EF-Tu can bind tRNAs transiently it cannot, to our knowledge, resolve kinetically trapped conformers or disrupt RNA-RNA interactions and therefore would not be considered an RNA chaperone. While it would be convenient to assume RNA modifying enzymes are all functioning as RNA chaperones *in vivo*, this would be a severe over-interpretation and most likely untrue for many examples. Instead it would be imperative to investigate each modifying enzyme individually for RNA chaperone activity separately from their modification activity.

As this thesis demonstrates, the lifecycle of tRNA is a complex cellular process involving many different processing and folding steps, and interaction partners. Since protein translation is critical for cell survival and tRNAs are the essential adaptor molecules, their structural integrity and conformation must be maintained throughout the lifetime of the tRNA. Interaction with modifying enzymes that also act as tRNA chaperones at the same time serves a critical function along this pathway.

Chapter 6 -
References

Abbasi-Mohed L, Mertel S, Gonsior M, Nouri-Vahid L, Kahrizi K, Cirak S, Wieczorek D, Motazacker M, Esmaeeli-Nieh S, Cremer K et al. 2012. Mutations in NSUN2 cause autosomal-recessive cognitive disorders. *American Journal of Human Genetics* **90**: 847-855.

Abbott JA, Francklyn CS, Robey-Bond SM. 2014. Transfer RNA and human disease. *Frontiers in Genetics* **5**.

Agarwalla S, Kealey J, Santi D, Stroud R. 2002. Characterization of the 23S ribosomal RNA m5U1939 methyltransferase from *Escherichia coli*. *The Journal of Biological Chemistry* **277**: 8835-8840.

Agris P. 2004. Decoding the genome: a modified view. *Nucleic Acids Research* **32**: 223-238.

Agris P, Sierzputowska-Gracz H, Smith C. 1986. Transfer RNA contains sites of localized positive charge: carbon NMR studies of [^{13}C]methyl-enriched *Escherichia coli* and yeast tRNA^{Phe}. *Biochemistry* **25**: 5126-5131.

Agris P, Vendeix F, Graham W. 2007. tRNA's wobble decoding of the genome: 40 years of modification. *The Journal of Molecular Biology* **366**: 1-13.

Aktas M, Gleichenhagen J, Stoll R, Narberhaus F. 2011. *S*-Adenosylmethionine-binding properties of a bacterial phospholipid *N*-methyltransferase. The *Journal of Bacteriology* **193**: 3473-3481.

Alexandrov A, Chernyakov I, Gu W, Hiley S, Hughes T, Grayhack E, Phizicky E. 2006. Rapid tRNA decay can result from lack of nonessential modifications. *Molecular Cell* **21**: 87-96.

Alexandrov A, Martzen M, Phizicky E. 2002. Two proteins that form a complex are required for 7-methylguanosine modification of yeast tRNA. *RNA* **8**: 1253-1266.

Alian A, Lee TT, Griner SL, Stroud RM, Finer-Moore J. 2008. Structure of a TrmA–RNA complex: A consensus RNA fold contributes to substrate selectivity and catalysis in m^{5}U methyltransferases. *PNAS* **105**: 6876-6881.

Altman S, Kirsebom L, Talbot S. 1995. Recent studies of ribonuclease P. *FASEB Journal* **7**: 7-14.

Anantharaman V, Koonin E, Aravind L. 2002. SPOUT: a class of methyltransferases that includes spoU and trmD RNA methylase superfamilies, and novel superfamilies of predicted prokaryotic RNA methylases. *The Journal of Molecular Microbiology and Biotechnology* **4**: 71-75.

Anderson J, Phan L, Cuesta R, Carlson B, Pak M, Asano K, Björk G, Tamame M, Hinnebusch A. 1998. The essential Gcd10p-Gcd14p nuclear complex is required

for 1-methyladenosine modification and maturation of initiator methionyl-tRNA. *Genes & Development* **12**: 3650-3662.

Anderson J, Phan L, Hinnebusch A. 2000. The Gcd10p/Gcd14p complex is the essential two-subunit tRNA(1-methyladenosine) methyltransferase of *Saccharomyces cerevisiae*. *PNAS* **97**: 5173-5178.

Ansmant I, Massenet S, Grosjean H, Motorin Y, Branlant C. 2000. Identification of the *Saccharomyces cerevisiae* RNA:pseudouridine synthase responsible for formation of psi(2819) in 21S mitochondrial ribosomal RNA. *Nucleic Acids Research* **28**: 1941-1946.

Ansmant I, Motorin Y, Massenet S, Grosjean H, Branlant C. 2001. Identification and characterization of the tRNA:Psi 31-synthase (Pus6p) of *Saccharomyces cerevisiae*. *The Journal of Biological Chemistry* **276**: 34934-34940.

Armstrong RD, Diasio RB. 1982. Improved measurement of thymidylate synthetase activity by a modified tritium-release assay. *The Journal of Biochemical and Biophysical Methods* **6**: 141-147.

Arnez J, Steitz T. 1994. Crystal structure of unmodified $tRNA^{Gln}$ complexed with glutaminyl-tRNA synthetase and ATP suggest a possible role for pseudo-uridines in stabilization of RNA structure. *Biochemistry* **33**: 7560-7567.

Auxilien S, El Khadali F, Rasmussen A, Douthwaite S, Grosjean H. 2007. Archease from *Pyrococcus abyssi* improves substrate specificity and solubility of a tRNA m5C methyltransferase. *The Journal of Biological Chemistry* **282**: 18711-18721.

Baba T, Ara T, Hasegawa M, Takai Y, Okumura Y, Baba M, Datsenko K, Tomita M, Wanner B, Mori H. 2006. Construction of *Escherichia coli* K-12 in-frame, single-gene knockout mutants: the Keio collection. *Molecular Systems Biology* **2**: 1-11.

Baker D, Youssef O, Chastkofsky M, Dy D, Terns R, Terns M. 2005. RNA-guided RNA modification: functional organization of the archaeal H/ACA RNP. *Genes & Development* **19**: 1238-1248.

Bakin A, Ofengand J. 1993. Four newly located pseudouridylate residues in Escherichia coli 23S ribosomal RNA are all at the peptidyltransferase center: Analysis by the application of a new sequencing technique. *Biochemistry* **32**: 9754-9762.

Balakin A, Smith L, Fournier M. 1996. The RNA world of the nucleolus: Two major families of small RNAs defined by different box elements with related functions. *Cell* **86**: 823-834.

Becker H, Motorin Y, Planta R, Grosjean H. 1997a. The yeast gene YNL292w encodes a pseudouridine synthase (Pus4) catalyzing the formation of psi55 in both mitochondrial and cytoplasmic tRNAs. *Nucleic Acids Research* **25**: 4493-4499.

Becker H, Motorin Y, Sissler M, Florentz C, Grosjean H. 1997b. Major identity determinants for enzymatic formation of ribothymidine and pseudouridine in the Tψ-loop of yeast tRNAs. *The Journal of Molecular Biology* **274**: 505-518.

Behm-Ansmant I, Branlant C, Motorin Y. 2007. The *Saccharomyces cerevisiae* Pus2 protein encoded by YGL063w ORF is a mitochondrial tRNA:Psi27/28-synthase. *RNA* **13**: 1641-1647.

Behm-Ansmant I, Grosjean H, Massenet S, Motorin Y, Branlant C. 2004. Pseudouridylation at position 32 of mitochondrial and cytoplasmic tRNAs requires two distinct enzymes in *Saccharomyces cerevisiae*. *The Journal of Biological Chemistry* **279**: 52998-53006.

Behm-Ansmant I, Urban A, Ma X, Yu U, Motorin Y, Branlant C. 2003. The *Saccharomyces cerevisiae* U2 snRNA:pseudouridine-synthase Pus7p is a novel multisite-multisubstrate RNA:Psi-synthase also acting on tRNAs. *RNA* **9**: 1371-1382.

Benítez- Páez A, Villarroya M, Armengod M. 2012. The *Escherichia coli* RlmN methyltransferase is a dual-specificity enzyme that modifies both rRNA and tRNA and controls translational accuracy. *RNA* **18**: 1783-1795.

Bergstrom D, Leonard N. 1972. Photoreaction of 4-thiouracil with cytosine. Relation to photoreactions in *Escherichia coli* transfer ribonucleic acids. *Biochemistry* **11**: 1-9.

Bhaskaran H, Rodriguez-Hernandez A, Perona JJ. 2012. Kinetics of tRNA folding monitored by aminoacylation. *RNA* **18**: 569-580.

Bishop A, Xu J, Johnson R, Schimmel P, de Crécy-Lagard V. 2002. Identification of the tRNA dihydrouridine synthase family. *The Journal of Biological Chemistry* **277**: 25090-29295.

Björk G, Isaksson L. 1970. Isolation of mutants of *Escherichia coli* lacking 5-methyluracil in transfer ribonucleic acid or 1-methylguanine in ribosomal RNA. *The Journal of Molecular Biology* **51**: 83-100.

Björk GR, Neidhardt FC. 1975. Physiological and biochemical studies on the function of 5-methyluridine in the transfer ribonucleic acid of *Escherichia coli*. *The Journal of Bacteriology* **124**: 99-111.

Blattner F, Plunkett III G, Bloch C, Perna N, Burland V, Riley M, Collado-Vides J, Glasner J, Rode C, Mayhew G et al. 1997. The complete genome sequence of *Escherichia coli* K-12. *Science* **277**.

Byrne R, Jenkins H, Peters D, Whelan F, Stowell J, Aziz N, Kasatsky P, Rodnina M, Koonin E, Konevega A et al. 2015. Major reorientiation of tRNA substrates defines specificity of dihydrouridine synthases. *PNAS* **112**: 6033-6037.

Byrne R, Konevega A, Rodnina M, Antson A. 2010. The crystal structure of unmodified $tRNA^{Phe}$ from *Escherichia coli*. *Nucleic Acids Research* **38**: 4154-4162.

Cabello-Villegas J, Nikonowicz E. 2005. Solution structure of Ψ32-modified anticodon stem-loop of *Escherichia coli* $tRNA^{Phe}$. *Nucleic Acids Research* **33**: 6961-6971.

Carlile T, Rojas-Duran M, Zinshteyn B, Shin H, Bartoli K, Gilbert W. 2014. Pseudouridine profiling reveals regulated mRNA pseudouridylation in yeast and human cells. *Nature* **515**: 143-146.

Carre D, Thomas G, Favre A. 1974. Conformation and functioning of tRNAs: cross-linked tRNAs as substrate for tRNA nucleotidyl-transferase and aminoacyl synthetases. *Biochimie* **56**: 1089-1101.

Cavaillé J, Chetouani F, Bachellerie J. 1999. The yeast *Saccharomyces cerevisiae* YDL112w ORF encodes the putative 2'-O-ribose methyltransferase catalyzing the formation of Gm18 in tRNAs. *RNA* **5**: 66-81.

Cerrudo CS, Ghiringhelli PD, Gomez DE. 2014. Protein universe containing a PUA RNA-binding domain. *FEBS Journal* **281**: 74-87.

Chakshusmathi C, Kim S, Rubinson D, Wolin S. 2003. A La protein requirement for efficient pre-tRNA folding. *EMBO Journal* **22**: 6562-6572.

Chan C, Pang Y, Deng W, Babu I, Dyavaiah M, Begley T, Dedon P. 2012. Reprogramming of tRNA modifications controls the oxidative stress response by codon-biased translation of proteins. *Nature Communications* **3**: 1-9.

Charette M, Gray MW. 2000. Pseudouridine in RNA: what, where, how, and why. *IUBMB Life* **49**: 341-351.

Charpentier B, Muller S, Branlant C. 2005. Reconstitution of archaeal H/ACA small ribonucleoprotein complexes active in pseudouridylation. *Nucleic Acids Research* **33**: 3133-3144.

Chen C, Deutscher M. 2005. Elevation of RNase R in response to multiple stress conditions. *The Journal of Biological Chemistry* **280**: 34393-34396.

Cheng X, Kumar S, Posfai J, Pflugrath J, Roberts R. 1993. Crystal structure of the HhaI DNA methyltransferase complexed with S-adenosyl-L-methionine. *Cell* **74**: 299-307.

Chernyakov I, Whipple J, Kotelawala L, Grayhack E, Phizicky E. 2008. Degradation of severa hypomodified mature tRNA species in *Saccharomyces cerevisiae* is mediated by Met22 and the 5'-3' exonucleases Rat1 and Xrn1. *Genes & Development* **22**: 1369-1380.

Cleland W. 1973. Derivation of rate equations for multisite ping-pong mechanisms with ping-pong reactions at one or more sites. *The Journal of Biological Chemistry* 248: 8353-8355.

Clodi E, Semrad K, Schroeder R. 1999. Assaying RNA chaperone activity *in vivo* using a novel RNA folding trap. *EMBO Journal* **18**: 3776-3782.

Coetzee T, Herschlag D, Belfort M. 1994. *Escherichia coli* proteins, including ribosomal protein S12, facilitate *in vitro* splicing of phage T4 introns by acting as RNA chaperones. *Genes & Development* **8**: 1575-1588.

Cole P, Crothers D. 1972. Conformational changes of transfer ribonucleic acid. Relaxation kinetics of the early melting transition of methionine transfer ribonucleic acid (*Escherichia coli*). *Biochemistry* **11**: 4368-4374.

Cole P, Yang S, Crothers D. 1972. Conformational changes of transfer ribonucleic acid. Equilibrium phase diagrams. *Biochemistry* **11**.

Copela L, Fernadez C, Sherrer R, Wolin S. 2008. Competition between the Rex1 exonuclease and the La protein affects both Trf4p-mediated RNA quality control and pre-tRNA maturation. *RNA* **14**: 1214-1227.

Crothers D, Cole P, Hilbers C, Shulman R. 1974. The molecular mechanism of thermal unfolding of *Escherichia coli* formylmethionine transfer RNA. *The Journal of Molecular Biology* **87**: 63-88.

Dalluge J, Hamamoto T, Horikoshi K, Morita R, Stetter K, McCloskey J. 1997. Posttranscriptional modification of tRNA in psychrophilic bacteria. *The Journal of Bacteriology* **179-6**.

Dalluge J, Hashizume T, Sopchik A, McCloskey J. 1996. Conformational flexibility in RNA: the role of dihydrouridine. *Nucleic Acids Research* **24**: 1073-1079.

Davanloo P, Sprinzl M, Watanabe K, Albani M, Kersten H. 1979. Role of ribothymidine in the thermal stability of transfer RNA as monitored by proton magnetic resonance. *Nucleic Acids Research* **6**: 1571-1581.

Davis D. 1995. Stabilization of RNA stacking by pseudouridine. *Nucleic Acids Research* **23**: 5020-5026.

Davis D. 1998. Biophysical and conformational properties of modified nucleosides in RNA (nuclear magnetic resonance studies). in *Modification and Editing of RNA* (eds. H Grosjean, R Benne), pp. 103-112. ASM Press, Washington DC.

Davis D, Veltri C, Nielson L. 1998. An RNA model system for investigation of pseudouridine stabilization of the codon-anticodon interaction in $tRNA^{Lys}$, $tRNA^{His}$ and $tRNA^{Tyr}$. *The Journal of Biomolecular Structure and Dynamics* **15**: 1121-1132.

Davis F, Allen F. 1957. Ribonucleic acids from yeast which contain a fifth nucleotide. *The Journal of Biological Chemistry* **227**: 907-915.

De Bie L, Roovers M, Oudjama Y, Wattiez R, Tricot C, Stalon V, Droogmans L, Bujnicki J. 2003. The yggH gene of *Escherichia coli* encodes a tRNA (m^7G46) methyltransferase. *The Journal of Bacteriology* **185**: 3238-3243.

Del Campo M, Kaya Y, Ofengand J. 2001. Identification and site of action of the remaining four putative pseudouridine synthases in Escherichia coli. *RNA* **7**: 1603-1615.

Dennis P, Omer A. 2005. Small non-coding RNAs in archaea. *Current Opinion in Microbiology* **8**: 685-694.

Deutscher M. 2003. Degradation of stable RNA in bacteria. *The Journal of Biological Chemistry* **278**: 45041-45044.

Di Matteo G, Salerno M, Guarguaglini G, Di Fiore B, Palitti F, Lavia P. 1998. Interactions with single-stranded and double-stranded DNA-binding factors and alternative promoter conformation upon transcriptional activation of the *Htf9-a/RanBP1* and *Htf9-c* genes. *The Journal of Biological Chemistry* **273**: 495-505.

Dillon S, Zhang X, Trievel R, Cheng X. 2005. The SET-domain protein superfamily: protein lysine methyltransferases. *Genome Biology* **6**: 227.

Dixon M, Huang S, Matthews R, Ludwig M. 1996. The structure of the C-terminal domain of methionine synthase: presenting S-adenosylmethionine for reductive methylation of B12. *Structure* **4**: 1263-1275.

Droogmans L, Roovers M, Bujnicki J, Tricot C, Hartsch T, Stalon V, Grosjean H. 2003. Cloning and characterization of tRNA (m^1A58)methyltransferase (TrmI) from *Thermus thermophilus* HB27, a protein required for cell growth at extreme temperatures. *Nucleic Acids Research* **31**: 2148-2156.

Dunkle JA, Vinal K, Desai PM, Zelinskaya N, Savic M, West DM, Conn GL, Dunham CM. 2014. Molecular recognition and modification of the 30S ribosome by the aminoglycoside-resistance methyltransferase NpmA. *PNAS* **111**: 6275-6280.

Duraffour S, Ishchenko A, Saparbaev M, Crance J, Garin D. 2007. Substrate specificity of homogeneous monkeypox virus uracil-DNA glycosylase. *Biochemistry* **46**: 11874-11881.

Easton LE, Shibata Y, Lukavsky PJ. 2010. Rapid, nondenaturing RNA purification using weak anion-exchange fast performance liquid chromatography. *RNA* **16**: 1-7.

Edmonds C, Crain P, Gupta R, Hashizume T, Hocart C, Kowalak J, Pomerantz S, Stetter K, McCloskey J. 1991. Posttranscriptional modification of tRNA in thermophilic archaea (Archaebacteria). *The Journal of Bacteriology* **173**: 3138-3148.

Elkins P, Watts J, Zalacain M, van Thiel A, Vitazka P, Redlak M, Andraos-Selim C, Rastinejad F, WM H. 2003. Insights into catalysis by a knotted TrmD tRNA methyltransferase. *The Journal of Molecular Biology* **333**: 931-949.

Fauman E, Blumenthal R, Cheng X. 1999. Structure and evolution of AdoMet-dependent methyltransferases. in *S-Adenosylmethionine-dependent Methyltransferases: Structures and Functions* (eds. X Cheng, R Blumenthal), pp. 1-38. World Scientific Publishing, Singapore.

Favre A, Michelson A, Yaniv M. 1971. Photochemistry of 4-thiouridine in *Escherichia coli* transfer RNA_1^{Val}. *The Journal of Molecular Biology* **58**: 367-379.

Feder M, Pas J, Wyrwicz L, Bujnicki J. 2003. Molecular phylogenetics of the RrmJ/fibrillarin superfamily of ribose 2'-O-methyltransferases. *Gene* **302**: 129-138.

Fersht A. 1998. *Structure and mechanism in protein science: a guide to enzyme catalysis and protein folding*. W.H. Freeman and Company.

Fleissner E, Borek E. 1962. A new enzyme of RNA synthesis: RNA methylase. *PNAS* **48**: 1199-1203.

Foster P, Huang L, Santi DV, Stroud RM. 2000. The structural basis for tRNA recognition and pseudouridine formation by pseudouridine synthase I. *Nature Structural & Molecular Biology* **7**: 23-27.

Freude K, Hoffmann K, Jensen L, Delatycki M, des Portes V, Moser B, Hamel B, van Bokhoven H, Moraine C, Fryns J et al. 2004. Mutations in the *FTSJ1* gene coding for a novel *S*-adenosylmethionine-binding protein cause nonsyndromic X-linked mental retardation. *American Journal of Human Genetics* **75**: 305-309.

Friedt J, Leavens FM, Mercier E, Wieden HJ, Kothe U. 2014. An arginine-aspartate network in the active site of bacterial TruB is critical for catalyzing pseudouridine formation. *Nucleic Acids Research* **42**: 3857-3870.

Frye M, Watt F. 2006. The RNA methyltransferase Misu (NSun2) mediates Myc-induced proliferation and is upregulated in tumors. *Current Biology* **16**: 971-981.

Galardi S, Fatica A, Bachi A, Scaloni A, Presutti C, Bozzoni I. 2002. Purified box C/D snoRNPs are able to reproduce site-specific 2'-O-methylation of target RNA *in vitro*. *Molecular and Cellular Biology* **22**: 6663-6668.

Gehrig S, Eberle M, Botschen F, Rimbach K, Eberle F, Eigenbrod T, Kaiser S, Holmes W, Erdmann V, Sprinzl M et al. 2012. Identification of modifications in microbial, native tRNA that suppress immunostimulatory activity. *Journal of Experimental Medicine* **209**: 225-233.

Giegé R, Jühling F, Pütz J, Stadler P, Sauter C, Florentz C. 2012. Structure of transfer RNAs: similarity and variability. *Wiley Interdiscip Rev RNA* **3**: 37-61.

Goedecke K, Pigmot M, Goody R, Scheidig A, Weinhold E. 2001. Structure of the N6-adenine DNA methyltransferase M.TaqI in complex with DNA and a cofactor analog. *Nature Structural Biology* **8**: 121-125.

Gong W, O'Gara M, Blumenthal R, Cheng X. 1997. Structure of pvu II DNA-(cytosine N4) methyltransferase, an example of domain permutation and protein fold assignment. *Nucleic Acids Research* **25**: 2702-2715.

Greenberg R, Dudock B. 1980. Isolation and characterization of m^5U-methyltransferase from *Escherichia coli*. *The Journal of Biological Chemistry* **255**: 8296-8302.

Großhans H, Lecointe F, Grosjean H, Hurt E, Simos G. 2001. Pus1p-dependent tRNA pseudouridylation becomes essential when tRNA biogenesis is compromised in yeast. *The Journal of Biological Chemistry* **276**: 46333-46339.

Gu X, Ivanetich K, Santi D. 1996. Recognition of the T-arm of tRNA by tRNA (m^5U54)-methyltransferase is not sequence specific. *Biochemistry* **35**: 11652-11659.

Gu X, Liu Y, Santi D. 1999. The mechanism of pseudouridine synthase I as deduced from its interaction with 5-fluorouracil-tRNA. *PNAS* **96**: 14270-14275.

Gu X, Ofengand J, Santi DV. 1994. *In vitro* methylation of *Escherichia coli* 16S rRNA by tRNA (m^5U54)-methyltransferase. *Biochemistry* **33**: 2255-2261.

Gu X, Santi D. 1990. High-level expression of *Escherichia coli* tRNA (m^5U54)-methyltransferase. *DNA and Cell Biology* **9**: 273-278.

Gu X, Santi DV. 1991. The T-arm of tRNA is a substrate for tRNA (m^5U54)-methyltransferase. *Biochemistry* **30**: 2999-3002.

Gu X, Santi DV. 1992. Covalent adducts between tRNA (m^5U54)-methyltransferase and RNA substrates. *Biochemistry* **31**: 10295-10302.

Gu X, Yu M, Ivanetich K, Santi DV. 1998. Molecular recognition of tRNA by tRNA pseudouridine 55 synthase. *Biochemistry* **37**: 339-343.

Gurha P, Gupta R. 2008. Archaeal Pus10 proteins can produce both pseudouridine 54 and 55 in tRNA. *RNA* **14**: 2521-2527.

Gustafsson C, Björk GR. 1993. The tRNA-(m^5U54)-methyltransferase of *Escherichia coli* is present in two forms *in vivo*, one of which is present as bound to tRNA and to a 3'-end fragment of 16S rRNA. *The Journal of Biological Chemistry* **268**: 1326-1331.

Gustafsson C, PH L, Hagervall T, Esberg K, Björk G. 1991. The *trmA* promoter has regulatory features and sequence elements in common with the rRNA P1 promoter family of *Escherichia coli*. *The Journal of Bacteriology* **173**: 1757-1764.

Gutgsell N, Englund N, Niu L, Kaya Y, Lane BG, Ofengand J. 2000. Deletion of the Escherichia coli pseudouridine synthase gene truB blocks formation of pseudouridine 55 in tRNA in vivo, does not affect exponential growth, but confers a strong selective disadvantage in competition with wild-type cells. *RNA* **6**: 1870-1881.

Hagervall T, Ericson J, Esberg K, Li J, Björk G. 1990. Role of tRNA modification in translational fidelity. *Biocheimica et Biophysica Acta* **1050**: 263-266.

Hall K, Sampson J, Uhlenbeck O, Redfield A. 1989. Structure of an unmodified tRNA molecule. *Biochemistry* **28**: 5794-5801.

Hamdane D, Guelorget A, Guerineau V, Golinelli-Pimpaneau B. 2014. Dynamics of RNA modification by a multi-site-specific tRNA methyltransferase. *Nucleic Acids Research* **42**: 11697-11706.

Hamma T, Ferré-D'Amaré AR. 2006. Pseudouridine synthases. *Chemistry & Biology* **13**: 1125-1135.

Hamma T, Reichow S, Varani G, Ferré-D'Amaré A. 2005. The Cbf5-Nop10 complex is a molecular bracket that organizes box H/ACA RNPs. *Nature Structural & Molecular Biology* **12**: 1101-1107.

Harrington K, Nazarenko I, Dix D, Thompson R, Uhlenbeck O. 1993. *In vitro* analysis of translational rate and accuracy with an unmodified tRNA. *Biochemistry* **32**: 7617-7622.

Helm M, Brulé H, Françoise D, Cepanec C, Leroux J, Giegé R, Florentz C. 1998. The presence of modified nucleotides is required for cloverleaf folding of a human mitochondrial tRNA. *Nucleic Acids Research* **26**: 1636-1643.

Hicks D, Janarthanan B, Vardarajan R, Kulkarni S, Khoury T, Dim D, Budd G, Yoder B, Tubbs R, Schreeder M et al. 2010. The expression of TRMT2A, a novel cell cycle regulated protein, identifies a subset of breast cancer patients with HER2 over-expression that are at an increased risk of recurrence. *BMC Cancer* **10**: 1-7.

Hoang C, Chen J, Vizthum CA, Kandel JM, Hamilton CS, Mueller EG, Ferré-D'Amaré AR. 2006. Crystal structure of pseudouridine synthase RluA: indirect sequence readout through protein-induced RNA structure. *Molecular Cell* **24**: 535-545.

Hoang C, Ferré-D'Amaré AR. 2001. Cocrystal structure of a tRNA Psi55 pseudouridine synthase: nucleotide flipping by an RNA-modifying enzyme. *Cell* **107**: 929-939.

Hoang C, Ferré-D'Amaré AR. 2004. Crystal structure of the highly divergent pseudouridine synthase TruD reveals a circular permutation of a conserved fold. *RNA* **10**: 1026-1033.

Hoang C, Hamilton C, Mueller E, Ferré-D'Amaré A. 2005. Precursor complex structure of pseudouridine synthase TruB suggests coupling of active site perturbations to an RNA-sequestering peripheral protein domain. *Protein Science* **14**: 2201-2206.

Holley R, Apgar J, Everett G, Madison J, Marquisee M, Merrill S, Penswick J, Zamir A. 1965. Structure of a ribonucleic acid. *Science* **147**: 1462-1465.

Hopper A, Furukawa A, Pham H, Martin N. 1982. Defects in modification of cytoplasmic and mitochondrial transfer RNAs are caused by single nuclear mutations. *Cell* **28**: 543-550.

Hori H, Suzuki T, Sugawara K, Inoue Y, Shibata T, Kuramitsu S, Yokoyama S, Oshima T, Watanabe K. 2002. Identification and characterization of tRNA (Gm18) methyltransferase from *Thermus thermophilus* HB8: domain structure and conserved amino acid sequence motifs. *Genes to Cells* **7**: 259-272.

Hori H, Yamazaki N, Matsumoto T, Watanabe Y, Ueda T, Nishikura K, Kumagai I, Watanabe K. 1998. Substrate recognition of tRNA (guanosine-2')-methyltransferase from *Thermus thermophilus* HB27. *The Journal of Biological Chemistry* **273**: 25721-25727.

Horie N, Hara-Yokoyama M, Yokoyama S, Watanabe K, Kuchino Y, Nishimura S, Miyazawa T. 1985. Two $tRNA^{Ile}$ species from an extreme thermophile, *Thermus thermophilus* HB8: Effect of 2-thiolation of ribothymidine on the thermostability of tRNA. *Biochemistry* **24**: 5711-5715.

Howland J. 1990. *Biochemistry: By D Voet and JG Voet*. John Wiley and Sons, New York.

Huang L, Pookanjanatavip M, Gu X, Santi DV. 1998. A conserved aspartate of tRNA pseudouridine synthase is essential for activity and a probable nucleophilic catalyst. *Biochemistry* **37**: 344-351.

Huang Y, Komoto J, Konishi K, Takata Y, Ogawa H, Gomi T, Fujioka M, Takusagawa F. 2000. Mechanisms for auto-inhibition and forced product release in glycine N-methyltransferase: crystal structures of wild-type, mutant R175K and S-adenosylhomocysteine-bound R175K enzymes. *The Journal of Molecular Biology* **298**: 149-162.

Hurd R, Reid B. 1979. Nuclear magnetic resonance studies on the tertiary folding of transfer ribonucleic acid: assignment of the 7-methylguanosine resonance. *Biochemistry* **18**: 4017-4024.

Hussain S, Sajini A, Blanco S, Dietmann S, Lombard P, Sugimoto Y, Paramor M, Gleeson J, Odom D, Ule J et al. 2013. NSun2-mediated cytosine-5 methylation of vault noncoding RNA determines its processing into regulatory small RNAs. *Cell Reports* **4**: 255-261.

Ishida K, Kunibayashi T, Tomikawa C, Ochi A, Kanai T, Hirata A, Iwahita C, Hori H. 2011. Pseudouridine at position 55 in tRNA controls the contents of other modified nucleotides for low-temperature adaptation in the extreme-thermophilic eubacterium Thermus thermophilus. *Nucleic Acids Research* **39**: 2304-2318.

Ishihama A. 2000. Functional modulation of *Escherichia coli* RNA polymerase. *Annual Reviews of Microbiology* **54**.

Ishitani R, Yokoyama S, Nureki O. 2008. Structure, dynamics, and function of RNA modification enzymes. *Current Opinion in Structural Biology* **18**: 330-339.

Jarrett J, Huang S, Matthews R. 1998. Methionine synthase exists in two distinct conformations that differ in reactivity toward methyltetrahydrofolate, adenosylmethionine, and flavodoxin. *Biochemistry* **37**: 5372-5382.

Johansson MJO, Byström AS. 2002. Dual function of the tRNA(m5U54)methyltransferase in tRNA maturation. *RNA* **8**: 324-335.

Jones CN, Jones CI, Graham WD, Agris PF, Spremulli LL. 2008. A disease-causing point mutation in human mitochondrial $tRNA^{Met}$ rsults in tRNA misfolding leading to defects in translational initiation and elongation. *The Journal of Biological Chemistry* **283**: 34445-34456.

Kadaba S, Krueger A, Trice T, Krecic A, Hinnebusch A, Anderson J. 2004. Nuclear surveillance and degradation of hypomodified initiator tRNAMet in *S. cerevisiae*. *Genes & Development* **18**: 1227-1240.

Kadaba S, Wang X, Anderson J. 2006. Nuclear RNA surveillance in *Saccharomyces cerevisiae*: Trf4p-dependent polyadenylation of nascent hypomethylated tRNA and an aberrant form of 5S rRNA. *RNA* **12**: 508-521.

Kamalampeta R, Keffer-Wilkes L, Kothe U. 2013. tRNA binding, positioning, and modification by the pseudouridine synthase Pus10. *The Journal of Molecular Biology* **425**: 3863-3874.

Kamalampeta R, Kothe U. 2012. Archaeal proteins Nop10 and Gar1 increase the catalytic activity of Cbf5 in pseudouridylating tRNA. *Scientific Reports* **2**: 663.

Kambampati R, Lauhon C. 2000. Evidence for the transfer of sulfane sulfur from IscS to ThiI during the *in vitro* biosynthesis of 4-thiouridine in *Escherichia coli* tRNA. *The Journal of Biological Chemistry* **275**: 10727-10730.

Kaya Y, Ofengand J. 2003. A novel unanticipated type of pseudouridine synthase with homologs in bacteria, archaea, and eukarya. *RNA* **9**: 711-721.

Kealey J, Gu X, Santi D. 1994. Enzymatic mechanism of tRNA (m^5U54) methyltransferase. *Biochimie* **76**: 1133-1142.

Kealey J, Lee S, Floss H, Santi D. 1991. Stereochemistry of methyl transfer catalyzed by tRNA (m5U54)-methyltransferase - evidence for a single displacement mechanism. *Nucleic Acids Research* **19**: 6465-6468.

Kealey J, Santi D. 1991. Identification of the catalytic nucleophile of tRNA (m^5U54)methyltransferase. *Biochemistry* **30**: 9724-9728.

Khan M, Rafiq M, Noor A, Hussain S, Flores J, Rupp V, Vincent A, Malli R, Ali G, Khan F et al. 2012. Mutation in *NSUN2*, which encodes an RNA methyltransferase, causes autosomal-recessive intellectual disability. *American Journal of Human Genetics* **90**: 856-863.

Kim S, Quigley G, Suddath F, McPherson A, Sneden D, JJ K, Weinzierl J, Rich A. 1973. Three-dimensional structure of yeast phenylalanine transfer RNA: Folding of the polynucleotide chain. *Science* **179**: 285-288.

Kim YE, Hipp MS, Bracher A, Hayer-Hartl M, Hartl FU. 2013. Molecular chaperone functions in protein folding and proteostasis. *Annual Review of Biochemistry* **82**: 323-355.

King RD, Lu C. 2014. An investigation into eukaryotic pseudouridine synthases. *The Journal of Bioinformatics and Computational Biology* **12**: 1450015.

King T, Liu B, McCully R, Fournier M. 2003. Ribosome structure and activity are altered in cells lacking snoRNPs that form pseudouridines in the peptidyl transferase center. *Molecular Cell* **11**: 425-435.

Kinghorn SM, O'Byrne CP, Booth IR, Stansfield I. 2002. Physiological analysis of the role of truB in Escherichia coli: a role for tRNA modification in extreme temperature resistance. *Microbiology* **148**: 3511-3520.

Kiss-Laszlo Z, Henry Y, Bachellerie J, Caizergues-Ferrer M, Kiss T. 1996. Site-specific ribose methylation of preribosomal RNA: a novel function for small nucleolar RNAs. *Cell* **85**: 1077-1088.

Kiss-Laszlo Z, Henry Y, Kiss T. 1998. Sequence and structural elements of methylation guide snoRNAs essential for site-specific ribose methylation of pre-rRNA. *EMBO Journal* **17**: 797-807.

Kiss T, Fayet-Lebaron E, Jady B. 2010. Box H/ACA small ribonucleoproteins. *Molecular Cell* **37**: 597-606.

Kitagawa M, Ara T, Arifuzzaman M, Ioka-Nakamichi T, Inamoto E, Toyonaga H, Mori H. 2005. Complete set of ORF clones of *Escherichia coli* ASKA library (A Complete Set of *E. coli* K-12 ORF Archive): Unique resources for biological research. *DNA Research* **12**: 291-299.

Klug A, Ladner J, Robertus J. 1974. The structural geometry of co-ordinated base changes in transfer RNA. *The Journal of Molecular Biology* **89**: 511-516.

Komine Y, Adachi T, Inokuchi H, Ozeki H. 1990. Genomic organization and physical mapping of the transfer RNA genes in *Escherichia coli* K12. *The Journal of Molecular Biology* **212**: 579-598.

Kowalak J, Dalluge J, McCloskey J, Stetter K. 1994. The role of posttranscriptional modificaiton in stabilization of transfer RNA from hyperthermophiles. *Biochemistry* **33**: 7869-7876.

Kuhsel M, Strickland R, Palmer J. 1990. An ancient group I intron shared by eubacteria and chloroplasts. *Science* **250**: 1570-1573.

Lamichhane T, Blewett N, Crawford A, Cherkosova V, Iben J, Begley T, Farabaugh P, Maraia R. 2013. Lack of tRNA modification isopentenyl-A37 alters mRNA decoding and causes metabolic deficiencies in fission yeast. *Molecular and Cellular Biology* **33**: 2928-2929.

Lauhon C, Erwin W, Ton G. 2004. Substrate specificity for 4-thiouridine modification in *Escherichia coli*. *The Journal of Biological Chemistry* **279**: 23022-23029.

Lecointe F, Simos G, Sauer A, Hurt E, Motorin Y, Grosjean H. 1998. Characterization of yeast protein Deg1 as pseudouridine synthase (Pus3) catalyzing the formation of psi 38 and psi 39 in tRNA anticodon loop. *The Journal of Biological Chemistry* **273**: 1316-1323.

Lee TT, Agarwalla S, Stroud RM. 2004. Crystal Structure of RumA, an Iron-Sulfur Cluster Containing *E. coli* Ribosomal RNA 5-Methyluridine Methyltransferase. *Structure* **12**: 397-407.

Lee TT, Agarwalla S, Stroud RM. 2005. A unique RNA fold in the RumA-RNA-Cofactor ternary complex contributes to substrate selectivity and enzymatic function. *Cell* **120**: 599-611.

Lee T, Feig A. 2008. The RNA binding protein Hfq interacts specifically with tRNAs. *RNA* **14**: 514-523.

Levinger L, Vasisht V, Greene V, Bourne R, Birk A, Kolla S. 1995. Sequence and structure requirements for Drosophila tRNA 5'- and 3'-end processing. *The Journal of Biological Chemistry* **270**: 18903-18909.

Li J, Esberg B, Curran J, Björk G. 1997. Three modified nucleosides present in the anticodon stem and loop influence the *in vivo* aa-tRNA selection in a tRNA-dependent manner. *The Journal of Molecular Biology* **271**: 209-221.

Li L, Ye K. 2006. Crystal structure of an H/ACA box ribonucleoprotein particle. *Nature* **443**: 302-307.

Li R, Ge HW, Cho SS. 2013. Sequence-dependent base-stacking stabilities guide tRNA folding energy landscapes. *The Journal of Physical Chemistry B* **117**: 12943-12952.

Li X, Zhu P, Ma S, Song J, Bai J, Sun F, Yi C. 2015. Chemical pulldown reveals dynamic pseudouridylation of the mammalian transcriptome. *Nature Chemical Biology* **11**: 592-597.

Li Z, Deutscher M. 1996. Maturation pathways for *E. coli* tRNA precursors: A random multienzyme process *in vivo*. *Cell* **86**: 503-512.

Li Z, Reimers S, Pandit S, Deutscher M. 2002. RNA quality control: degradation of defective transfer RNA. *EMBO Journal* **21**: 1132-1138.

Liu B, Yang X, Wang K, Tan W, Li H, Tang H. 2007. Real-time monitoring of uracil removal by uracil-DNA glycosylase using fluorescent resonance energy transfer probes. *Analytical Biochemistry* **366**: 237-243.

Lomax MIS, Greenberg GR. 1967. A new assay of thymidylate synthetase activity based on the release of tritium from deoxyuridylate-5-^{3}H. *The Journal of Biological Chemistry* **242**: 109-113.

Machnicka M, Milanowska K, Osman Oglu O, Purta E, Kurkowska M, Olchowik A, Januszewski W, Kalinowski S, Dunin-Horkawicz S, Rother K et al. 2012. MODOMICS: a database of RNA modification pathways. in *Nucleic Acid Research*, pp. 262-267.

Madsen C, Mengel-Jorgensen J, Kirpekar F, Douthwaite S. 2003. Identifying the methyltransferases for m(5)U747 and m(5)U1939 in 23S rRNA using MALDI mass spectrometry. *Nucleic Acids Research* **31**: 4738-4746.

Maglott E, Deo S, Przykorska A, Glick G. 1998. Conformational transitions of an unmodified tRNA: Implications for RNA folding. *Biochemistry* **37**: 16349-16359.

Masaki H, Ogawa T. 2002. The modes of action of colicins E5 and D, and related cytotoxic tRNases. *Biochimie* **84**: 433-438.

Massé E, Gottesmann S. 2002. A small RNA regulates the expression of genes involved in iron metabolism in *Escherichia coli*. *PNAS* **99**: 4620-4625.

Massenet S, Motorin Y, Lafontaine D, Hurt E, Grosjean H, Branlant C. 1999. Pseudouridine mapping in the *Saccharomyces cerevisiae* spliceosomal U small nuclear RNAs (snRNAs) reveals that pseudouridine synthase Pus1p exhibits a dual substrate specificity for U2 snRNA and tRNA. *Molecular and Cellular Biology* **19**: 2142-2154.

Massenet S, Mougin A, Branlant C. 1998. Posttranscriptional modifications in the U small nuclear RNAs. in *Modification and Editing of RNA* (ed. H Grosjean), pp. 223-262. ASM Press, Washington, DC.

Matsumoto K, Toyooka T, Tomikawa C, Ochi A, Takano Y, Takayanagi N, Endo Y, Hori H. 2007. RNA recognition mechanism of eukaryotic tRNA (m^7G46) methyltransferase (Trm8-Trm82 complex). *FEBS Letters* **581**: 1599-1604.

McClain W, Seidman J. 1975. Genetic perturbations that reveal tertiary conformation of tRNA precursor molecules. *Nature* **257**: 106-110.

McCleverty C, Hornsby M, Spraggon G, Kreusch A. 2007. Crystal structure of human Pus10, a novel pseudouridine synthase. *The Journal of Molecular Biology* **373**: 1243-1254.

Megel C, Morelle G, Lalande S, Duchêne A, Small I, Maréchal-Drouard L. 2015. Surveillance and cleavage of eukaryotic tRNAs. *International Journal of Molecular Sciences* **16**: 1873-1893.

Michel G, Sauvé V, Larocque R, Li Y, Matte A, Cygler M. 2002. The structure of the RlmB 23S rRNA methyltransferase reveals a new methyltransferase fold with a unique knot. *Structure* **10**: 1303-1315.

Miller J, Hussain Z, Schweizer M. 1976. The involvment of the anticodon adjacent modified nucleoside N-[9-(β-D-ribofuranosyl) purine-6-ylcarbamoyl]-threonine in the biological function of *E. coli* $tRNA^{Ile}$. *Nucleic Acids Research* **3**: 1185-1202.

Min J, Zhang X, Cheng X, Grewal S, Xu R. 2002. Structure of the SET domain histone lysine methyltransferase Clr4. *Nature Structural Biology* **9**: 828-832.

Miracco E, Mueller E. 2011. The products of 5-fluorouridine by the action of the pseudouridine synthase TruB disfavor one mechanism and suggest another. *The Journal of American Chemical Society* **133**: 11826-11829.

Mizutani K, Machida Y, Unzai S, Park S, Tame J. 2004. Crystal structures of the catalytic domains of pseudouridine synthases RluC and RluD from *Escherichia coli*. *Biochemistry* **43**: 4454-4463.

Motorin Y, Grosjean H. 1999. Multisite-specific tRNA:m5C-methyltransferase (Trm4) in yeast *Saccharomyces cerevisiae*: identification of the gene and substrate specificity of the enzyme. *RNA* **5**: 1105-1118.

Motorin Y, Helm M. 2010. tRNA stabilization by modified nucleotides. *Biochemistry* **49**: 4934-4944.

Motorin Y, Keith G, Simon C, Foiret D, Simos G, Hurt E, Grosjean H. 1998. The yeast tRNA:pseudouridine synthase Pus1p displays a multisite substrate specificity. *RNA* **4**: 856-869.

Mueller E. 2002. Chips off the old block. *Nature Structural & Molecular Biology* **9**: 320-322.

Mueller E, Buck C, Palenchar P, Barnhart L, Paulson J. 1998. Identification of a gene involved in the generation of 4-thiouridine in tRNA. *Nucleic Acids Research* **26**: 2606-2610.

Nelson D, Cox M. 2005. *Lehninger Principles of Biochemistry*. W. H. Freeman and Company, New York.

Neumann P, Lakomek K, Naumann P, Erwin W, Lauhon C, Ficner R. 2014. Crystal structure of a 4-thiouridine synthetase-RNA complex reveals specificity of tRNA U8 modification. *Nucleic Acids Research* **42**: 6673-6685.

Newby M, Greenbaum N. 2001. A conserved pseudouridine modification in eukaryotic U2 snRNA induces a change in branch-site architecture. *RNA* **7**: 833-845.

Nishikura K, De Robertis E. 1981. RNA processing in microinjected *Xenopus* oocytes: sequential addition of base modifications in a spliced transfer RNA. *The Journal of Molecular Biology* **145**: 405-420.

Nishimasu H, Ishitani R, Yamashita K, Iwashita C, Hirata A, Hori H, Nureki O. 2009. Atomic structure of a folate/FAD-dependent tRNA T54 methyltransferase. *PNAS* **106**: 8180-8185.

Nishimura S, Taya Y, Kuchino Y, Ohashi Z. 1974. Enzymatic synthesis of 3-(3-amino-3-carboxypropyl)uridine in *Escherichia coli* phenylalanine transfer RNA: transfer of the 3-amino-3-carboxypropyl group from S-adenosylmethionine. *Biochemical and Biophysical Research Communications* **57**: 702-708.

Nordlund M, Johansson J, von Pawel-Rammingen U, Byström A. 2000. Identification of the *TRM2* gene encoding the tRNA(m^5U54)methyltransferase of *Saccharomyces cerevisiae*. *RNA* **6**: 844-860.

Nurse K, Wrzesinski J, Bakin A, Lane B, Ofengand J. 1995. Purification, cloning, and properties of the tRNA pseudouridine 55 synthase from *Escherichia coli*. *RNA* **1**: 102-112.

Ny T, Björk G. 1980. Cloning and restriction mapping of the *trmA* gene coding for transfer ribonucleic acid (5-methyuridine)-methyltransferase in *Escherichia coli* K-12. *The Journal of Bacteriology* **142**: 371-379.

Nyhan W. 2001. Nucleotide synthesis via salvage pathway. in *Encyclopedia of Life Sciences*. John Wiley & Sons, Ltd.

O'Connor M, Gregory S. 2011. Inactivation of the RluD pseudouridine synthase has minimal effects on growth and ribosome function in wild-type Escherichia coli and Salmonella enterica. *The Journal of Bacteriology* **193**: 154-162.

Ochi A, Makabe K, Kuwajima K, Hori H. 2010. Flexible recognition of the tRNA G18 methylation target site by TrmH methyltransferase through first binding and induced fit processes. *The Journal of Biological Chemistry* **285**: 9018-9029.

Ofengand J. 2002. Ribosomal RNA pseudouridines and pseudouridine synthases. *FEBS Letters* **512**: 17-25.

Okamoto H, Watanabe K, Ikeuchi Y, Suzuki T, Endo Y, Hori H. 2004. Substrate tRNA recognition mechanism of tRNA (m7G46) methyltransferase from *Aquifex aeolicus*. *The Journal of Biological Chemistry* **279**: 49151-49159.

Omer A, Ziesche S, Ebhardt H, Dennis P. 2002. *In vitro* reconstitution and activity of a C/D box methylation guide ribonucleoprotein complex. *PNAS* **99**: 5289-5294.

Ow M, Kushner S. 2002. Initiation of tRNA maturation by RNase E is essential for cell viability in *Escherichia coli*. *Genes & Development* **16**: 1102-1115.

Pan H, Agarwalla S, Moustakas D, Finer-Moore J, Stroud RM. 2003. Structure of tRNA pseudouridine synthase TruB and its RNA complex: RNA recognition through a combination of rigid docking and induced fit. *PNAS* **100**: 12648-12653.

Persson B, Gustafsson C, Berg D, Björk G. 1992. The gene for a tRNA modifying enzyme, m5U54-methyltransferase is essential for viability in *Escherichia coli*. *PNAS* **89**: 3995-3998.

Persson B, Jäger G, Gustafsson C. 1997. The spoU gene of *Escherichia coli*, the fourth gene of the spoT operon, is essential for tRNA (Gm18) 2'-O-methyltransferase activity. *Nucleic Acids Research* **25**: 4093-4097.

Phannachet K, Elias Y, Huang R. 2005. Dissecting the roles of a strictly conserved tyrosine in substrate recognition and catalysis by pseudouridine 55 synthase. *Biochemistry* **44**: 15488-15494.

Phannachet K, Huang R. 2004. Conformational change of pseudouridine 55 synthase upon its association with RNA substrate. *Nucleic Acids Research* **32**: 1422-1429.

Phizicky EM, and Anita K. Hopper. 2010. tRNA Biology Charges to the Front. *Genes & Development* **24**: 1832–1860.

Preumont A, Snoussi K, Stroobant V, Collet J, Van Schaftingen E. 2008. Molecular identification of pseudouridine-metabolizing enzymes. *The Journal of Biological Chemistry* **283**: 25238-25246.

Purich D. 2010. *Enzyme Kinetics: Catalysis & Control: A Reference Theory and Best-Practice Methods*. Elsevier, London.

Purta E, van Vliet F, Tricot C, De Bie L, Feder M, Skowronek K, Droogmans L, Bujnicki J. 2005. Sequence-structure-function relationships of a tRNA (m7G46) methyltransferase studied by homology modeling and site-directed mutagenesis. *Proteins: Structure, Function, and Bioinformatics* **59**: 482-488.

Putz J, Florentz C, Benseler F, Giegé R. 1994. A single methyl group prevents the mischarging of a tRNA. *Nature Structural Biology* **1**: 580-582.

Rajkowitsch L, Chen D, Stampfl S, Semrad K, Waldsich C, Mayer O, Jantsch MF, Konrat R, Blasi U, Schroeder R. 2007. RNA chaperones, RNA annealers and RNA helicases. *RNA Biology* **4**: 118-130.

Ramabhadran T, Jagger J. 1976. Mechanism of growth delay induced in *Escherichia coli* by near ultraviolet radiation. *PNAS* **73**: 59-63.

Ramamurthy V, Swann SL, Paulson JL, Spedaliere CJ, Mueller EG. 1999a. Critical aspartic acid residues in pseudouridine synthases. *The Journal of Biological Chemistry* **274**: 22225-22230.

Ramamurthy V, Swann SL, Spedaliere CJ, Mueller EG. 1999b. Role of cysteine residues in pseudouridine synthases of different families. *Biochemistry* **38**: 13106-13111.

Ramser J, Winnepenninckx B, Lenski C, Errijgers V, Platzer M, Schwartz C, Meindi A, Kooy R. 2004. A splice site mutation in the methyltransferase gene *FTSJ1* in Xp11.23 is associated with non-syndromic mental retardation in a large Belgian family (MRX9). *The Journal of Medical Genetics* **41**.

Ranjan N, Rodnina M. 2016. tRNA wobble modifications and protein homeostasis. *Translation* **4**: 1-11.

Rashid R, Liang B, Baker D, Youssef O, He Y, Phipps K, Terns R, Li H. 2006. Crystal structure of a Cbf5-Nop10-Gar1 complex and implications in RNA-guided pseudouridylation and dyskeratosis congentia. *Molecular Cell* **21**: 249-260.

Raychaudhuri S, Niu L, Conrad J, Lane BG, Ofengand J. 1999. Functional effect of deletion and mutation of the Escherichia coli ribosomal RNA and tRNA pseudouridine synthase RluA. *The Journal of Biological Chemistry* **274**: 18880-18886.

Reddy R, Busch H. 1988. Small nuclear RNAs: RNA sequences, structure, and modifications. in *Structure and function of major and minor small nuclear*

ribonucleoprotein particles (ed. M Birnsteil), pp. 1-37. Springer-Verlag Press, Heidelberg.

Reinhold-Hurek B, Shub D. 1992. Self-splicing introns in tRNA genes of widely divergent bacteria. *Nature* **357**: 173-176.

Rider L, Ottosen M, Gattis S, Palfey B. 2009. Mechanism of dihydrouridine synthase 2 from yeast and the importance of modifications for efficient tRNA reduction. *The Journal of Biological Chemistry* **284**: 10324-10333.

Robertus J, Ladner J, Finch J, Rhodes D, Brown R, Clark B, Klug A. 1974. Structure of yeast phenylalanine tRNA at 3 Å resolution. *Nature* **250**: 546-551.

Rodriguez V, Chen Y, Elkahloun A, Dutra A, Pak E, Chandrasekharappa S. 2007. Chromosome 8 BAC array comparative genomic hydridization and expression analysis identify amplification and overexpression of TRMT12 in breast cancer. *Genes, Chromosomes & Cancer* **46**: 694-707.

Roovers M, Wouters J, Bujnicki J, Tricot C, Stalon V, Grosjean H, Droogmans L. 2004. A primordial RNA modification enzyme: the case of tRNA (m^1A) methyltransferase. *Nucleic Acids Research* **32**: 465-476.

Sabina J, Söll D. 2006. The RNA-binding PUA domain of archaeal tRNA-guanine transglycosylase is not required for archaeosine formation. *The Journal of Biological Chemistry* **281**: 6993-7001.

Sampson J, Uhlenbeck O. 1988. Biochemical and physical characterization of an unmodified yeast phenylalanine transfer RNA transcribed *in vitro*. *PNAS* **85**: 1033-1037.

Santi DV, Hardy LW. 1987. Catalytic mechanism and inhibition of tRNA (uracil-5-) methyltransferase: Evidence for covalent catalysis. *Biochemistry* **26**: 8599-8606.

Sarin L, Leidel S. 2015. Modify or die? - RNA modification defects in metazoans. *RNA Biology* **11**: 1555-1567.

Schaefer K, Altman S, Söll D. 1973. Nucleotide modification *in vitro* of the precursor of transfer RNA^{Tyr} of *Escherichia coli*. *PNAS* **70**: 3626-3630.

Schiffer S, Rösch S, Marchfelder A. 2002. Assigning a function to a conserved group of proteins: the tRNA 3'-processing enzymes. *EMBO Journal* **21**: 2769-2777.

Schubert H, Wilson K, Raux E, Woodcock S, Warren M. 1998. The X-ray structure of a cobalamin biosynthetic enzyme, cobalt-precorrin-4 methyltransferase. *Nature Structural Biology* **5**: 585-592.

Schubert HL, Blumenthal RM, Cheng X. 2003. Many paths to methyltransfer: a chronicle of convergence. *Trends in Biochemical Sciences* **28**: 329-335.

Schwartz S, Bernstein DA, Mumbach MR, Jovanovic M, Herbst RH, Leon-Ricardo BX, Engreitz JM, Guttman M, Satija R, Lander ES et al. 2014. Transcriptome-wide mapping reveals widespread dynamic-regulated pseudouridylation of ncRNA and mRNA. *Cell* **159**: 148-162.

Seidel A, Brunner S, Seidel P, Fritz G, Herbarth O. 2006. Modified nucleosides: an accurate tumour marker for clinical diagnosis of cancer, early detection and therapy control. *British Journal of Cancer* **94**: 1726-1733.

Seidman J, McClain W. 1975. Three steps in conversion of large precursor RNA into serine and proline transfer RNAs. *PNAS* **72**: 1491-1495.

Semrad K, Green R, Schroeder R. 2004. RNA chaperone activity of large ribosomal subunit proteins from *Escherichia coli*. *RNA* **10**: 1855-1860.

Serebrov V, Clarke R, Gross H, Kisselev L. 2001. Mg^{2+}-induced tRNA folding. *Biochemistry* **40**: 6688-6698.

Serebrov V, Vassilenko K, Kholod N, Gross H, Kisselev L. 1998. Mg^{2+} binding and structural stability of mature and in vitro synthesized unmodified *Escherichia coli* $tRNA^{Phe}$. *Nucleic Acids Research* **26**: 2723-2728.

Shisler K, Broderick J. 2012. Emerging themes in radical SAM chemistry. *Current Opinion in Structural Biology* **22**: 701-710.

Sivaraman J, Sauve V, Larocque R, Stura EA, Schrag J, Cygler M, Matte A. 2002. Structure of the 16S rRNA pseudouridine synthase RsuA bound to uracil and UMP. *Nature Structural & Molecular Biology* **9**: 353-358.

Spedaliere CJ, Hamilton CS, Mueller EG. 2000. Functional importance of motif I of pseudouridine synthases: Mutagenesis of aligned lysine and proline residues. *Biochemistry* **39**: 9459-9465.

Sprinzl M, Horn C, Brown M, Ioudovitch A, Steinberg S. 1998. Complation of tRNA sequences and sequences of tRNA genes. *Nucleic Acids Research* **26**: 148-153.

Stein A, Crothers D. 1976. Equilibrium binding of magnesium(II) by *Escherichia coli* $tRNA^{fMet}$. *Biochemistry* **15**: 157-160.

Sundaram M, Durant P, Davis D. 2000. Hypermodified nucleosides in the anticodon of tRNALys stabilize a canonical U-turn structure. *Biochemistry* **39**: 12575-12584.

Suzuki T, Nagao A. 2011. Human mitochondrial diseases caused by lack of taurine modifications in mitochondiral tRNAs. *Wiley Interdiscip Rev RNA* **2**: 376-386.

Thapa K, Oja T, Metsä-Ketelä M. 2014. Molecular evolution of the bacterial pseudouridine-5'-phosphate glycosidase protein family. *FEBS Journal* **281**: 4439-4449.

Toh S, Mankin A. 2008. An indigenous posttranscriptional modification in the ribosomal peptidyl transferase center confers resistance to an array of protein synthesis inhibitors. *The Journal of Molecular Biology* **380**: 593-597.

Tollervey D, Kiss T. 1997. Function and synthesis of small nucleolar RNAs. *Current Opinions in Cell Biology* **9**: 337-342.

Tomikawa C, Yokogawa T, Kanai T, Hori H. 2010. N^7-Methylguanine at position 46 (m^7G46) in tRNA from *Thermus thermophilus* is required for cell viability at high temperatures through a tRNA modification network. *Nucleic Acids Research* **38**: 942-957.

Urban A, Behm-Ansmant I, Branlant C, Motorin Y. 2009. RNA sequence and two-dimensional structure features required for efficient substrate modification by the *Saccharomyces cerevisiae* RNA:{Psi}-synthase Pus7p. *The Journal of Biological Chemistry* **284**: 5845-5858.

Urbonavičius J, Auxilien S, Walbott H, Trachana K, Golinelli-Pimpaneau B, Brochier-Armanet C, Grosjean H. 2008. Acquisition of a bacterial RumA-type tRNA(uracil-54, C5)-methyltransferase by Archaea through an ancient horizontal gene transfer. *Molecular Microbiology* **67**: 323-335.

Urbonavičius J, Durand JMB, Björk GR. 2002. Three modifications in the D and T arms of tRNA influence translation in *Escherichia coli* and expression of virulence genes in *Shigella flexneri*. *The Journal of Bacteriology* **184**: 5348-5357.

Urbonavičius J, Jäger G, Björk GR. 2007. Amino acid residues of the *Escherichia coli* tRNA(m^5U54)methyltransferase (TrmA) critical for stability, covalent binding of tRNA and enzymatic activity. *Nucleic Acids Research* **35**: 3297-3305.

Urbonavičius J, Skouloubris S, Myllykallio H, Grosjean H. 2005. Identification of a novel gene encoding a flavin-dependent tRNA:m^5U methyltransferase in bacteria - evolutionary implications. *Nucleic Acids Research* **33**: 3955-3964.

Veerareddygari G. 2014. Mechanistic investigations of pseudouridine synthases: a surprising glycal intermediate lies on the reaction pathway. in *Chemistry*, p. 220. University of Kentucky, Louisville, Kentucky.

Wang H, Boisvert D, Kim K, Kim R, Kim S. 2000. Crystal structure of a fibrillarin homologue from *Methanococcus jannaschii*, a hyperthermophile, at 1.6 Å resolution. *EMBO Journal* **19**: 317-323.

Watanabe K, Shinma M, Oshima T, Nishimura S. 1976. Heat-induced stability of tRNA from an extreme thermophile, *Thermus thermophilus*. *Biochemical and Biophysical Research Communications* **72**: 1137-1144.

Wei F, Suzuki T, Watanabe S, Kimura S, Kaitsuka T, Fujimura A, Matsui H, Atta M, Michiue H, Fontecave M et al. 2011. Deficit of tRNA(Lys) modification by

Cdkal1 causes the development of type 2 diabetes in mice. *Journal of Clinical Investigation* **121**: 3598-3608.

Whipple J, Lane E, Chernyakov I, D'Silva S, Phizicky E. 2011. The yeast rapid tRNA decay pathway primarily monitors the structural integrity of the acceptor and T-stems of mature tRNA. *Genes & Development* **25**: 1173-1184.

Willis I. 1993. RNA polymerase III. Genes, factors and transcriptional specificity. *European Journal of Biochemistry* **212**: 1-11.

Withers M, Wernisch L, Reis M. 2006. Archaeology and evolution of transfer RNA genes in the *Escherichia coli* genome. *RNA* **12**: 933-942.

Wolin S, Cedervall T. 2002. The La Protein. *Annual Reviews of Biochemistry* **71**: 375-403.

Wright JR, Keffer-Wilkes LC, Dobing SR, Kothe U. 2011. Pre-steady-state kinetic analysis of the three Escherichia coli pseudouridine synthases TruB, TruA, and RluA reveals uniformly slow catalysis. *RNA* **17**: 2074-2084.

Wu G, Adachi H, Ge J, Stephenson D, Query C, Yu Y. 2016. Pseudouridines in U2 snRNA stimulate the ATPase activity of Prp5 during spliceosome assembly. *EMBO Journal* **35**: 654-667.

Wu J, Santi D. 1987. Kinetic and catalytic mechanism of *Hha*I methyltransferase. *The Journal of Biological Chemistry* **262**: 4778-4786.

Wurm J, Griese M, Bahr U, Held M, Heckel A, Karas M, Soppa J, Wöhnert J. 2012. Identification of the enzyme responsible for N1-methylation of pseudouridine 54 in archaeal tRNAs. *RNA* **18**: 412-420.

Xiao B, Jing C, Wilson J, Walker P, Vasisht N, Kelly G, Howell S, IA T, Blackburn G, Gamblin S. 2003. Structure and catalytic mechanism of the human histone methyltransferase SET7/9. *Nature* **421**: 652-656.

Yamagami R, Yamashita K, Nishimasu H, Tomikawa C, Ochi A, Iwahita C, Hirata A, Ishitani R, Nureki O, Hori H. 2012. The tRNA recognition mechanism of folate/FAD-dependent tRNA methyltransferase (TrmFO). *The Journal of Biological Chemistry* **287**: 42480-42494.

Yan F, LaMarre J, Röhrich R, Wiesner J, Jomaa H, Mankin A, Galonić Fujimori D. 2010. RlmN and Cfr are radical SAM enzymes involved in methylation of ribosomal RNA. *The Journal of American Chemical Society* **132**: 3953-3964.

Yang S, Crothers D. 1972. Conformational changes of transfer ribonucleic acid. Comparison of the early melting transition of two tyrosine-specific transfer ribonucleic acids. *Biochemistry* **11**: 4375-4381.

Yarian C, Basti M, Cain R, Ansari G, Guenther R, Sochacka E, Czerwinska G, Malkiewicz A, Agris P. 1999. Structural and functional roles of the N1- and N3-protons of ψ at tRNA's position 39. *Nucleic Acids Research* **27**: 3543-3549.

Zebarjadian Y, King T, Fournier MJ, Clarke L, Carbon J. 1999. Point mutations in yeast CBF5 can abolish *in vivo* pseudouridylation of rRNA. *Molecular and Cellular Biology* **19**: 7461-7472.

Zegers I, Gigot D, van Vliet F, Tricot C, Aymerich S, Bujnicki J, Kosinski J, Droogmans L. 2006. Crystal structure of *Bacillus subtilis* TrmB, the tRNA (m^7G46) methyltransferase. *Nucleic Acids Research* **34**: 1925-1934.

Zhang X, Tamaru H, Khan S, Horton J, Keefe L, Selker E, Cheng X. 2002. Structure of the *Neurospora* SET domain protein DIM-5, a histone H3 lysine methyltransferase. *Cell* **111**: 117-127.

Zheng Y, Bruice T. 1997. A theoretical examination of the factors controlling the catalytic efficiency of a transmethylation enzyme: catechol *O*-methyltransferase. *The Journal of American Chemical Society* **119**: 8137-8145.

Zhou H, Liu Q, Yang W, Goa Y, Teng M, Niu L. 2009. Monomeric tRNA (m6G46) methyltransferase from *Escherichia coli* presents a novel structure at the function-essential insertion. *Proteins: Structure, Function, and Bioinformatics* **76**: 512-515.

Zhou J, Liang B, Li H. 2011. Structural and functional evidence of high specificity of Cbf5 for ACA trinucleotide. *RNA* **17**: 244-250.

Zhu L, Deutscher M. 1987. tRNA nucleotidyltransferase is not essential for *Escherichia coli* viability. *EMBO Journal* **6**: 2473-2477.

Appendix I

TrmA amino acid sequence alignment with 23S rRNA *E. coli* methyltransferases RumA and RumB, as well as *S. cerevisiae* homolog Trm2p and human homolog TRMT2A. Conserved motif sequences are underlined. Residues targeted for mutation in TrmA are bolded and coloured as described in Figure 4.2.

```
                 ....|....| ....|....| ....|....| ....|....| ....|....|
                         10         20         30         40         50
TrmA             MTPEHLPTEQ YEAQLAEKVV RLQSMMAPFS D--------- ----------
RumA             CGGCQQQHAS VDLQQRSKSA ALARLMKH-- ---------- ----------
RumB             CRSCQWITQP IPEQLSAKTA DLKNLLADFP VE-------- ----------
Trm2p            SSGSQLEFLT YDDQLELKRK TIMNAYKFFA PRL------- ---------V
TRMT2A           ---------P YAEQLERKQL ECEQVLQKLA KEIGSTNRAL LPWLLEQRHK
Clustal Co                    *   *


                 ....|....| ....|....| ....|....| ....|....| ....|....|
                        60         70         80         90        100
TrmA             --LVPEVFR- ----SPVSHY RMRAEFRIWH D-GD------ -DLYHII---
RumA             --EVSEVIA- ----DVPWGY RRRARLSLNY LPKT------ -QQLQMG---
RumB             --EWCAPVS- ----GPEQGF RNKAKMVVSG SVEK------ -PLLGML---
Trm2p            AEKLLPPFDT TVASPLQFGY RTKITPHFDM PKRKQKELSV RPPLGFGQKG
TRMT2A           HNKACCPLEG VRPSPQQTEY RNKCEFLVGV GVDG------ -EDNTVG---
Clustal Co              .            : * :    .                .


                 ....|....| ....|....| ....|....| ....|....| ....|....|
                       110        120        130        140        150
TrmA             ---F-DQ--- -QTKSRI-RV DSFPAASELI NQLM---TAM IA--GVRNNP
RumA             ---F-RK--- -AGSSDIVDV KQCPILVPQL EALLPKVRA- ----CLGSLQ
RumB             ---H-RD--- -GTP---EDL CDCPLYPASF APVFAALKPF IARAGLTPYN
Trm2p            RPQWRKDTLD IGGHGSILDI DECVLATEVL NKGLTNERRK FEQ-EFKN--
TRMT2A           ---C-RLGKY KGGTCAVAAP FDTVHIPEAT KQVVKAFQEF IRSTPYSAYD
Clustal Co                           .            .


                 ....|....| ....|....| ....|....| ....|....| ....|....|
                       160        170        180        190        200
TrmA             VLRHKLFQID YLTTLSN--Q AVVSLLYHK- --------KL DDEWRQEAEA
RumA             AMRH-LGHVE LV---QATSG TLM-ILRH-- ---------- TAPLSSADRE
RumB             VARK-RGELK YILLTESQSD GGMMLRFVLR SDTKLAQLRK ALPWLQEQLP
Trm2p            ---YKKGAT- -ILLREN--- -TTI---LDP SK-------- ---------P
TRMT2A           PETY-TGHWK QLTVRTSRRH QAMAIAYFHP ---------- -QKLSPEELA
Clustal Co                :


                 ....|....| ....|....| ....|....| ....|....| ....|....|
                       210        220        230        240        250
TrmA             LRDALRAQNL NVHLIGRATK TKIELDQ-D- --------YI DERL------
RumA             KLECF----- -----SHSEG LDLYLAPDS- --------EI LETVSG-E-M
RumB             QLKVITVNIQ PVHMAIMEGE TEIYLTEQQ- --------AL AER-------
Trm2p            TLEQLT---- -EEA-SRDEN GDISYVEVED KKNNVR--LA KTCVTNPRQI
TRMT2A           ELKTSLAQHF TAGPGRASGV TCLYFVEEGQ RKTPSQEGLP LEHVAG-DRC
Clustal Co         .                    :
```

```
                 ....|....| ....|....| ....|....| ....|....| ....|....|
                         260        270        280        290        300
TrmA             PVA-GKEMIY RQVENSFTQP NAAMNIQMLE WALDVT-KG- -----SKGDL
RumA             PWYDSNGLRL TFSPRDFIQV NAGVNQKMVA RALEWLDVE- -----PEDRV
RumB             ----FNDVPL WIRPQSFFQT NPAVASQLYA TARDWVRQL- -----PVKHM
Trm2p            VTEYVDGYTF NFSAGEFFQN NNSILPIVTK YVRDNLQAPA KGDDNKTKFL
TRMT2A           IHEDLLGLTF RISPHAFFQV NTPAAEVLYT VIQDWAQLD- -----AGSMV
Clustal Co                       * *  *      :      :               :
                                   X

                 ....|....| ....|....| ....|....| ....|....| ....|....|
                         310        320        330        340        350
TrmA             LELYCGNGNF SLALARNFDR VLATEIAKPS VAAAQYNIAA NHIDNVQIIR
RumA             LDLFCGMGNF TLPLATQAAS VVGVEGVPAL VEKGQQNARL NGLQNVTFYH
RumB             WDLFCGVGGF GLHCATPDMQ LTGIEIAPEA IACAKQSAAE LGLTRLQFQA
Trm2p            VDAYCGSGLF SICSSKGVDK VIGVEISADS VSFAEKNAKA NGVENCRFIV
TRMT2A           LDVCCGTGTI GLALARKVKR VIGVELCPEA VEDARVNAQD NELSNVEFHC
Clustal Co        :  ** * :  :  :      : . *      :  .. .      : .  :
                      I                  II

                 ....|....| ....|....| ....|....| ....|....| ....|....|
                         360        370        380        390        400
TrmA             MAAEEFTQAM NGVREFNRLQ GIDLKSYQCE TIFVDPPRSG LDSETEKMV-
RumA             ENLEEDVTKQ P--------- ---WAKNGFD KVLLDPARAG AAG-VMQQII
RumB             LDSTQFATA- ---------- ----QGEVPE LVLVNPPRRG IGKPLCDYLS
Trm2p            GKAEKLFESI D--------- ----TPSENT SVILDPPRKG CDELFLKQLA
TRMT2A           GRAEDLVPTL VS-------- ---RLASQHL VAILDPPRAG LHSKVILAIR
Clustal Co           .                             :::* * *         :
                                                     IV

                 ....|....| ....|....| ....|....| ....|....| ....|....|
                         410        420        430        440        450
TrmA             --QAYPRILY ISCNPETLCK NLETL-S--- -----QTHKV ERLALFDQFP
RumA             -KLEPIRIVY VSCNPATLAR DSEALLK--- -----AGYTI ARLAMLDMFP
RumB             -TMAPRFIIY SSCNAQTMAK DIRE--L--- -----PGYRI ERVQLFDMFP
Trm2p            -AYNPAKIIY ISCNVHSQAR DVEYFLKE-- -TENGSAHQI ESIRGFDFFP
TRMT2A           RAKNLRRLLY VSCNPRAAMG NFVDLCRAPS NRVKGIPFRP VKAVAVDLFP
Clustal Co              ::*  ***  :    :                .        .* **
                               VI

                 ....|....| ....|....| ....|....| ....|....| ....|....|
                         460        470        480        490        500
TrmA             YTHHMECGVL LTAK------ ---------- ---------- ----------
RumA             HTGHLESMVL FSRVK----- ---------- ---------- ----------
RumB             HTAHYEVLTL LVQQ------ ---------- ---------- ----------
Trm2p            QTHHVESVCI MKRI------ ---------- ---------- ----------
TRMT2A           QTPHCEMLIL FERVEHPNGT GVLGPHSPPA QPTPGPPDNT LQETGTFPSS
Clustal Co       * * *    : :
                  VIII
```